ADDIS ABABA UNIVERSITY

ADDIS ABABA INSTITUTE OF TECHNOLOGY (AAIT)

SCHOOL OF CIVIL AND ENVIRONMENTAL ENGINEERING

GEODESY AND GEOMATICS PROGRAM

ASSESSMENT OF SPATIO-TEMPORAL PATTERN OF WATER HYACINTH AND ITS DYNAMIC WITH SEASONAL CLIMATE VARIABILITY AND IMPACT ON EVAPOTRANSPIRATION OF LAKE TANA USING LANDSAT AND SENTINEL-2

TAKELE ABEBE

ADVISOR: Dr. BERHAN GESSESSE (ASSOCIATE PROFESSOR)

A THESIS SUBMITTED TO

SCHOOL OF CIVIL AND ENVIRONMENTAL ENGINEERING OF ADDIS ABABA UNIVERSITY IN PARTIAL FULFILLMENT OF THE REQUIREMENTS FOR DEGREE OF MASTER OF SCIENCE IN GEODESY AND GEOMATICS PROGRAM (IN SPECIALIZATION OF GEOMATICS)

ADDIS ABABA UNIVERSITY, ETHIOPIA

OCTOBER, 2020

APPROVAL SHEET

Addis Ababa Institute of Technology (AAIT)

School of Civil and Environmental Engineering

Geodesy and Geomatics Program

This is to certify that a thesis prepared by **Takele Abebe**, entitled: "Assessment of spatio-temporal pattern of water hyacinth and its dynamic with seasonal climate variability and impact on evapotranspiration of Lake Tana using Landsat and Sentinel-2", submitted in partial fulfillment of the requirements for the degree of Master of Science in Geodesy and Geomatics (in specialization of Geomatics) complies with the regulations of the University and meets the accepted standards with respect to the originality and quality.

Dr. Berhan Gessesse	_____	_____.
Advisors:	Signature	Date
Dr. Tulu Besha	_____	_____.
Internal examiner:	Signature	Date
Dr. Ermias Teferi	_____	_____.
External examiner:	Signature	Date
	_____	_____.
Chairperson:	Signature	Date

ACKNOWLEDGMENTS

First and for most, I would like to thanks the “Almighty GOD” who made it possible and for strength and patience that he gave me to complete the study successfully.

I wish to express my deepest and heartfelt gratitude to Dr. Berhan Gessesse, the principal supervisor of this thesis, for his continuous technical and scientific guidance, patience, motivation, and enthusiasm. He guided me in all facets of my research from the proposal conception to the final write-up.

My special thank goes to Mr. Gashew Mesafint, office expert and Mohammed Hassen, filed expert at ANRS Environment, Forest and Wildlife Protection and Development Authority they helped me to access transport service in the water hyacinth infested areas, a success of this thesis would not have been possible if it is not to do so as well as they provided the required information related to the status water hyacinth in Lake Tana.

My gratitude is belongs to Mr. Getachew Bayable, Worku Nega and Abel Balew for their technical and procedural advice and support starting from the proposal development to final thesis reviewing. I am very grateful to my best friend and colleague to Mr. Niguse Adane who helped me in the arrangement of a large number of climate data in MS-excel software into required form and provided other multi supports.

I would like to extend my appreciation to my family for their continuous support from lower grade education up to now. Special thank goes to my beloved fiancé Abeba Demle. I really appreciate her advice, support, encouragement, love, and understanding and tolerance me for my inconvenience to her. Finally, I want to thanks all of those people who helped me and their name are not listed here.

ABSTRACT

Lake Tana is the largest Lake in Ethiopia which has been invaded by water hyacinth since 2011. However, there is lack of reliable estimates of annual and seasonal water hyacinth distribution and extent. Therefore, this study aims to assess the spatio-temporal pattern of water hyacinth and it's dynamics with seasonal climate variability and impact on evapotranspiration using Landsat 7 ETM+, Landsat 8 OLI, Sentinel 2 and meteorological data. The area of water hyacinth and surface area of the Lake were mapped using supervised, unsupervised and manual digitizing image classification techniques. The trend of water hyacinth was determined using Mann-Kendall trend test and the impact of climate variability on water hyacinth spatial distribution was studied using Pearson correlation coefficient. The evapotranspiration and water losses were estimated from reference evapotranspiration computed using FAO-56 Penman-Monteith method and a crop coefficient value of 0.65 and 1.90. The results of the study revealed that there was a statistically significant increasing trend in annual spatial coverage of water hyacinth. The annual coverage areas of water hyacinth increased by 96% from 134ha in 2011 to 3019ha in 2019. However, the surface area of the Lake showed a decreasing trend. A total of 1834ha of the surface area of the Lake (0.6 % of the average surface area of the Lake) has lost over the last nine years. The annual maximum lake surface area was 306,399ha occurred in 2015 and the minimum was 302,952ha in 2019. The monthly and seasonal spatial-temporal dynamics of water hyacinth in Lake Tana exhibit a periodic cyclical pattern, reaching the highest peak in Bega followed by a decline to the least coverage level in Kiremt season. The highest growth areal extends of water hyacinth was 3830ha in 2018 November while, the minimum area was 396ha in 2017 July. The monthly surface area of the Lake was varied from 298,392ha in 2016 June to 317,257ha in 2018 July. The seasonal average surface area of the Lake was ranged between 301,817ha in Belg and 307,471ha in Kiremt season. The average daily evapotranspiration of water hyacinth in Lake Tana from 2016 September to 2018 December was 2.39 and 6.99 mm/day, and the average water loss in the Lake due the weed evapotranspiration was 35, 678 and 104,290 m3/day using Kc of 0.65 and 1.90 respectively. The total amount volume of water loss in Lake Tana from 2016 Sep to 2018 Dec was between 30,397,918 m^3 and 88,855,452 $m,^3$ the average value represents 0.21 % of the volume of the Lake using a Kc value of 0.65 and 1.90. The Pearson correlation of monthly water hyacinth and rainfall was significant moderately negative (r= -0.63, p=0.03). The correlation of mean monthly temperature and wind speed with water hyacinth was negative (r = -0.34, p = 0.28) and (r = -0.59, p = 0.04) respectively. The seasonal correlation of the area of water hyacinth with rainfall and wind speed was insignificant moderately negative (r= -0.72, p=0.49) and (r= -0.62, p=0.57). Low insignificant negative correlation (r = -0.36, p = 0.76) with mean temperature was also attained in seasonal period. In general, the climate variability in Lake Tana Basin showed a less and insignificant contribution for distribution and spread of water hyacinth in study period.

Keywords: Lake Tana, Water Hyacinth, Evapotranspiration, Water Loss, Climate Variability, Annual, Monthly and Seasonal Time Periods.

TABLE OF CONTENTS

ACKNOWLEDGMENTS iii
ABSTRACT iv
CHAPTER ONE 1
1 INTRODUCTION 1
1.1 Background 1
1.2 Statement of the Problem 3
1.3 Objectives of the Study 5
1.3.1 General Objective 5
1.3.2 Specifically, the study was guided by the following specific objectives. 5
1.4 Significant of the Study 6
1.5 Scope of the Study 6
1.6 Organization of the Study 6
CHAPTER TWO 7
2 LITERATURE REVIEW 7
2.1 Water Hyacinth 7
2.2 Factors influencing the Distribution and Expansion of Water Hyacinth 7
2.3 Impacts of Water Hyacinth 8
2.3.1 Reduction of Biodiversity 8
2.3.2 Blockage of Waterways, Hampering Fisheries, and Hydropower 8
2.3.3 Oxygen Depletion and Reduced Water Quality 9
2.3.4 Increased Evapotranspiration Rate 9
2.3.5 Affect Human Health 9
2.4 Control Option and Management of Water Hyacinth 10
2.4.1 Physical Control 10
2.4.2 Chemical Control 10
2.4.3 Biological Control 11
2.4.4 Integrated Control Approach: 11
2.5 The Origin and Distribution of the Invasive Water Hyacinth in Ethiopia 11

2.6 Impact of Climate Variability on Water Hyacinth Dynamics 13
2.7 Types Image Classification Method Used in Mapping of Water Hyacinth 14
2.7.1 Unsupervised ISODATA and Maximum Likelihood Classification (MLC) 14
2.7.2 Discriminant Analysis (DA) 15
2.7.3 Support Vector Machines (SVM) 15
2.7.4 Manual Digitizing Image Classification 16
2.8 The Role of Remote Sensing for Analyzing Spatio-Temporal Detection of Water Hyacinth 16
CHAPTER THREE 18
3 MATERIALS AND METHODS 18
3.1 Description of Lake Tana Basin 18
3.1.1 Location and Extent of the Study Area 18
3.1.2 Topography and Slope of Lake Tana Basin 19
3.1.3 Land Use and Land Cover of Lake Tana Basin 20
3.1.4 Climate of Lake Tana Basin 20
3.1.5 Hydrology and Hydrogeology of Lake Tana 21
3.2 Data Source 22
3.2.1 Remote Sensing Data 22
3.2.1.1 Landsat 7 Enhanced Thematic Mapper Plus (ETM+) Image 23
3.2.1.2 Landsat 8 Operational Land Imager (OLI) Image 23
3.2.1.3 Sentinal-2 Images 23
3.2.2 Meteorological Data 24
3.2.3 Ground Truth Points and Google Earth Data 25
3.3 Software Used for the Study 26
3.4 Methods of Data Analysis 27
3.4.1 Digital Image Preprocessing 27
3.4.1.1 Layer Stacking, Resampling, and Re-projection of the Images 28
3.4.2 Image Enhancement 28
3.5 Mapping and Detecting of the Spatio-Temporal Distribution of Water Hyacinth 29
3.6 Spatio-Temporal Monitoring of Water Surface Area of Lake Tana 30

3.6.1 Normalized Difference Water Index (NDWI) and Modified NDWI (MNDWI) 30
3.7 Accuracy Assessment 32
3.8 Spatio-Temporal Change Detection Analysis of water hyacinth and Surface Area of Lake Tana 33
3.9 Post Classification Approach 33
3.10 Trend Analysis of Annual Water Hyacinth Area and Surface Area of Lake Tana 33
3.10.1 Sen's Slope Estimator Test 34
3.11 Analysis of Meteorological Dataset in Lake Tana Basin 35
3.11.1 Analysis of Rainfall Data in Lake Tana Basin 35
3.11.1.1 Lake Areal Rainfall of Lake Tana Basin 35
3.11.2 Analysis of Temperature Data in Lake Tana Basin 36
3.11.3 Analysis of Wind Speed, Relative Humidity and Sunshine Hour Data in Lake Tana Basin 36
3.12 Evapotranspiration of Water Hyacinth (ETc) and Water Losses in Lake Tana 37
3.12.1 Crop Coefficient (Kc) 37
3.12.2 Referenced Evapotranspiration (ET_0) 38
3.12.3 Estimation of Water Losses Due to Evapotranspiration of Water Hyacinth 41
3.13 Correlational Analysis 42
CHAPTER FOUR 43
4 RESULTS AND DISCUSSION 43
4.1 Image Classification Accuracy Assessment 43
4.2 Water Hyacinth Spectral Response Profiles 44
4.3 Results of Spatio-Temporal Distribution of Water Hyacinth in Lake Tana 45
4.3.1 Annual Spatio-Temporal Distribution of Water Hyacinth in Lake Tana 45
4.3.2 Monthly Spatio-Temporal Distribution of Water Hyacinth in Lake Tana 50
4.3.3 Seasonal Spatio-Temporal Distribution of Water Hyacinth in Lake Tana 54
4.4 Spatio-Temporal Change Detection of Water Hyacinth in Lake Tana 55
4.4.1 Annual Spatio-Temporal Trend of Water Hyacinth in Lake Tana 55
4.4.2 Monthly and Seasonal Spatio-Temporal Change Detection of Water Hyacinth 57
4.5 Spatio-Temporal Change Detection of Surface Area of Lake Tana 59

4.5.1 Spatio-Temporal Change of Annual Surface Area of Lake Tana 59
4.5.2 Monthly and Seasonal Spatio-Temporal Change of Surface Area of Lake Tana 60
4.6 Analysis of Spatio-Temporal Distribution of Climate Variability in Lake Tana Basin. 62
4.6.1 Analysis of Rainfall Data in Lake Tana Basin 62
4.6.2 Analysis of Temperature Data in Lake Tana Basin 66
4.6.3 Analysis of Wind Speed, Relative Humidity and Sunshine Hour Data 68
4.7 Estimation Water Losses Due To Evapotranspiration of Water Hyacinth..... 70
4.8 The Association of Water Hyacinth Area with Climate Elements and Surfaces Area of Lake Tana 73
CHAPTER FIVE 76
5 CONCLUSIONS AND RECOMMENDATIONS 76
5.1 Conclusions 76
5.2 Recommendations 78
REFERENCE 79
Appendices 94

LIST OF FIGURES

Figure 3.1 Locational map of the Lake Tana Basin 18
Figure 3.2 Topographic map of Lake Tana Basin 19
Figure 3.3: Methodological flow chart of the research process. 27
Figure 4.1 Ground GPS points overlaid over 2019 January Sentinel- 2 raw image (TCI). 43
Figure 4.2 Spectral reflectance of water hyacinth derived from Sentinel-2 and Landsat 8 of Lake Tana 45
Figure 4.3 GPS points collected in 2011 by Tewabe, (2015) overlaid on a classified map of 2011 Jan in this study 46
Figure 4.4 Water hyacinth infestation in 2019 hot-spot areas (Kebeles) within the Lakeshore ... 47
Figure 4.5 spatio-temporal distribution and extent of water hyacinth in Lake Tana (2011- 2019) 49
Figure 4.6 Monthly spatio-temporal variation of water hyacinth area in Lake Tana 51
Figure 4.7 Monthly spatio-temporal distribution and extent of water hyacinth in Lake Tana 53
Figure 4.8 Area of Lake Tana occupied by water hyacinth as measured from satellite imagery . 56
Figure 4.9 Seasonal change patterns of water hyacinth area from 2016 Oct to 2019 Jan 58
Figure 4.10 Annual water surface area change of Lake Tana from 2011 to 2019 60
Figure 4.11 Monthly spatio-temporal variations in surface area of Lake Tana from 2016-2018. 61
Figure 4.12 Mean monthly rainfall pattern of class 1 stations from 2011 to 2018 years 64
Figure 4.13 Variation of total annual rainfall in the Basin from 2011 to 2018 years 64
Figure 4.14 Spatial interpolation of total annual mean rainfall (mm) of Lake Tana Basin from 2011–2018 years using Ordinary Kriging method 65
Figure 4.15 Maximum, mean and minimum monthly mean temperature distribution of Lake Tana Basin from 2011- 2018 years 67
Figure 4.16 Spatial interpolation of annual mean temperature (℃) of the Basin from 2011 - 2018 68
Figure 4.17 water hyacinth evapotranspiration in Lake Tana from 2017 Jan – 2018 Dec 72
Figure 4.18 water losses due to water hyacinth evapotranspiration in Lake Tana (2017 -2018) . 73

LIST OF TABLES

Table 3.1 Sentinel -2 data descriptions 24
Table 4.1 Results of accuracy assessment of water hyacinth and water surface 44
Table 4.2 Area of water hyacinth coverage from 2011 January to 2019 January 45
Table 4.3 Monthly areal coverage of water hyacinth (ha) of the study area (2016 Sep -2018 Dec) 50
Table 4.4 Seasonal mean area of water hyacinth from 2016 Oct – 2019 Jan 54
Table 4.5 Result of the Mann-Kendall trend test for annual water hyacinth area and surface area of Lake Tana. 56
Table 4.6 Monthly spatio-temporal distribution change of water hyacinth (ha) in Lake Tana 57
Table 4.7 Monthly and seasonal surface area of Lake Tana (ha) from 2016 Jan to 2018 Dec..... 61
Table 4.8 Total annual and seasonal mean rainfall (mm) from 2011 to 2018 years..... 63
Table 4.9 Mean monthly rainfall (mm) of Lake Tana Basin from 2011-2018 years..... 63
Table 4.10 Mean annual and seasonal temperature variation in the study area (2011 -2018)..... 66
Table 4.11 Maximum, mean and minimum monthly mean temperature (℃) variation of Lake Tana Basin from 2011 to 2018 years 67
Table 4.12 Monthly mean wind speed (m/s) at 2m above the ground surface from 2011 to 2018 69
Table 4.13 Mean monthly relative humidity (%) of the study area from 2011 to 2018 69
Table 4.14 Mean monthly sunshine hours (hr/day) of the study area from 2011 to 2018..... 69
Table 4.15 Reference evapotranspiration, evapotranspiration and water losses of water hyacinth from 2016 September to 2018 December 70
Table 4.16 Result of correlation of water hyacinth with climatic elements and surface area of Lake Tana..... 73

ACRONYMS

ANRS	Amhara National Regional State
BoEPLAU	Bureau of Environmental Protection, Administration and Use
℃	Degree Centigrade
ERDAS	Earth Resources Data Analysis System
ET_0	Referenced Evapotranspiration
ETM+	Enhanced Thematic Mapper Plus
FAO	Food and Agricultural Organization
GIS	Geographic Information System
GPS	Global Positioning System
ha	Hectares
Kc	Crop Coefficient
LULC	Land Use/Land Cover
m	Meter
MLC	Maximum Likelihood Classification
mm	Millimeter
MNDWI	Modified Normalized Difference Water Index
MS	Multispectral
MSI	Multispectral Instruments
NDWI	Normalized Difference Water Index
NMA	National Meteorological Agency
NMSA	National Meteorological Services Agency
OLI	Operational Land Imager
RS	Remote Sensing
SNAP	Sentinel Application Platform
TIRS	Thermal Infrared Sensor
USGS	United State Geological Survey
UTM	Universal Transform Mercator
WGS	World Geodetic System
WH	Water Hyacinth
XLSTAT	Statistical Software for Microsoft Excel

CHAPTER ONE

1 INTRODUCTION

1.1 Background

Water hyacinth, Eichhornia crassipes, is known as one of the world's worst weeds (Holm et al., 1977), invading aquatic ecosystems and native to the Amazon Basin in South America (Tellez et al., 2008). It has been identified as one of the 100 most serious aquatic weed problems by the International Union for Conservation of Nature (IUCN) (Tellez et al., 2008) recognized as one of the top ten ecologically dangerous and worst invasive weed (Patel, 2012). It becomes a major challenges in water body of more than 50 countries in the world (Tellez et al., 2008; Patel, 2012; Samuel and Netsanet, 2014) with a permanent impacts on fishery industry and agricultural production, canals of hydroelectric power plants, water transport and rivers, and environmental balance, human health, evapotranspiration of water, irrigation, navigation, livestock watering, aquatic biodiversity and others (Navarro and Phiri, 2000).

It was originally distributed by human activities from the Amazon Basin in tropical South America to different parts of the world (Dagno et al., 2012). In Ethiopia, water hyacinth was officially reported in the 1950s in Aba Samuel Reservoir, in the outskirts of Addis Ababa (Stroud, 1994). According to UNEP, (2013); Samuel and Netsanet, (2014), the weed was announced in 1956 in Lake Koka and Awash River. As sporadic visits including some clean-up attempts made during 1959, 1968, 1979 and 1988, the infestation of water hyacinth in Baro, Gillo, and Akobo Rivers of western Ethiopia was observed (Rezene, 2005). However, Lake Tana was infested by water hyacinth in September 2011 (Wassie et al., 2014). Following this infestation, BoEPLAU made a physical removal campaign, an estimated that between 90 – 95 % of the water hyacinth was removed from the Lake (Wassie et al., 2014). A study conducted in 2012 by a team member from the Bureau of Agriculture, Bureau of Water, Bureau of Tourism, BoEPLAU, Bahir Dar University and Agricultural Research Institute of Amhara Region showed that the water hyacinth coverage was 20,000ha (Wassie et al., 2014). This coverage continues to escalate 50,000ha in 2014 and close to one-third or more than 30% of the shoreline of the north-eastern part of the Lake's shore was invaded by water hyacinth while an intervention made on it (Wassie et al., 2014). Furthermore, an assessment made by Wassie et al., (2015) showed that the estimate of water hyacinth infestation coverage was approximately 34,500ha in 2015.

The water hyacinth causes loss of water rapidly through its broad leaves, which is about 3.5 times that of a free water surface (Gopal, 1987). Timmer and Weldon, (1966) indicated that the water loss through evapotranspiration from water hyacinth was 3.7 times greater than from open water. On the contrary, a study conducted by (Agutu et al., 2018) in Lake Naivasha, Kenya found out areas covered by water hyacinth had lower water loss than open water surface areas of the lake. Water losses increase through evapotranspiration and considered as one of the most important weed problems in water bodies, which require tools to reduce water losses (Ali and Khedr, 2018). Thus, estimating water losses through evapotranspiration of water hyacinth is very important for hydrological management and allows a better knowledge and understanding of the mechanisms and regularities that guides the water circulation in nature.

Climate change has profound effects on the distribution and location of water hyacinth in water bodies (Center et al., 2002) because it can cause significant impacts on water resources by resulting changes in hydrological cycle (Sewnet and Kameswara, 2011). The growth rate of water hyacinth in most open water bodies are driven by climate change and variability, high recharge from sewage disposal and nutrients from anthropogenic activities (Palmer et al., 2015). Change in temperature, rainfall, sea-level rise significantly affect the vegetation of coastal and wetland ecosystems (Erwin, 2009). For example, warming temperatures due to climate change have created favorable growing conditions for water hyacinth across most of the world (Stephenson et al., 1980). However, a high increase in temperature reduces the growth and productivity of aquatic plant by enhancing evaporation from them (Wrona et al., 2006). Rainfall and floods swept agricultural runoff and nutrient-rich sediment into the lake. The influx of fertilizer and sediments could have stimulated a new outbreak of water hyacinth (Fusilli et al., 2013). Seasonal dynamism and abundance of water hyacinth in Winam Gulf of Lake Victoria with the seasonal climatic variability data study shows seasonal–climatic factors directly affects the seasonal spatio-temporal pattern and distribution of the water hyacinth (Ouma et al., 2005).

The distribution and location of water hyacinth can be predicted based on seasonal climatic variations. Observed climatic and quantified water hyacinth distributions via satellite and meteorological data can be correlated to understand the seasonal-climatic factor, and subsequently derive information system is invaluable for advising the stakeholders: transportation, lake management and fishing industries (Ouma et al., 2005). This could be done

using remote sensing technology since it is an efficient method for environmental monitoring over aquatic ecosystems where the area is large, access is limited, and the weeds are not easy to see from a distance (Rajapakse et al., 2006). Remotely sensed imagery used to map and monitor seasonal and yearly changes in the extent of aquatic plant cover (Welch et al., 1988; Nohara, 1991; Everitt et al., 1999). Moreover, the availability of automated, reliable and real-time remote sensing data is important in detecting the distribution and location of aquatic weeds in water bodies (Cavalli et al., 2009). Satellite sensors capable of recording continual coverage of the earth surface provides spatial data for both short and long-term monitoring, which is crucial for evaluating the intervention made on the control and management of water hyacinth in the lakes (Penatti et al., 2015). Satellite images such as Landsat 8 and Sentinel 2 with a high revisit time, large coverage (swath-width), high radiometric, spatial and spectral resolution allows for detecting and mapping the spatial configuration of water hyacinth (Thamaga and Dube, 2018). Similarly, Landsat 7 ETM+ data is capable of mapping and monitoring of water hyacinth (Shekede et al., 2008; Dube et al., 2017a). In general, satellite data used to study the spatio-temporal distribution and configuration of water hyacinth in a timely and cost-effective way (Shekede et al., 2008; Dube et al., 2014).

Therefore, obtaining information about the distribution and extent of water hyacinth weed in Lake Tana shoreline is crucial based on seasonal climatic variability in order to understand the evolution of the invasion, to determine affected areas, to relate water hyacinth abundance with environmental parameters and to gauge the efficacy of control measures and management actions. This study sought to map the annual, monthly and seasonal spatio-temporal infestation of the weed in Lake Tana; identify the relationship of water hyacinth area with rainfall, temperature, wind speed and surface area of the Lake, and estimate the water losses through water hyacinth from the Lake by using remote sensing images and meteorological data.

1.2 Statement of the Problem

Lake Tana is the largest Lake in Ethiopia which accounts for 50% of the freshwater resource of the country. The Basin in its natural state has a high potential for agriculture, livestock, water resource, forest and wildlife, tourism, and fishery development besides too high biological diversity (Goraw and Shimelis, 2017). However, this multi-purpose Lake is invaded by one of the most ecologically dangerous weed, water hyacinth since 2011. Measurements such as

physical removal to control the proliferation of water hyacinth have been tried in the Lake. Even if a tremendous amount of human labor, time and money has been exerted each year by both surrounding community and government, its coverage continues to escalate from 20,000ha in 2012 to more than 50,000ha in 2014 (Wassie et al., 2014 and 2015). This is due to water hyacinth once established is it very difficult to manage and eradication often impossible. Continuous monitoring of its status is a mandatory part of its management (Wassie et al., 2015). However, their outcome of the intervention on the control and management of hyacinth is not systematically assessed, documented and shared to the stakeholders. Data about the follow-ups and sustainability of the community-based water hyacinth removal in Lake Tana was scarce (Wassie et al., 2014).

Accurate, reliable, and timely information on the spatio-temporal distribution and configuration of water hyacinth is important in tracing their evolution, and propagation in affected areas, as well as the potential vulnerable areas (Thamaga and Dube, 2018). The evolution of invasion water hyacinth and rapidity and direction of spread requires a detailed understanding of the impacts of climate, topography, soil, and anthropogenic factors on weeds' propagation and spread (Thamaga and Dube, 2018). Single date weed information could not provide a full understanding on their spatio-temporal variability. Comprehensive information on the spatial distribution of water hyacinth and its annual and seasonal variability is critical in managing water resources (Molinos et al., 2015). Due to this, continuous observation and monitoring of the proliferation of aquatic weeds are essential for proper water resource management and for the development of appropriate weed control strategies and prioritizations of most infested areas (Albright et al., 2004). Moreover, developing accurate, spatially explicit, fine-scale records on rates of invasions is a high priority (Panetta and Lawes, 2005). However, the studies conducted in Lake Tana regarding to spatial coverage of water hyacinth so far were deal about a single time. The long term spatial distribution and extent of the weed and its monthly and seasonal dynamics; surface area variability of the Lake; the impact of climate variability for the invasive water hyacinth proliferation as well as the impact of water hyacinth on evapotranspiration and water losses in Lake Tana has not been addressed. In addition, the infestation areal coverage of water hyacinth in Lake Tana reported previously is a source of conflict among the stakeholders (Derseh et al., 2019). High discrepancy has existed between the areas of water hyacinth of

50,000ha and 2279.4ha, excluding the infestation area in the flood plain estimated in 2014 and 2018 October respectively.

Therefore, a scientific approach is necessary to better understand the annual and seasonal spatio-temporal variation of the area covered by the water hyacinth and surface area of the Lake to support management actions using free accessible satellite images such as Sentinel-2 MSI which is capable of detecting and mapping the spatio-temporal variability and extent of water hyacinth in lakes with an alternatively of Landsat images in case of heavy cloud covers in seasonal periods. The study was tried to show the annual, monthly and seasonal of spatio-temporal distribution of water hyacinth and surface area of the Lake, and the impact climate factors to the spatio-temporal dynamics of the invasive weed. Beyond this, the study was attempted to estimate the evapotranspiration of water hyacinth and water losses in Lake Tana.

1.3 Objectives of the Study

1.3.1 General Objective

The general objective of this study was to examine the spatio-temporal pattern of water hyacinth, and it's dynamic with seasonal climate variability and impact on evapotranspiration of Lake Tana by using satellite imagery and meteorological data.

1.3.2 Specifically, the study was guided by the following specific objectives.

- To assess the annual spatio-temporal distribution of water hyacinth in Lake Tana from 2011 to 2019 using Landsat and Sentinel-2 satellite imageries.
- To compute the monthly and seasonal spatio-temporal dynamics of water hyacinth from 2016 to 2019 using Landsat and Sentinel-2 satellite imageries.
- To analyze the climate variability of Lake Tana Basin from 2011 to 2018.
- To evaluate the impact of water hyacinth expansion on the evapotranspiration and water loss in Lake Tana from 2016 to 2018 and,
- To investigate the association between the area of water hyacinth with climate elements and surface area the Lake.

1.4 Significant of the Study

The results of the study basically will answers the questions of what is the trend of water hyacinth and surface area of the Lake looks like and the impact of climate factors on the distribution and expansion water hyacinth in addition to estimation of water losses from the Lake. This information is important to the lake managers, environmentalists, botanists, fisher folk, decision supporters and other stakeholders for sustainable management of the Lake, and to do any kind of tasks related to their profession or interest on the lake. Moreover, based on the results obtained from the study, the community may put pressure on the government to take tangible and consistent management in Lake Tana. Besides, the study will provide firsthand information for the other researchers who have an interest to conduct further study related to water hyacinth cover change and water hyacinth evapotranspiration in Lake Tana or other water bodies especially from the perspective of climate variability using remote sensing data.

1.5 Scope of the Study

The scope of the study was focus on spatially within the Lake Tana and its Basin. The study was assessed the annual, monthly and seasonal spatio-temporal dynamics of water hyacinth and surface area of the Lake and the impact of climate variability on seasonal spatio-temporal distribution of the weed besides the evapotranspiration of water hyacinth and water losses in the Lake was estimated using Landsat 7, Landsat 8, Sentinel-2, Ground truth points, Google earth and meteorological data. The annual study covering the time frame between 2011 and 2019, excluding 2013 and the monthly and seasonal analyze covering the time periods from 2016 September to 2019 January.

1.6 Organization of the Study

The thesis is organized into five chapters. Followed by this section of the thesis, the second chapter describes the literature review which gives emphasis on concepts of the water hyacinth, the origin, occurrence, distribution of the invasive water hyacinth, its impacts on water bodies, and its relationship with climate variability and other details. The third chapter provides an overall description of data sets and the way how the research was conducted. The fourth chapter deals with the results and discussion. The conclusions and recommendations part of the thesis is presented in chapter five.

CHAPTER TWO

2 LITERATURE REVIEW

2.1 Water Hyacinth

Water hyacinth is a free-floating perennial aquatic plant native to tropical and sub-tropical South America; with bright green, waxy leaves and attractive, violet flowers that has yellow stripes banner petals. The leaves are arranged in a rosette. The leaf stem usually is somewhat to completely swollen and filled with spongy tissue and thus acts as a float (Tewabe, 2015). The weed is recognized as one of the top ten ecologically dangerous and worst invasive weed (Patel, 2012), invading aquatic ecosystems since the weed can quickly dominate waterways due to its rapid leaf production, fragmentation of daughter plants, and copious seed production and germination (Rajapakse et al., 2006). The weed quickly invaded, colonized slow-moving waters resulting in thick and extensive mats, prevents from accessing of water surface if proper management would not been applied (Edwards and Musil, 1975) which degrade aquatic ecosystems and limit their utilization (Hill and Coetzee, 2008).

Water hyacinth a native to the Amazon Basin in South America has emerged as a major weed in more than 50 countries in the tropical and subtropical regions of the world with profuse and permanent impacts (Téllez et al., 2008; Villamagna and Murphy, 2010; Patel, 2012). Water hyacinth was introduced in to different parts of the world as a beautiful garden plant (Shanab et al., 2010). It was originally distributed by human activities from the Amazon Basin in tropical South America to different parts of the world (Dagno et al., 2012) and New Zealand was largely facilitated by human activities. It was first recorded in Africa in Egypt in 1879 and later colonized water bodies, such as the Incomati River in Mozambique in 1946, the Zambezi River and some rivers in Ethiopia in 1956 (Dagno et al., 2012).

2.2 Factors influencing the Distribution and Expansion of Water Hyacinth

Water hyacinth grows quickly, faster than any other saltwater, freshwater, or terrestrial vascular aquatic plant (Teygeler, 2000). Water hyacinth can reproduce both vegetatively and sexually by seeds produced under favorable climatic conditions (Penfound and Earle, 1948), flowering occurs mostly during spring and summer seasons although the weed can grow and reproduce throughout the year (Tiwari et al., 2007). In addition to climate change, human activities and the

unplanned occupation of land in aquatic basins can drive cultural eutrophication, which leads to the degradation of water quality, an increase in the concentrations of nutrients, and alterations to the composition of freshwater biodiversity (Callisto et al., 2013). The major factors which affect the growth of the weed are phosphorus, nitrogen, temperature, pH, salinity, and lake depth (Derseh et al., 2019). The availability of phosphorus has been regarded as one of the most important factors for determining phytoplankton biomass and water quality in lakes and temperate wetlands (Dilon and Rigler, 1974) of tropical and subtropical regions. No single factor can possibly be responsible for the proliferation of water hyacinth in a Lake rather than a multifaceted phenomenon that is a function of rainfall, light, climate, wave action, flooding and wash out of shore/river plants as well as nutrients (Albright et al., 2004).

2.3 Impacts of Water Hyacinth

Water hyacinth has become a major pest in waterways around the world. It is one of the top 10 worst aquatic invasive species in the world (Patel, 2012). Its rampant growth can destroy native habitats, and high rates of transpiration through the weed's leaves during summer can cause up to four times the loss of water from normal water surface evaporation (Dagno et al., 2007).

2.3.1 Reduction of Biodiversity

Today alien invasions species are a major factor for the destruction of biodiversity in the world (Vila et al., 2011). Water hyacinth is challenging the ecological stability of freshwater water bodies (Khanna et al., 2011; Gichuki et al., 2012), out-competing all other species growing in the vicinity, posing a threat to aquatic biodiversity (Patel, 2012). Besides, suppressing the growth of native plants and negatively affecting microbes, water hyacinth prevents the growth and abundance of phytoplankton under large mats, ultimately affecting fisheries (Villamagna and Murphy, 2010; Gichuki et al., 2012).

2.3.2 Blockage of Waterways, Hampering Fisheries, and Hydropower

The dense mats disrupt socioeconomic and subsistence activities (Ship and Boat navigation, restricted access to water for recreation, fisheries, and tourism) if waterways are blocked, water pipes clogged (Ndimele and Jimoh, 2011; Patel, 2012). The weed mats have further invaded fishing grounds and blocked waterways. For fishermen, the hyacinth mats reduce their catch by covering grounds, delaying access to markets because of loss of output, increasing fishing costs because of the time and effort spent in clearing waterways, forcing translocation, and causing

loss of nets (http://projects.infonile.org/a_weed_grown_out_of_control/index.html). water hyacinth causes large impact in different hydropower schemes for instance the Owen Falls hydropower scheme on Lake Victoria is a victim of the weeds rapid reproduction rates and an increasing amount of time and money having to be invested in clearing the weed to prevent it from entering to the turbine and causing damage and power interruptions (Minakawa et al., 2008). Costs of cleaning intake screens at the Owen Falls hydroelectric power plant were calculated to be $1 million United States dollars (USD) per year (Mailu, 2001).

2.3.3 Oxygen Depletion and Reduced Water Quality

Large water hyacinth mats prevent the transfer of oxygen from the air to the water surface or decrease oxygen production by other plants and algae (Villamagna and Murphy, 2010). When the plant dies and sinks to the bottom the decomposing biomass depletes oxygen content in the water body (EEA, 2012). Dissolved oxygen levels can reach dangerously low concentrations for fish. Furthermore, low dissolved oxygen conditions catalyze the release of phosphorus from the sediment which in turn accelerates eutrophication and can lead to a subsequent increase in water hyacinth (Bicudo et al., 2007). Death and decay of water hyacinth vegetation in large masses deteriorate the water quality and the quantity of potable water and increases treatment costs for drinking water (Mironga et al., 2011; Patel, 2012).

2.3.4 Increased Evapotranspiration Rate

The water hyacinth losses water rapidly through its broad leaves, which is about 3.5 times that of a free water surface (Gopal, 1987). Different studies suggest various rate of evapotranspiration of water hyacinth. A water loss through evapotranspiration from water hyacinth was 3.7 times greater than from open water (Timmer and Weldon, 1967). The rate of water loss through evapotranspiration by weed is more than 1.8 times than that of evaporation from open water this leads to high reduction water content on a surface (Ndimele et al., 2011 cited in (Haider, 1989)). On the contrary, areas covered by water hyacinth has lower water loss than open water surface areas of the lake (Agutu et al., 2018).

2.3.5 Affect Human Health

Water hyacinth offers a micro-habitat for a variety of disease vectors such as snails, malaria, schistosomiasis and lymphatic filariasis. The weed provides a natural habitat for organisms that spread diseases such as bilharzia and malaria. It also harbors snakes and it has an itching effect

on human skin. Water hyacinth has been recognized as the most damaging aquatic weed (Mujere, 2015).

2.4 Control Option and Management of Water Hyacinth

Water hyacinth control is absolutely essential; intensified monitoring, mitigation, and management measures are needed to keep water hyacinth at unproblematic levels. If water hyacinth is not checked, it will choke out all water life, bring to a halt any economic activity on water bodies and drastically affect the environment. Control methods include reduction of water nutrients, use of physical barriers (manual and mechanical), biological and chemical control (MNR, 1994). Each method has its own benefits and drawbacks and the goal of most management efforts is to minimize economic costs and ecological change (MNR, 1994). The following is a description of the major control methods and their cost-effectiveness.

2.4.1 Physical Control

The physical method employed the mechanical removal of the weed through machines, destruction Boats, Dredgers, and weed harvesters and manual removal methods using human power (MNR, 1994; Worku and Sahile, 2018). Manual and mechanical techniques of water hyacinth require the support of water and land-based vehicles for transporting the large quantities of water hyacinth which is removed due to the large biomass of the weed which can have a density of up to 200 tons per acre. The manual and mechanical methods are environmentally friendly; expensive especially high cost of machinery; problematic to dispose of the weed; slow and often inefficient; effective only for small areas and difficult to organize and sustain manual laborers (Patel, 2012).

2.4.2 Chemical Control

This involves the application of herbicides such as Paraquat, Amitrole, 2, 4-D, Diquat and Glysophate for the reduction of water hyacinth populations. Chemical control is quick, effective and less expensive than mechanical control but its management demands more skill. The herbicide decomposes rapidly and lasts for about a week (Villamagna and Murphy, 2010). This method has been found effective for smaller areas infestation and less effective of large area coverage. The limitation of this method remains its negative impact on the environment and communities, especially in where the water is used for drinking and washing purpose. Long term use may degrade water quality and put aquatic life at risk with significant socio-economic

impacts if beneficial or designated uses of the water body such as drinking and preparing food are affected (Dagno et al., 2012).

2.4.3 Biological Control

This control method is based on the use of natural enemies of water hyacinth to reduce the population density of a pest. Adult beetles feed on leaves which increase transpiration and places the plant under stress. Several insects and fungi have been identified as biological control enemies for dangerious of water hyacinth. The weed's natural enemies include a variety of weevils, moth and fungi. These natural enemies reduce water hyacinth vigor by decreasing plant size, vegetative reproduction, and flower and seed production. They also facilitate the transfer and ingress of deleterious microorganisms associated with the weevils (both fungi and bacteria) into the plant tissues (Venter et al., 2012). This is environmentally safe; however, it may take time to establish and is labor-intensive. Biological techniques of controlling spread of water hyacinth is the most environmental friendly method for long-term time, being relatively easy to use, and beneficial as it is the only economical and sustainable viable approach (Mujere, 2015).

2.4.4 Integrated Control Approach:

To sustainably supervise and manage the extent of the unfamiliar species; an integrated manage advance is necessary, where substance, mechanical and normal controls are used jointly. Different management method addition to each other and where likely have a preservative effect (Worku and Sahile, 2018).

2.5 The Origin and Distribution of the Invasive Water Hyacinth in Ethiopia

In Ethiopia, this weed was officially reported in the 1950s in Aba Samuel Reservoir, in the outskirts of Addis Ababa, and immediately invaded Koka Reservoir and Awash River (Stroud, 1994). The weed infestation in Ethiopia has been observed on a large scale in many water bodies of the country such as Awash River Basin (Koka Reservoir), Abbay River Basin, Baro-Akobo River Basin and Rift Valley Basins System resulting severity of problems on water resource (Rezene, 2005; Firehun, 2017). Some of the major problems are destroying the fishery industry and agricultural production, clogging canals of hydroelectric power plants, hindrance to water transport and rivers, and creating serious environmental imbalance, causing human health problems, losing of water by increase evapotranspiration, reduction of biodiversity affecting irrigation, navigation and livestock watering (Hailu et al., 2004). To control of the expansion of

water hyacinth in Wonji-Shoa Sugar estate a total of 100,000 USD was incurred from 2000 to 2013 time periods however, there is lack of comprehensive local estimates of economic impacts of the weed in the other affected areas of Ethiopian water bodies have not been done yet (Firehun et al., 2014). Its recent infestation in Lake Tana has created serious social, economic and environmental problems and has become a serious concern by the government, public, and academia. In September 2011, it was officially recognized that one of the top ten ecologically dangerous and worst invasive weed infested Lake Tana. The weed is rapidly expanding and covered 50,000ha of water and land surface with more than 130 km of the shore (Wassie et al., 2014), close to one-third or more than 30% of the shoreline of the north-eastern part of the Lake's shore was invaded by water hyacinth while an intervention made on it (Wassie et al., 2014). The estimate of water hyacinth infestation coverage in 2015 was reduced to 34,500 ha Wassie et al., (2015). However, the results of Wassie et al., 2014 and 2015 complained by the result estimated by the government of office, the spatial coverage of hyacinth is less 5000ha in the growing season (Derseh et al., 2019).

Water hyacinth in Lake Tana causing several problems; destroying the fishery industry and agricultural production, making cattle sick, clogging canals of hydroelectric power plants and creating serious environmental imbalance. Very serious disturbance to Boat transport, and infrastructure such as water supply by obstructive the consumption points, port facilities. The invasion is putting the aquatic biodiversity of Lake Tana at extreme risk. Under heavy infestation, the socio-economic structure, food supply and health of the societies exist around the Lake are extremely worried. In the surrounding areas, great problems on different types of diseased exposed the likes of malaria and bilharzia and snakes, water dirty creation the supply unsuitable for drinking and other domestic use (Erkie, 2017; Worku and Sahile, 2018; http://projects.infonile.org/a_weed_grown_out_of_control/index.html).

To control the spread of water hyacinth in Lake Tana mechanical and manual methods have been applied so far. Since 2014, more than 1,018,227 people were participated in Lake Tana to manually remove the weed for the last six years (Implementation Guideline on Use of Neochetina Weevils for Water Hyacinth Control around Lake Tana, 2018). But, the weed is still flourishing and creates severe problems (Wassie et al., 2014 and 2015). To complement the local community physical removal campaign, Gondar and Bahir Dar Universities, Private Companies

and Global Coalition for the Restoration of Lake Tana have tested harvesters, locally made and purchased from abroad since 2017. However, due to the reason for the efficacy and the high operating costs of the machines; lack of strategically important landing sites, such as ports, road accesses and shallowness of the Lake Tana the harvester machines are utilizing in limited areas. Due to this ANRS Environment, Forest and Wildlife Protection and Development Authority, Bahir Dar University and Global Coalition for Lake Tana Restoration prepared a guideline entitled as "Implementation Guideline on Use of Neochetina Weevils for Water Hyacinth Control around Lake Tana" in 2018 that allows an integrated control method of water hyacinth to be applied in Lake Tana.

2.6 Impact of Climate Variability on Water Hyacinth Dynamics

Climate variability is the way climate fluctuates yearly as above or below of long-term average value. Climate variability refers to shorter-term (daily, seasonal, annual, inter-annual, several years) variations in climate, including fluctuations associated with, for example, teleconnection systems, El Niño (warming) or La Niña (cool) events, which is spatial and season-specific. Seasonal climate forecasts provide an indication of how variable the rainfall might be compared to past years and is therefore considered as information that could help to prepare for and adapt to climate variability (Getachew, 2017).

The growth rate of water hyacinth in many open water bodies is cuased by climate change and variability, high recharge from sewage disposal and nutrients due to anthropogenic activities (Palmer et al., 2015). Climate change has profound effects on the distribution of water hyacinth (Center et al., 2002). Because changes in climate alter the characteristics of water include high nutrient loading from the catchment to the lakes (Sewnet and Kameswara, 2011; Dhir, 2015). Alteration in factors such as temperature, rainfall, sea-level rise affects the vegetation of coastal and wetland ecosystems to a significant extent (Erwin, 2009). An increase in nutrient concentrations, temperature and sediment accumulation (siltation) are supposed to support the growth of emergent macrophytes leading to their increased vegetation cover, hence altering the community structure (Dhir, 2015). The rains and floods swept agricultural runoff and nutrient-rich sediment into the lake. The influx of fertilizer and sediments could have stimulated a new outbreak of the floating vegetation and, in particular, of the water hyacinth (Fusilli et al., 2013). On the other side, water hyacinth tolerates drought well because it can survive in moist

sediments up to several (Mujere, 2015). Warming temperatures due to climate change have created favorable growing conditions for water hyacinth across most of the world (Stephenson et al., 1980). However, a high increase in temperature enhances evaporation which further leads to water loss from the wetland patches and reduces plant productivity (Scavia et al., 2002). Rainfall and temperatures directly influence the ecological functioning within the lake, which in turn affects the health status of the water hyacinth. The current-wind factor influences mobility and geographic positioning from time-to-time on the lake. The changes in wind/current directions and speeds may create backward–forward mobility within the seasons (Ouma et al., 2005).

2.7 Types Image Classification Method Used in Mapping of Water Hyacinth

Estimation of invasive wetland vegetation biomass at species level using multispectral remote sensing is challenging. This is because different plant invasive species have similar spectral reflectance during growing season among different types of wetlands (Ozesmi & Bauer, 2002). A variety of classification algorithms have been developed and used to map the spatial distribution of invasive water hyacinth in the freshwater ecosystem (Thamaga and Dube, 2018). The following are some of the classification algorithms used to map the spatial distribution of water hyacinth.

2.7.1 Unsupervised ISODATA and Maximum Likelihood Classification (MLC)

The Maximum likelihood Classifier is selected as one of the commonly used method giving the much better and visualizes results, which it quantitatively evaluates both the variance and covariance of the category spectral response patterns when classifying an unknown pixel (Lillesand et al., 2008). According to (Xie et al., 2008) MLC is typically stared as a classic and most extensively used supervised classification for satellite images resting on the statistical distribution pattern. Cheruiyot et al., (2014) evaluate the Normalized Difference Vegetation Index (NDVI) slicing and maximum likelihood classifier in terms of delineation of aquatic plants and estimation of its surface extent, the results showed MLC gives an average classification accuracy of 80% is better than NDVI slicing at 75%.

Unsupervised algorithms often attempt to find groups or clusters in data that are spectrally similar. The basic assumption in unsupervised classification is that values with a given cover type should be close together (Omo-Irabor, 2016). The advantages of unsupervised technique are that it is faster, free from human errors and there is no requirement of detailed prior knowledge

(Nath et al., 2014). Ouma et al., (2005) used Unsupervised ISODATA (Iterative Self-Organizing Data Analysis) clustering technique to separate water hyacinth from water surface for mapping and quantifying the area of the weed.

2.7.2 Discriminant Analysis (DA)

Fernandez, (2002) describes discriminant analysis as a multivariate statistical classifier used to model group discrimination based on observed predictor variables of remote sensing in each observation into one of the groups. DA seeks linear combinations that optimally classify each land cover type or hyacinth age group (Sibanda et al., 2015). DA utilized a discriminant function to distinguish land cover types into classes based on a measure of generalized squared distances. Within-group covariance matrices were derived categorizing all the samples into clusters which they had least generalized squared distances to producing classification and cross-validates results. Xu et al, (2005) produced higher results with an overall classification accuracy of 74.45% with a method of DA. Thamaga and Dube, (2018) maps the distribution of water hyacinth with overall classification accuracy of 73% and 63.34% using Sentinel -2 and Landsat 8 imageries respectively by using a discriminant analysis method. However, Dube et al., (2017) found a high overall accuracy result of 95% using a DA classification algorithm in detecting of spatio-temporal of water hyacinth through Landsat 8 imagery.

2.7.3 Support Vector Machines (SVM)

The support vector machine (SVM) approach is one of the successful machine learning algorithms for classifying high dimensional remotely sensed data sets. Training sites are selected to create hyper planes to separate dataset into predefined number of classes represented by training areas (Topaloğlu et al., 2016). The SVM is based on statistical learning theory (Vapnik, 1998) and works on the principle of optimal separation of classes. SVM's adopted the method of structural risk minimization for class member discrimination which minimizes the classification error on unseen data without making prior assumptions on the probability distribution of the data (Mountrakis and Ogole, 2011). Thus, the selected decision boundary (represented by a hyper plane in feature space) will be one that leaves the greatest margin between the two classes, where the margin is defined as the sum of the distances to the hyper plane from the closest cases of the two classes (Vapnik, 1998). For linearly non-separable classes, the restriction that all training data of a given class lie on the same side of the optimal hyper plane can be relaxed by

introducing a slack variable. SVM is important for satellite imageries that have unknown distributions. However, the performance of the SVM algorithm is sensitive to the choice of kernel function and the setting of its associated parameters (Thamaga and Dube, 2018).

2.7.4 Manual Digitizing Image Classification

This method is based on manual on-screen digitizing, evolving extraction of spatial information from satellite images or graphical map by digitizing the required objects or classes on the computer screen via proper software (Sahin et al., 2014). Manual visual classification techniques are better suited for smaller-scale studies and studies that require fine detail classification, especially when analyzing aquatic vegetation habitats which lack distinctive differences in color and texture (Cobbing, 2006).

2.8 The Role of Remote Sensing for Analyzing Spatio-Temporal Detection of Water Hyacinth

Remote sensing and geographic information systems (GIS) have risen as important tools in the management and inventory of aquatic macrophytes (Krishnaveni, 2010). Many satellite-borne sensors over the past 30 years have been employed to gather information on invasive water hyacinth and study the biological activity of the weed occurring within water bodies (Cavalli et al., 2009). Research literature work done in mapping the spatial distribution of water hyacinth in lakes and dams published in remote sensing journals has shown an increase (Thamaga and Dube, 2018). This is links to remote sensing ability to provide several new advantages that can quickly and synoptically monitor and manage large areas. Current and historical remote sensing data have been used to assess the status and level of degradation and has helped to select the best restoration scenario for many wetland ecosystems (Alexandridis et al., 2007). Remote sensing technologies have many potential applications for assessing the spatio-temoral spread of aquatic invasive vegetation in a timely and cost-effective approach (Shekede et al., 2008; Dube et al., 2014). Besides, as Penatti et al., (2015) satellite sensors capable of recording continual coverage the portion of the earth surface provides spatial data for both short and long-term monitoring, which is crucial for evaluating the intervention made on the control and management of water hyacinth in the lakes. Remote sensing imagery having high spectral and spatial characteristics helps to enhance monitoring of the spread and spatial locational distribution of invasive water hyacinth (Thamaga and Dube, 2018). The availability of automated, reliable and real-time

remote sensing data helps to monitor the spread of aquatic weeds, over water bodies. Hence, the use of satellite imagery has proved to be a reliable primary data source and has become frequently used in aquatic ecosystem research (Aplin, 2005), crucial in mapping and detecting of LULC (water hyacinth with its' surrounding wetland species) due to the satellite sensors could provide high-quality data (DeFries et al., 2004).

Landsat 8 OLI sensor is very useful to water related studies, due to the sensor's possesses improved spectral, spatial, temporal and radiometric characteristics (Dube et al., 2017b) that can discriminate or separate water hyacinth from other co-existing species in lakes, helps for mapping the evolution of spatial and temporal distribution, and quantifying extent of water hyacinth at a low or no cost over time and space (Dube et al., 2017a). Since water hyacinth is an evergreen species, detecting their coverage will not be restricted by seasonal variation but largely determined by the sensor's spatial and vegetation characteristics. Sentinel-2 data is capability mapping the spatial areal coverage of water hyacinth, especially in lakes where it was previously a challenging task with broadband multispectral sensors (Thamaga and Dube, 2018).

Therefore, Remote sensing technology has many attributes that would be beneficial for us to detect, map and monitor invasion species. Spatial heterogeneity complicates the study of seasonal and long-term trends of biological invasion. The multi-date nature of satellite imagery permits monitoring dynamic features of the landscape and thus provides a means to detect major land cover changes and quantify the rates of change (Joshi et al., 2004).

CHAPTER THREE

3 MATERIALS AND METHODS

3.1 Description of Lake Tana Basin

3.1.1 Location and Extent of the Study Area

Lake Tana Basin is located in the northwestern plateau of Ethiopia. Geographically, it extends from 10.9^{o} N to 12.8^{o} N latitude and 36.7^{o} E to 38.2^{o} E longitude. The Basin area of the Lake is approximately 15,123 square kilometers, of which 3046 is the Lake area. Lake Tana is a shallow lake with a maximum depth of 14 meter and average depth of 8 meter. The volume of the Lake is 28.4 km^{3}, and has maximum length of 90 km and width of 65 km (Goraw and Shimelis, 2017). The Basin is located in an area where water resources issues are critical for sustainable development, locally and regionally. It constitutes the upper catchment of the Blue Nile River (Abay River) which has about 60% contribution to the main Nile River flow (Agizew, 2010).

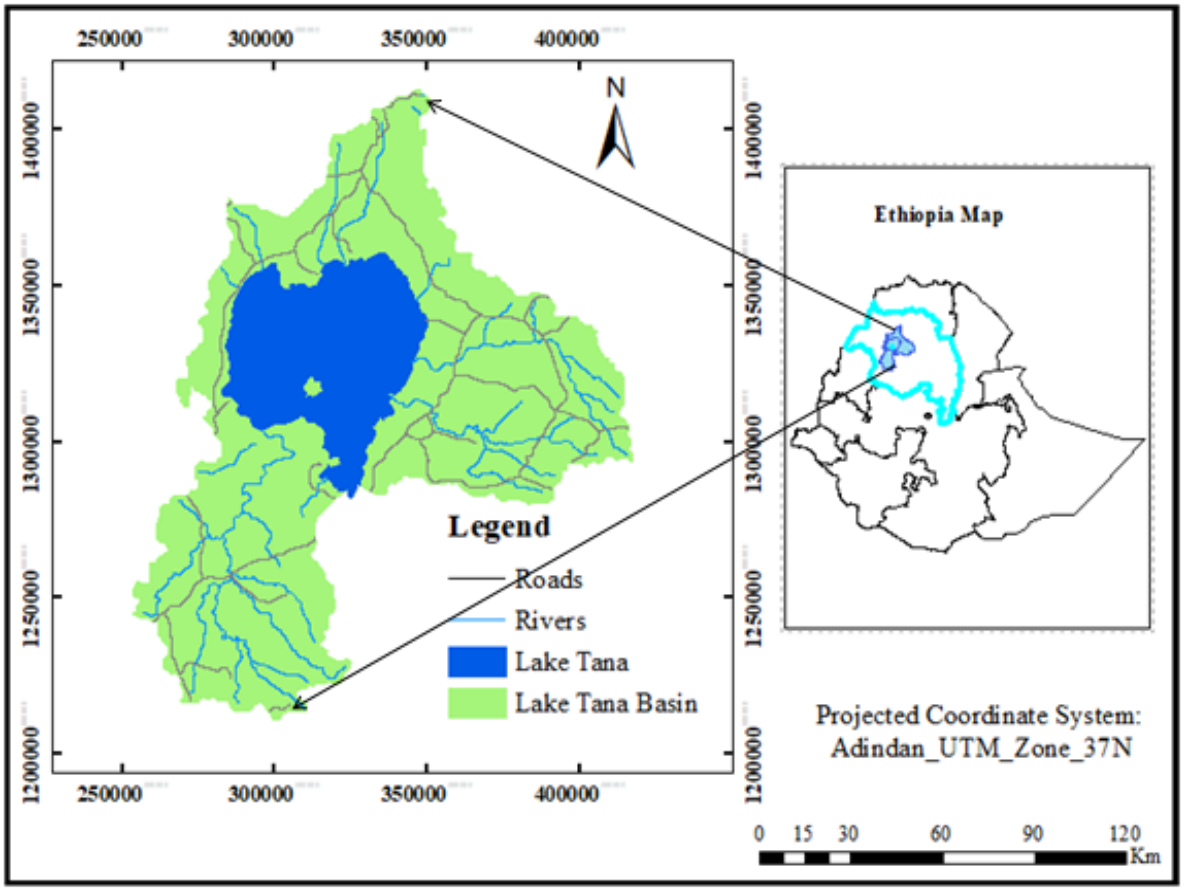

Figure 3.1 Locational map of the Lake Tana Basin

3.1.2 Topography and Slope of Lake Tana Basin

The total catchment area of Lake Tana Basin in excess of 15 000 Km^2 constitutes of several streams and catchments that all drain into Lake. The Basin close to the Lake is lowlands and away from the Lake is mountainous area. The mean altitude of the Basin is 2035 meter above mean sea level with a large portion elevation fall in the range 1686 - 2500 meter. Some areas close to the watershed divide have an altitude of 2500-4113 meter. Mountain Choke and Guna make a solid boundary in the south and east of the Basin. The Chilga Mountain Ridge and Gondar Graben form the boundary in the north. The Gilgel Abay rises in elevated terrain that occurs off the flanks of Mt Choke and flows across largely basaltic terrain into the Lake Tana. The slopes of the Basin are generally converged into Lake Tana (Getachew, 2010). Based on topographic classification indicated in REDECO and HSD (2002), the Basin can be grouped into five relief types (Agizew, 2010). These are flat areas with slopes between 0-2%, undulating terrain with slopes between 2-10%, rolling land with 10-15% slope, hilly areas having slopes of 15-30% and steeply dissected and mountainous lands of slope > 30% .

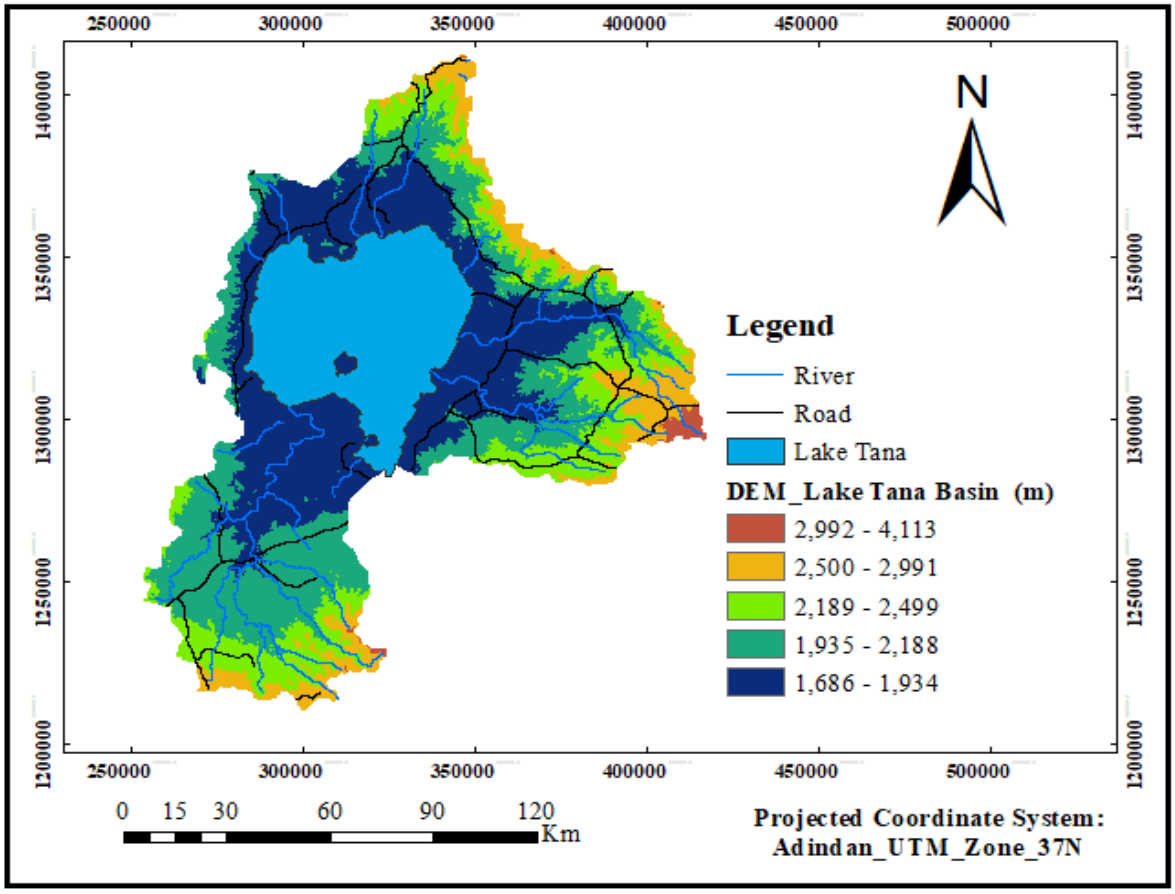

Figure 3.2 Topographic map of Lake Tana Basin

3.1.3 Land Use and Land Cover of Lake Tana Basin

The Lake Tana Basin consists of 347 Kebeles (the lowest administrative units) and 21 Woredas (districts) in four administrative zones (Wassie et al., 2014). A significant part of the Basin is designated for crop production using rain-fed agriculture making it vulnerable to drought and flooding. The dominantly crop types practiced in the Basin are Barley, Maize and Teff. Because of the growing population pressure, cultivation is also practiced on marginal lands with a resulting increase in upstream soil erosion and sedimentation in downstream areas (Getachew, 2010). The low-lying parts of the Basin bordering Lake Tana are extensive floodplains which is highly suitable for farming practices. The coastal land found all bordering of Lake Tana is valuable for agricultural purposes. Two major urban centers of the country, Bahir Dar and Gondar City, with more than 200, 000 inhabitants are also found in the Basin (Agizew, 2010). Most of the Lake Tana Sub Basin is characterized by cropland with scarce woodlands while only a few limited areas of highlands are forested (less than 1% of the Basin). The major land cover types are cropland (45%), woody land (18%), water body (20%), grassland (13%), bare land (2%), and urban/built (0.2 %). Other land cover types include open shrub lands and plantation, mainly eucalyptus (Getachew, 2010).

3.1.4 Climate of Lake Tana Basin

Lake Tana Basin is located in a region where the annual rainfalls are more than 900 mm with a unimodal pattern. According to the traditional climate classification of Ethiopia, most of the study area falls in Woina-Dega zone (1500-2300m altitude) with a mean annual temperature of 16-20°C, temperature decreases with altitude at an average lapse rate of 5 °C in 1000m (Agizew, 2010).

The rainfall climate is highly seasonal with more than 78% of the rainfall occurring in the Kiremt season (June-September) whereas low rainfall was received in December, January, February and March months. Based on rainfall data of the stations located within and around the Basin, the mean annual rainfall of Lake Tana Basin from 2011 to 2018 was estimated to be 1331mm. The maximum mean monthly temperature occurred in Belg (April) which was 29.4 ℃ (followed by 29.3℃ March) whereas the minimum mean monthly temperature was recorded during Bega season (October - January), mainly in December and January which was 10 ℃ and 10.1℃ respectively with mean annual temperature of 19.5 °C.

The mean monthly wind speed varied from 0.8 m/s at Bahir Dar to 2.08 m/s at Aykel station. The wind speed increase from south to north (Agizew, 2010). A slight seasonal variation in wind speed is shown in kiremt season, and monthly wind speed showed an increasing pattern starting from October/November (0.81/0.82m/s) and attaining its peak in April/May (1.25/1.23m/s) when the monsoon climate approaches the Basin. A general south-north and west-east increase in wind energy distribution for Ethiopia characterized the wind speeds as stronger and weaker, respectively, during dry and wet seasons in the highland regions of Ethiopia (Mulugeta and Drake, 1996).

The average sunshine hour length extended from 4.4 hours in Kiremt season to 9.2 hours in Belg season. The sunshine hour length during the wet season appeared to be in accordance with the diurnal rainfall pattern where the formation of clouds and rainfall generally occurs in the afternoon and evening hours. The temporal variability of the sunshine hour is relatively high with a standard deviation of about 1.7 hours. The relative humidity of the Basin during the time period of 2011 -2018 was varied from 39.9% in April month to 81.3% in August.

3.1.5 Hydrology and Hydrogeology of Lake Tana

Lake Tana Basin comprises different catchments that all discharge into the Lake. About forty percent of the Basin, mainly located in the western and lower parts of the various catchments, is yet ungauged. More than ninety percent of the runoff is contributed by four major rivers: Megech, Rib, Gumara and Gilgel Abay (Kebede et al., 2006). In the downstream reaches of the major river systems are Megech, Gumara, Rib, Gigel Abay, Koga, Memera, Garno and Dirma. Gumara is one of the main rivers on the east side discharging to the Lake Tana. It source's is Guna Mountain, and drops its load in the low land to the mouth of Lake Tana. Megech River drains Northern highlands and flows toward Lake Tana. The River changed its course in kola Diba village and deposited large sediment in the flat land. Ribb River drains from highlands of Debre Tabor and flows across the flat land from Woreta to Lake Tana. There are extensive flood plains in the downstream ends of Ribb and Gumara River, which prone to long term flooding. Analysis of the stream flow data from the gauged catchments indicated that runoff is highly seasonal with more than 75 percent of the annual volume concentrated in the Kiremt season. Flooding of low-lying areas due to an overflow of the major rivers and the rising lake level is a frequent problem in the wet season (Agizew, 2010). Lake Tana discharges into the Abay River

with a long-term mean annual runoff volume of 3.7 square kilometers, which is about 8% of the Blue Nile flow at Rosaires Dam in Sudan (Conway, 2000). The formation of Lake Tana is believed to be associated with a volcanic activity that created a barrier to the south during the Pleiocene (Mohr, 1962). In the study area, shallow groundwater flow systems controlled by local topography are important. The existence of Lake Tana graven also favour regional and probably deeper groundwater flows. Based on recorded piezometric levels, the groundwater flow direction is found to be consistent with the surface water drainage (Agizew, 2010).

3.2 Data Source

3.2.1 Remote Sensing Data

To detect and map the annual, monthly and seasonal spatio-temporal distribution pattern of water hyacinth and surface area of the Lake, the study has been utilized Landsat 7 ETM+ and Landsat 8 OLI from United States Geological Survey (USGS) website (http://glovis.usgs.gov/web-link), and Sentinel-2 MSI remotely satellite images from Sentinel Hub (https://scihub.copernicus.eu/). For the annual spatio-temporal trend of water hyacinth and area of Lake Tana all the images covering the time frame between 2011 and 2019 (excluding 2013 year due to WH was unable to identified in satellite images) were acquired during the dry season (January month) since the good availability of cloud free images: Landsat 7 was acquired on18/01/2011 and 23/01/2012; Landsat 8 was acquired on 16/01/2014 and 19/01/2015 and Sentinel-2 image was acquired on 18/01/2016, 22/01/2017, 17/01/2018 and 22/01/2019. On the other hand, for analyzing the monthly and seasonal spatio-temporal dynamics of water hyacinth and surface area of the Lake and identifying the impact of climate variability on the spread of the weed a number of Landsat 8 and Sentinel 2 images were used for the time periods from 2016 Sep to 2019 Jan because of the water hyacinth at monthly level once again has not been visible for all months before 2016 Sep. The most of the monthly images were acquired between 20 -30/31 days of the month. The study area is covered by two separate Landsat 7 Scenes with path/row of 170/51 and170/52, one Landsat 8 Scene with path/row of 170/52 and three Sentinel-2 Tiles. Due to this, a total of 83 images were downloaded and of these 41 images (such as four (4) Landsat 7 images for 2011 and 2012; two (2) Landsat 8 images for 2014 and 2015; seventeen (17) Landsat 8 and sixty (60) Sentinel-2 images for 17 and 20 months respectively from 2016 Sep to 2019 Jan time period) have been classified for the final LULC map of water hyacinth and water surface of the Lake.

3.2.1.1 Landsat 7 Enhanced Thematic Mapper Plus (ETM+) Image

Landsat Enhanced Thematic Mapper Plus Sensor (ETM+) was carried on Landsat 7 since July 1999 with a 16 days revisit period of the ETM+ sensor. Landsat 7 ETM+ images consist of eight spectral bands with a spatial resolution of 30 m, Bands 1-5 and 7 which are Multi-spectral (MS) images. While Band 8 is panchromatic with 15 m resolution and Band 6 is thermal with a resolution of 60m. Landsat 7 ETM+ data is capable of mapping and monitoring of water hyacinth (Shekede et al., 2008; Dube et al., 2017a). All ETM+ sensor bands can collect one of two gain settings (high or low) for increased radiometric sensitivity and dynamic range whereas ETM+ Band 6 collects both high and low gain for all scenes (ERDAS Imagine, 2005).

3.2.1.2 Landsat 8 Operational Land Imager (OLI) Image

Landsat Operational Land Imager (OLI) and Thermal Infrared Sensor (TIRS), Landsat 8 was launched on February 11, 2013, could be downloaded from the United States Geological Survey website (http://earthexplorer.usgs.gov) which is free of charge. It has 11 bands; Band 1 to 7, 9 are MS, and Band 8 is panchromatic while Band 10 and 11 are thermals. The spatial resolution of Landsat 8 is 15m, 30m and 100m for MS, PAN, and TIRS respectively. Ultra-blue Band 1 is useful for coastal and aerosols studies while Band 9 is useful for cirrus cloud detection. The approximate scene size of Landsat 8 images is 170 km north-south by 183 km east-west (USGS, 2013; Abel, 2018). Landsat 8 OLI sensor, an improved spectral, spatial, temporal and radiometric characteristics is very important to water related studies, can discriminate or separate water hyacinth from the co-existing species in lakes (Dube et al., 2017a).

3.2.1.3 Sentinal-2 Images

Sentinel-2 mission, launched on 23/06/2015, is a land monitoring constellation of two satellites (Sentinel- 2A and Sentinel- 2B) equipped with Multispectral Instruments (MSI) capable of acquiring 13 bands information at different spatial resolutions (10m, 20m and 60m) without thermal infrared bands ensuring a better data continuity than other relevant satellites, such as SPOT and Landsat satellite series, due to its high spatial resolution and short revisit time. Sentinel-2 MSI which is an improved spectral and spatial resolution sensor has the capability to detect and map the spatial configuration of water hyacinth (Thamaga and Dube, 2018). Bands 2, 3, 4 and 8 of 10m resolution meet the basic requirements for land use land cover classification; six bands at 20m resolution provide additional information on vegetation detecting. The

remaining three bands at 60m used in atmospheric and geophysical parameters studies. Sentinel-2A provides more details in the NIR and SWIR band range, which is helpful for agriculture, forest monitoring, and natural disaster management applications (Zhang et al., 2017). The temporal resolution of Sentinel-2 is 10 days with one satellite and will be 5 days with 2 satellites that will create a huge amount of Earth observation data for several research and application projects (Marangoz et al., 2017). Sentinel -2B launched in March 2017 helps to shorten the Sentinel satellite revisit periods (Zhang et al., 2017). Sentinel images series are capable of downloading freely from Sentinel Hub, which was owned by ESA (https://scihub.copernicus.eu/). Besides, freely available satellite information analysis software Sentinel Application Platform (SNAP) is also provided, which in comparison with ENVI, QGIS and ERDAS Imagine, is specially customized for Sentinel series.

Table 3.1 Sentinel -2 data descriptions

Sentinel-2 Bands	Wavelength (nanometer)	Resolution (meter)
Band 1- Coastal aerosol	443	60
Band 2 –Blue	490	10
Band 3- Green	560	10
Band 4-Red	665	10
Band 5 –RE 1	705	20
Band 6-RE 2	740	20
Band 7-RE 3	783	20
Band 8–NIR	842	10
Band 8a-NIR narrow	865	20
Band 9-Water vapor	945	60
Band 10-SWIR(Cirrus)	1380	60
Band 11-SWIR 1	1610	20
Band 12-SWIR 2	2190	20

NIR: Near-infrared; SWIR: shorter wave infrared and RE: red edge.

3.2.2 Meteorological Data

The daily and monthly climate data such as precipitation, temperature, wind speed, relative humidity and sunshine hours were acquired from Ethiopian National Meteorological Agency for the years 2010 to 2018, the rainfall and temperature data were collected from 19 and 17 meteorological stations respectively and wind speed, relative humidity and sunshine hour's data obtained from 4 class one stations. Rainfall, temperature and wind speed data were utilized to study the correlation between climate elements and area change of water hyacinth. Temperature,

wind speed, relative humidity and sunshine hour's data were used to estimate reference evapotranspiration in turn helps to compute evapotranspiration of water hyacinth and water losses in Lake Tana.

3.2.3 Ground Truth Points and Google Earth Data

Ground truth data have provided reliable data to guide the analytical process, such as creating samples to support supervised classification; to verify, evaluate and assess the results of remote sensing investigations and provide information to model the spectral behavior of specific landscape features (Lillesand et al., 2008). In this study, field data collection had been conducted from May 07 to 09, 2019 to record the location of water hyacinth and other land cover classes using Handheld Global Position System (GPS Garmin 64) in three infested woredas such as Libo Kemkem (Agid Qirgna Kebele), Gondar Zuria (Shagomengie Kebele) and Denbiya (Gorgora Kebele) and a check has also been done in southern shore of the Lake using a Boat at Debre Mariam Island around Bahir Dar City which was free of water hyacinth infestation. A total of 51 Ground GPS points, and more than 179 reference points from the Google Earth were randomly identified. These data were used for assessing the accuracy of the final classified map, creating training samples and image interpretation during image classification process. High-resolution Google Earth Imagine was used as a complementary reference to distinguish confusing water hyacinth class from other aquatic vegetation. In addition, photographs and other essential information were generated which helps to identify and quantify of the area of water hyacinth and map-making. During the field work, physical removal of water hyacinth through machine harvesters and human labors has been observed in northern and eastern shore of Lake Tana. The surrounding communities were working with payments in all infested kebeles which bordering the Lake. Two active harvesting machines, imported from aboard have participated in the removal of the invasive hyacinth in Shagomengie Kebele which depth is enough for machine operation and one idle machine made by Bahir Dar University and his partner was also available in the place.

3.3 Software Used for the Study

ArcGIS 10.5, Earth Resources Data Analysis System (ERDAS) Imagine 2015, Statistical Software such as Microsoft Excel (MS-excel) and XLSTAT, Sentinel Application Platform (SNAP) and Google Earth Pro 2019 software were used to accomplish this study.

Software	Applications
ERDAS IMAGINE 2015	To process Landsat 7 and 8 images (layer stacks, radiometric correction, mosaic, subset, classification, accuracy assessment, change detection analysis and other processes).
ARCGIS 10.5	To prepare map layout, spatial data interpolation, manual digitizing, area calculation and post image classification.
GOOGLE EARTH PRO 2019	Used as a base map in visual image interpretation, and to generate coordinate points for all images.
SNAP	For processing of Sentinel -2 images (layer stack, mosaic and subset, radiometric correction, resampling, and classification).
XLSTAT 2019/ MS EXCEL	To develop correlation statistics, trend and draw different graphs.
CROPWAT 8.0	To compute reference evapotranspiration of water hyacinth.

3.4 Methods of Data Analysis

The overall methodological flow chart of the study is presented below.

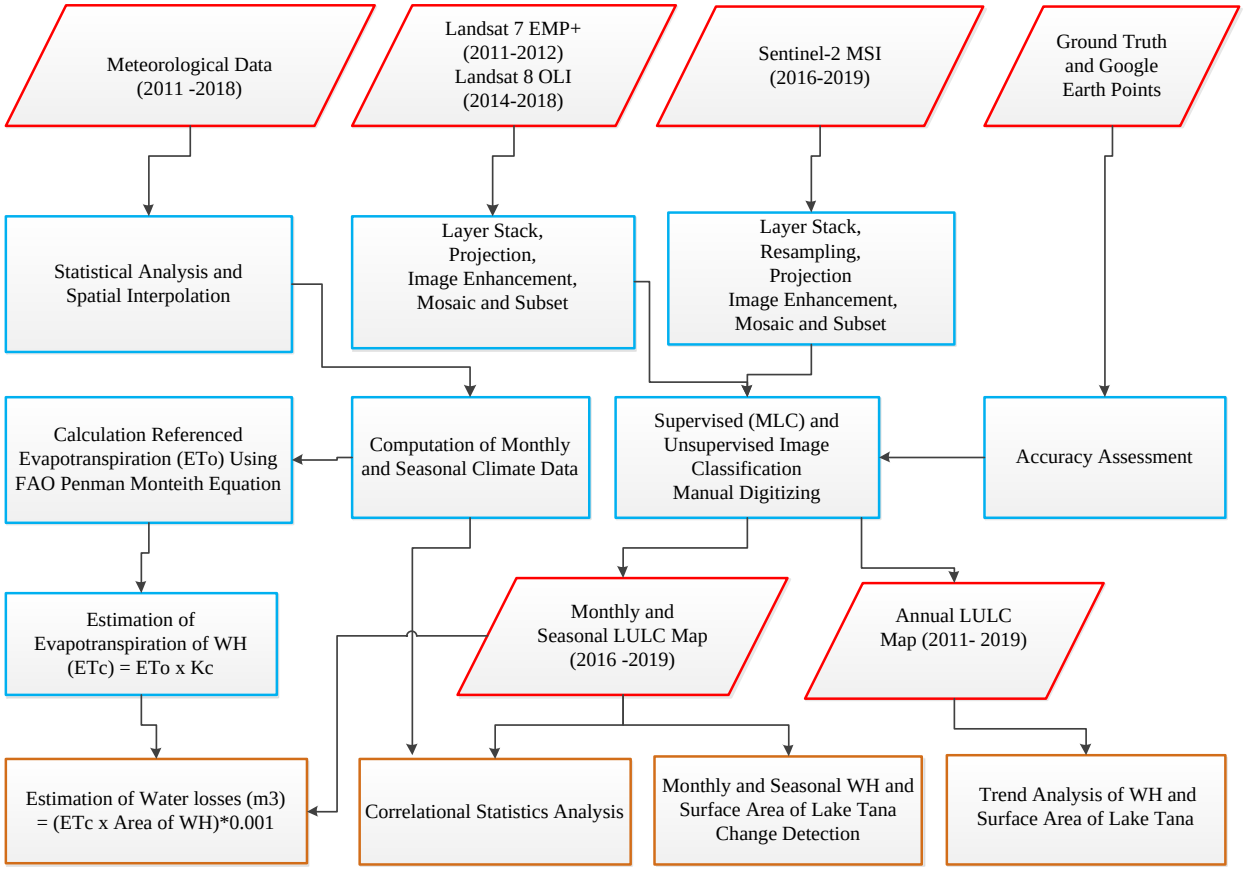

Figure 3.3: Methodological flow chart of the research process.

3.4.1 Digital Image Preprocessing

Satellite imagery is affected by various factors, which decrease the image quality. Image preprocessing is necessary before the information is extracted from the image because it ensures that the image is as close as to the true radiant energy and spatial characteristics at the time of data collection (Mohammed, 2016). Digital image processing involves manipulation and interpretation of digital images through the help of computer application software. It is helpful to increase the quality of an image and maintain the quality of the image for the purpose of interpretation and classification; it is possible to minimize interpretation errors since the image can easily be manageable in a computer (Abel, 2018). Therefore, preprocessing consists of series of sequential operations, including atmospheric correction or normalization, image registration, and geometric correction. Pre-processing functions involve those operations that are normally required prior to the main data analysis and extraction of information.

3.4.1.1 Layer Stacking, Resampling, and Re-projection of the Images

Layer stacking is a method to build a new multiband file from geo-referenced images of various pixel sizes, extents, and projections (Sisay et al., 2016). The original Landsat 8 OLI and Landsat 7 ETM+ satellite imagery have eleven and seven bands respectively. Those bands are existed separately from each other and have their own information about the earth's features. To have good spectral information about the earth's surface, each band should be stacked together and produce a single multispectral image. For Landsat 7 ETM+ except Band 6 all bands were stacked together whereas Landsat 8 Band 2-7 were layer stacked (Topaloglu et al., 2016; Worku, 2018) Due to Band 6 and 10, 11 are thermal bands for Landsat 7 and 8 respectively. Band 1 and 9 of Landsat 8 data are used for aerosol and cirrus cloud detection respectively not important for this application. For Sentinel-2 data, among the 13 multispectral bands; Band 2 - 8, Band 8a, Band 11 and 12 which having 10m and 20m spectral resolution were stacked together (Shoko and Mutanga, 2017; Thamaga and Dube, 2018). Afterward, 10m and 20m spectral resolution bands of Sentinel-2 image were resampled to 10m using nearest neighbour resampling method to make all the bands to have a similar resolution and pixel number (Marangoz et al., 2017). Band 1, 9 and 10 were excluded due to the bands are relevance for the detection of atmospheric features, such as aerosol and water vapor (Thamaga and Dube, 2018). Landsat 7, 8 and Sentinel-2 data are acquired in Universal Transform Mercator (UTM) Coordinate System and World Geodetic System (WGS -84) to make them compatible with local datum system, the projection transformation were carried out and assigned to the Adindan _UTM_ Zone_37N coordinate system projection for all the three data sets.

3.4.2 Image Enhancement

Image enhancement is used to make the image to have better visual interpretation and understanding. The advantage of digital imagery is that it allows us to manipulate the digital pixel values in an image (Lillesand et al., 2008). Although radiometric corrections for illumination, atmospheric influences, and sensor characteristics may be done prior to distribution of data to the user, the image may still not be optimized for visual interpretation (Fundament of remote sensing: A Canada Centre for remote sensing tutorial, nd). The image should be improved to increase the quality of visual perception of human beings to make it more appropriate and clearly visible for the required application. Wide ranges of enhancement techniques are available depending on the user’s purpose, which is ranging from simple contrast

stretching. Therefore, histogram matching and equalization, brightness inversion, haze and noise reduction were applied for increasing the visual distinctions between features in a scene doing different procedures to manipulate the contrast and spatial features of an image in this study. In addition, the scan line errors in the Landsat 7 images were removed by Focal Analysis tool in the Spatial Enhancement extension of ERDAS Imagine.

3.5 Mapping and Detecting of the Spatio-Temporal Distribution of Water Hyacinth

Estimation of invasive wetland vegetation biomass at species level using multispectral remote sensing is challenging. This is because different plant invasive species have similar spectral reflectance during growing season among different types of wetlands (Ozesmi & Bauer, 2002). However, there are several different remote sensing image classification techniques that can be used to analyses imagery and are based on a set of user-defined parameters; these are Manual Visual Classification (Digitizing) and Automated (Unsupervised Classification and Supervised Classification) Methods (Ozesmi and Bauer, 2002). Depending on the chosen classification technique, different results could be obtained from the same image and thus the skill of the "classifier" is paramount to the outcome (Fordham, 2012). The primary advantage of using an automated remote sensing technique is that once the system is correctly configured, the user can repeat the technique on several images, in relatively quick succession and use hard or soft classifiers to achieve the most accurate representation (Cobbing, 2006). The automated techniques can be quicker, and each replicate has the same degree of error, resulting in consistent results, allowing for less bias, but then may not be as accurate as visual classification techniques. Manual visual classification techniques are better suited for smaller-scale studies and studies that require fine detail classification, especially when analyzing aquatic vegetation habitats which lack distinctive differences in color and texture (Cobbing, 2006). To study the annual and seasonal spatio-temporal distribution of water hyacinth supervised image classification and manual digitizing techniques have been applied for this study. Manual digitizing employed because of satellite images in summer seasons were covered with heavy clouds and in a situation of the biomass of water hyacinth were not scattered. From the supervised image classification type maximum likelihood classification (MLC) algorithm was used since it quantitatively evaluates both the variance and covariance of the category spectral response patterns when classifying an unknown pixels (Landgrebe, 2003). MLC was employed when water hyacinth is found to be scattered over the Lake, difficult to applied manual digitizing method.

3.6 Spatio-Temporal Monitoring of Water Surface Area of Lake Tana

Surface water bodies are dynamic in nature because they shrink or expand with time, owing to a number of natural and human-induced factors. Variations in water bodies have significant impacts on other natural resources and human assets and further influence the environment (Karpatne et al., 2016). Spatio-temporal monitoring of water body dynamics is thus essential for understanding global or regional water availability, providing descriptive insights about the natural processes that shape the storage of water resources besides understanding the impact of water hyacinth on it.

The principle of extracting surface water from optical images is the obviously lower reflectance of water, compared to that of other land cover types, in infrared channels (Huang et al., 2018). Based on this, many methods have been developed for extracting water areas from optical remote sensing imagery. A simple method is to density slice a single infrared band to derive a water map (Frazier and Page, 2000). Either supervised or unsupervised classification methods (Ozesmi and Bauer, 2002) were used to generate land cover maps, from which water maps could be extracted. Decision trees were also built using multispectral bands to delineate water coverage from others (Acharya et al., 2016; Olthof, 2017). However, the problem with this kind of method is that their classification rules are difficult to build and sometimes not robust enough to be universally applicable (Huang et al., 2018). Normalized difference water index (NDWI) (McFeeters, 1996), and modified NDWI (MNDWI) (Xu, 2006) are among many water indices that are calculated from two or more bands, an easy and effective way to identify the differences between water and non-water area.

3.6.1 Normalized Difference Water Index (NDWI) and Modified NDWI (MNDWI)

McFeeters's, (1996) NDWI can be regarded as the first generation of water index which is developed to maximize the reflectance of a water body by using green wavelength, minimize the low reflectance in Near-IR, mathematically computed as follows:

$$\text{NDWI} = \frac{\text{Green}-\text{NIR}}{\text{Green}+\text{NIR}} \quad \text{(1)}$$

Where, NIR=Band 5 in Landsat 8 image and NIR = Band 8 in Sentinel-2. NDWI values greater than zero are assumed to represent water surfaces, while NDWI values less than, or equal to zero are non-water surfaces (McFeeters, 1996). However, this is not true in water regions with a built-up land background. The extracted water information in those regions often mixed with built-up

land noise. Thus, Xu (2006) found that the Short-wave Infrared (SWIR) band which able to reflect some subtle characteristics of water, and so replaced the NIR band in NDWI with the Short Wave Infrared band and proposed the Modified Normalized Difference Water Index (MNDWI). It is now widely accepted that MNDWI is more stable and reliable than NDWI because the SWIR band is less sensitive in built up surface within the water body than the NIR band.

$$\text{MNDWI} = \frac{\text{Green} - \text{SWIR}}{\text{Green} + \text{SWIR}} \quad \text{(2)}$$

Where, SWIR= Band 6 in Landsat 8 image and SWIR = Band 11 in Sentinel-2, the Green Band has the spatial resolution of 10m, while the SWIR Band (Band 11) has the spatial resolution of 20m. Thus, MNDWI needs to be calculated at a spatial resolution of either 10m or 20m. Top of atmosphere (TOA) reflectance of Band 11 at 10m resolution was produced by downscaling the original 20m Band 11 to 10m resolution using the resampling technique. Then, the values of MNDWI were calculated from each image using the Raster Calculator Tool in the Spatial Analyst extension in ArcGIS to extract water information.

Thresholding is one of the most critical issues in using water indices to extract water bodies. Base on the reflectance characteristics of water, NDWI and MNDWI values for water are usually greater than 0. A threshold of 0 is often applied to extract water from index images (Xu, 2006). However, it has been suggested that adjustment of the threshold value could usually achieve better extraction results (Ji al., 2009). This is especially tricky when thresholding either a time series of images that cover the same water body or a single image that covers a group of water bodies because automation would be impossible if manual adjustments on the threshold value for each image were required. Many studies have been devoted to working on this issue (Huang et al., 2018). Therefore, the ISODATA algorithm, unsupervised classification followed by the reclassification method using Reclassify Tools from Spatial Analysis Tools extension was performed to extract seasonal dynamics of surface area of Lake Tana in the case of cloud-free images from 2016 to 2019 time period (https://www.youtube.com/watch?v=520VZV9LoNk). Then after, the digitized area of water hyacinth and the extracted water body using unsupervised classification method was overlaid to model spatio-temporal change of the two classes.

3.7 Accuracy Assessment

One of the most important final steps in the classification process is accuracy assessment. The aim of accuracy assessment is to quantitatively assess how effectively the pixels are sampled into the correct land cover classes (Sophia et al., 2017). Accuracy assessment was carried out using Ground truth points that were collected with Handheld GPS and Google Earth generated points to assess the accuracy (Amare, 2015; Abel, 2018). The classification accuracy was assessed by calculating the Kappa coefficient 'k' and overall accuracy. The kappa statistics is an estimate of the measure of overall agreement between image data and the reference data. Its coefficient falls typically on a scale between 0 and 1, where the latter indicates complete agreement and is often multiplied by 100 to give a percentage measure of classification accuracy (Worku, 2018).

$$K = \frac{N\sum_{i=1}^{r} xii - \sum_{i=1}^{r}(xi+ * x+i)}{N^2 - \sum_{i=1}^{r}(xi+ * x+i)} \quad \ldots\ldots\ldots\ldots\ldots\ldots\ldots\ldots \text{(3)}$$

Where k is kappa statistics, n is total samples, xii is the number in row i and column i, xi+ is row total. X+i is column total. As Yetnayet et al., (2017) kappa values are characterized into 3 groupings: a value greater than 0.80 (80%) represents strong agreement, a value between 0.40 and 0.80 (40 to 80%) represents moderate agreement, and a value below 0.40 (40%) represents the poor agreement. The overall accuracy of the classified image compares how each of the pixels is classified versus the actual land cover conditions obtained from their corresponding Ground truth data (Congalton, 1991).

$$\text{Overall accuracy}(OA(\%)) = \frac{\text{the sum of a correctly classified pixel (SCC)}}{\text{Total sample (TS)}} * 100 \quad \ldots\ldots\ldots \text{(4)}$$

Producer's Accuracy (Omission Error)

The total number of correct pixels in a category is divided by the total number of pixels of that category as derived from the reference data (i.e., the column total). This statistic indicates the probability of a reference pixel being correctly classified and is a measure of omission error, or error of exclusion. Omission error is obtained by deducting the Producer's Accuracy in percentage from 100 (https://web.uri.edu/ltrs/files/415AccuracyAssessment2018.pdf).

User's Accuracy (Commission Error)

If the total number of correct pixels in a category is divided by the total number of pixels that were actually classified in that category, the result is a measure of commission error, or error of

inclusion. Commission error computed as 100- User's Accuracy (%) (https://web.uri.edu/ltrs/files/415AccuracyAssessment2018.pdf).

3.8 Spatio-Temporal Change Detection Analysis of water hyacinth and Surface Area of Lake Tana

Change detection is the process of identifying differences in the state of an object or phenomenon by observing it at different times. Essentially, it involves the ability to quantify temporal effects using multitemporal data sets (Lu et al., 2004). Many change detection methods have been developed and used for various applications. For example, there are post-classification comparison, image differencing, image rationing, image regression, principal component analysis. However, they can be broadly divided into post-classification and spectral change detection approaches (Chen, 2000).

3.9 Post Classification Approach

The post classification method was deployed in the study to quantify the change area of water hyacinth and surface area of Lake Tana because this method is among the most widely applied techniques for change detection purposes (Mohammed, 2016). Numerous studies have been carried out using post-classification approach. In post-classification change detection approach two images from different dates are classified and labeled. The area of change is then extracted through the direct comparison of the classification results (Lunetta and Elvidge, 1999). A post-classification change detection method was computed using two independent images (thematic maps). Difference or change information was generated by comparing image area values of one data set with those of the corresponding layer of the second data set. The estimation for the rate of change for the different covers/uses was computed based on the following formula.

$$\%\ \text{Cover change} = \frac{Area\ i\ year\ x+1 - Area\ i\ year\ x}{\sum_{i=1}^{r} \text{Area i year x+1}} * 100 \quad \ldots\ldots (5)$$

Where Area i year x = area of cover i at the first date, Area i year x +1 = area of cover i at the second date, $\sum_{i=1}^{r} \text{Area i year x} + 1$ = total cover area at the second date.

3.10 Trend Analysis of Annual Water Hyacinth Area and Surface Area of Lake Tana

Trend is a statistic term used to detect whether there is a significant change of a variable over time detectable by statistical non-parametric and parametric procedures (Soni, 2017). To assess whether there is a decreasing or increasing trend of area water hyacinth and surface area of Lake

Tana or not change the Mann-Kendall trend test was applied for time series from 2011 to 2019 excluding 2013. Mann-Kendall test is distribution-free trend test, which considers the positive or negative course of successive values. It is also for identifying trends in time series data. One of the benefits of Mann-Kendall test is that the data need not confirm to any particular distribution (Sithranjan, 2012). This test identifies the sign of the difference between the later-measured data and the earlier-measured data. Each later-measured value is compared to all values measured earlier; resulting in a total of $n(n-1)/2$ possible pairs of data, where n is the total number of observations (Mondal et al., 2012). According to this test, H_0 show no trend if the data are independent and randomly ordered. This is tested against the alternative hypothesis Ha, which assumes that there is a trend. If the p-value is greater than the level of confidence alpha (α=0.05), there is no significant trend. On the other hand, if the p-value is less than the level of confidence alpha, there is a significant trend (Thenmozhi and Kottiswaran, 2016). The mathematical formula for Mann-Kendall statistic (S) is as follows:

$$S = \sum_{i=1}^{n-1} \sum_{j=i+1}^{n} \mathrm{sign}(yj - yi) \quad \text{…………………………} (6)$$

The trend test is applied to a time series y_i, which is ranked from i = 1,2,3, ... n – 1 and y_j, which is ranked from j = i + 1, i + 2, i + 3, ... n. Each of the data point's y_j is taken as a reference point, which is compared with the rest of the data points.

In the Mann-Kendall test, the computed difference between the later-measured value and all earlier-measured values, (yj-yi), where j>i, the integer value of 1, 0, or –1 indicates to positive differences, no differences, and negative differences, respectively (Getachew, 2017).

3.10.1 Sen's Slope Estimator Test

To estimate the true slope of an existing trend such as the amount of change per year, Sen's slop nonparametric method was used. Sen's slope estimator test is used for linear trend of data.

$$B1 = \mathrm{median}\left[\frac{(yj-yi)}{xj-xi}\right] \quad \text{…………………………} (7)$$

For all j > i and i = 1, 2… n-1 and j = 2, 3…, n; in other words, computing the slope for all pairs of data that used to compute S. The median of those slopes is the Sen's Slope estimator (Rahman and Begum, 2013).

3.11 Analysis of Meteorological Dataset in Lake Tana Basin

3.11.1 Analysis of Rainfall Data in Lake Tana Basin

All of the stations have missing data in their monthly rainfall series, with lower gaps observed in class 1 stations. Creation of continuous time series of data for each station was done by filling the gaps, therefore, preceded the analysis. Data gaps of a target stations may be filled by using available records of the station itself or observed values of nearby stations this could be by using of the mean of the data series or linear interpolation (Agizew, 2010). Thus, the missing values of a month were replaced by the long-term mean value of observed data for that month (Getachew, 2017) with cross-checking from the close neighboring station records in a similar time. Then, the total seasonal and annual rainfalls of the Basin were computed from monthly records of each station to study its impact on the distribution of water hyacinth.

3.11.1.1 Lake Areal Rainfall of Lake Tana Basin

Rainfall surface map of Lake Tana Basin of the stations was estimated using spatial interpolation method known as ordinary kriging and Thiessen polygon method. Ordinary kriging relies on spatial correlation structure of the data to determine the weighting values instead of weighting nearby data points by some power of their inverted distance and it is an effective spatial interpolation and mapping tool. Because it honors data locations provides unbiased estimates at unsampled locations and provides for minimum estimation variance. It is the best linear unbiased estimator (Getachew, 2017). Thiessen method is also the appropriate method to evaluate the average areal distribution of rainfall in an area affected by topography. The stations in and around the Sub Basin are included (Getachew, 2010). Agizew, (2010) stated that the kriging method best to estimate areal rainfall and Thiessen polygon is also considered to be acceptable.

Thiessen polygon method attempts to make allowance for irregularities in gauge locations by weighting the record of each gauge in proportion to the area which is closer to that gauge than to any other gauge. However, this method does not make any allowance for orographic influences in the basin; it gives an appropriate depth of rainfall in the basin. The average depth of rainfall is computed using the following formula (Getachew, 2010).

$$P = \frac{P1A1+P2A2......PnAn}{A1+A2...An} \quad (8)$$

Where P1, P2...Pn are the rainfall recorded at rain gauge stations with A1, A2….An as the polygon areas.

3.11.2 Analysis of Temperature Data in Lake Tana Basin

The minimum and the maximum temperature of the study area were assessed using observed data of 17 class 1 and class 3 stations with less than 18 % data gaps in the analysis period. The analysis involved checking for validity and homogeneity of the datasets, spatio-temporal characterization of the annual and seasonal temperature and creation of continuous temperature series by filling the missing data using long term mean. The observed monthly minimum and maximum temperature data were subjected to quality control to identify invalid and temporally inconsistent records identifying based on: checking whether the data is within valid ranges; both the minimum and maximum temperature data should be within valid ranges; checking whether the minimum temperature is less than the maximum; this is to ensure that the maximum temperature is always greater than the minimum and checking for suspicious data, maximum and minimum temperature should be in line with the normal climate condition of the study area (Agizew, 2010). Then after the mean monthly and seasonal temperature were correlate with the area of water hyacinth and used in estimation of reference evapotranspiration of the weed.

3.11.3 Analysis of Wind Speed, Relative Humidity and Sunshine Hour Data in Lake Tana Basin

Wind speed has numerous impacts on the water surface. The wind speeds refer to the average air speeds and they influence not only the current speeds (the average lake water motion (waves)), but also the mobility of the water hyacinth on the lake (Ouma et al., 2005). Mean monthly and seasonal wind speeds were correlated with the corresponding monthly, seasonal water hyacinth area to see it influence for weed spread. In addition, wind speed data was applied in the computation of reference evapotranspiration of water hyacinth. However, the computed mean monthly relative humidity and sunshine hour data recorded from Bahir Dar, Gondar, Debre Tabor and Dangila meteorological stations were only used to estimate the reference evapotranspiration of water hyacinth in Lake Tana.

3.12 Evapotranspiration of Water Hyacinth (ETc) and Water Losses in Lake Tana

Evapotranspiration is the process in which water is returned to the atmosphere by a combination of evaporation and transpiration (Getachew, 2010). Numerous modeling techniques are used to estimate wetland evaporation. These are either empirical formulae utilizing climatic data or models satisfying the energy and water balance equations. In using the water balance approach, the accuracy of the estimate of evaporation of wetland depends on other components of the water balance (precipitation, runoff, interaction with groundwater) (Mohamed et al., 2011). In this research FAO-56 Penman-Monteith (P-M) equation was used to compute evapotranspiration of water hyacinth. Average daily of water losses of evapotranspiration (ETc) of water hyacinth were calculated by the equation as follows (Rashed, 2014; Ali and El-Din Khedr, 2018; Sasaqi et al., 2019):

$$ET_C = ET_O K_C \quad \text{……..……..…} \quad (9)$$

Where: ETo: reference evapotranspiration in mm/day, Kc: crop coefficient.

3.12.1 Crop Coefficient (Kc)

Crop coefficient (Kc) is the ratio of the evapotranspiration of the crop (ETc) to a reference crop (ETo), which is representative of crop specific evaporation parameters (albedo, thermal emissivity, aerodynamic resistance, and minimum surface resistance) for the various phenological stages (Sasaqi et al., 2019). Average monthly crop coefficient (mm/day), Kc is obtained by applying the weather-based method of FAO Penman-Monteith equation (equation 10) or by dividing the average monthly water consumption (ETp) by the corresponding average monthly water losses (ETb) (equation 11) as follows (Rashed, 2014):

$$Kc = \frac{ETp}{ETo} \text{……...……} \quad (10)$$

$$Kc = \frac{ETp}{ETb} \text{……} \quad (11)$$

The Kc value for water hyacinth computed in different literature ranged from 0.65 to 1.90: Meleha, (2005) estimated the monthly average Kc value for water hyacinth by many empirical formulas as 1.48, 1.54, 1.38, 1.42, 1.96, 2.27, 2.41, 2.31, 2.20, 1.97, 1.62, 1.34 and 1.30 from November 2004 to November 2005 respectively gives an average of 1.83; Jiménez-Rodríguez et al., (2019) obtained the value Kc as 1.90 using an experiment conducted from December 2012 – January 2013; crop coefficient value of water hyacinth is 1.1 (light to moderate wind) and 1.15

(strong wind) (Dooenboss and Pruitt, 1992), and Rashed, (2014) computed Kc value of water hyacinth as 0.65 using FAO Penman-Monteith and 1.83 by dividing the average monthly water consumption by the corresponding average monthly water losses by carrying out water hyacinth water consumption experiment through its different growth stages of the weed from April 2008 to August 2009. To calculate the evapotranspiration of water hyacinth and water loss due to the weed in Lake Tana, a minimum crop coefficient (Kc) of 0.65 and a maximum Kc value of 1.90 were adopted from Rashed, (2014) and Jiménez-Rodríguez et al., (2019). Because to determine the Kc of water hyacinth specifically to Lake Tana climate condition a minimum of one year water consumption measurement of the weed through its different growth stages is required.

3.12.2 Referenced Evapotranspiration (ET_0)

ETo is the potential ET from a reference surface of a hypothetical green grass of uniform height, 0.12 m, well watered and actively growing and has a constant albedo of 0.23 with fixed surface resistance of 70 sm^{-1} (Allen et al., 1998). Daily evapotranspiration (ETo) was computed using the FAO-56 Penman-Monteith method (Allen et al., 1998) as follows:

$$ET_0 = \frac{[0.408\Delta\,(Rn-G)+\gamma\frac{900}{T+273}U_2(es-ea)]}{[\Delta+\gamma(1+0.34U_2)]} \quad \text{(12)}$$

Where ET_0 is referenced evapotranspiration in mm/day; Δ is the slope of saturation vapor pressure curve (kPa/°C); γ is psychrometric coefficient (kPa/°C); Rn is the net radiation at the surface (MJm^{-2}/d^{-1}); G is soil heat flux in $MJm^{-2}d^{-1}$, assumed zero on daily basis; T is mean daily air temperature in ^oC; U_2 is mean wind speed at 2m (m/s); (es-ea) is vapor pressure deficit (kPa).

FAO-56 Penman-Monteith methods used to compute the various terms of the Penman equation in order to simplify the ETo calculation, several terms are calculated separately as presented below (Allen et al., 1998).

1. Temperature (ºC)

Minimum, maximum and mean monthly temperatures were used to calculate the various terms of the Penman equation. The areal temperature of Lake Tana was computed from point observations of six stations namely Bahir Dar, Deq Istifanos, Enfranz, Gorgora, Maksegnit, and Woreta stations. Mean monthly temperature calculated from the maximum monthly air temperature, ºC and the minimum monthly air temperature, ºC.

$$T_{mean} = \frac{(Tmax) + (Tmin)}{2} \quad \text{(13)}$$

2. Mean Saturation Vapor Pressure Derived from Air Temperature(es)

Saturation vapor pressure is can be derived from air temperature. The relationship is expressed by:

$$\text{es(T)} = 0.611.\exp\left(\frac{17.27\text{T}}{\text{T}+237.3}\right) \quad \text{(14)}$$

es(T) = saturation vapor pressure (kPa) at the air temperature, T = air temperature, ºC. The mean saturation vapor pressure for a day, week, decade or month should be computed as the mean between the saturation vapor pressure at the mean daily maximum and minimum air temperature for that period.

$$\text{es(T)} = \frac{es(Tmax)+es(Tmin)}{2} \quad \text{(15)}$$

Where, es(Tmax) and es(Tmin) are the saturation vapor pressure at the daily maximum and minimum air temperatures were calculated as

$$\text{es(Tmax)} = 0.611.\exp\left(\frac{17.27T_{max}}{T_{max}+237.3}\right) \quad \text{(16)}$$

$$\text{es(Tmin)} = 0.611.\exp\left(\frac{17.27T_{min}}{T_{min}+237.3}\right) \quad \text{(17)}$$

3. Actual Vapor Pressure (e_a)

The actual vapor pressure was then calculated from the saturated vapor pressure and observed relative humidity (RH in %).

$$\text{ea(T)} = \text{es(T)}.\left(\frac{RH}{100}\right) \quad \text{(18)}$$

4. The Slope of Saturation Vapor Pressure Curve (**Δ**)

The slope of saturation vapor pressure is calculated from the temperature as follows.

$$\Delta = \frac{4098.\ \text{es(T)}}{(\text{T}+237.3)^2} \quad \text{(19)}$$

5. Psychrometric Constant

Psychrometric constant is the ratio of specific heat of moist air at constant pressure (cp) to the latent heat of vaporization. The specific heat at constant pressure is the amount of energy required to increase the temperature of a unit mass of air by one degree at constant pressure. As an average atmospheric pressure is used for each location, the psychrometric constant is kept constant for each location depending of the altitude.

$$\gamma = \frac{cp.P}{0.622\lambda} = 0.000665P \quad \text{..... (20)}$$

Where, cp is the specific heat of water at constant pressure is (0.001013 MJ kJ/kg/°C. The latent heat of vaporization (λ) and atmospheric pressure (P) were calculated as follows.

$$\lambda = 2.501 - (2.361 \times (10)^{-3}).T \quad \text{..... (21)}$$

$$P = 101.3.\left(\frac{293-0.0065Z}{293}\right)^{5.26} \quad \text{..... (22)}$$

T is temperature in °C and Z is altitude in meters above mean sea level.

6. Net Radiations (Rns):

It is the difference between incoming and outgoing radiation of both short and long wavelengths.

$$Rn = Rs(1-\alpha) - RL \quad \text{..... (23)}$$

Where: α is albedo of the water surface; Rs is solar radiation reaching the ground surface, and in the absence of observed data it can be estimated from readily available measurements using empirical relations; RL: is long wave radiation

$$Rs = (a_s + b_s \frac{n}{N})Ra \quad \text{..... (24)}$$

Where: N is the maximum possible duration of sunshine hours [hour], n: is the actual duration of sunshine [hour] Ra: is extraterrestrial radiation [MJ m-2 day-1], a_s and b_s are regression constant. Where no actual solar radiation data are available and no calibration has been carried out to improve as and b_s parameters, the values as =0.25 and bs = 0.50 are usually recommended.

7. Extraterrestrial Radiation (Ra)

The radiation striking a surface perpendicular to the sun's rays at the top of the earth's atmosphere, called the solar constant, is about 0.082 MJ m^{-2} min^{-1}. The local intensity of

radiation is, however, determined by the angle between the direction of the sun's rays and the normal to the surface of the atmosphere. This angle will change during the day and will be different at different latitudes and in different seasons. The extraterrestrial radiation, Ra, for each day of the year and for different latitudes can be estimated from the solar constant, the solar declination and the time of the year by:

$$R_a = 37.59 d_r[\omega_s \sin(\varphi)\sin(\delta) + \sin(\omega_s)\cos(\delta)] \quad \ldots\ldots (25)$$

Where φ is latitude (rad) and the other terms are functions of the position of the sun: dr is the relative distance between the sun and the earth, ωs sunset hour angle (rad), δ solar declination angle (rad)

8. The Inverse Relative Distance Earth-Sun (dr) and Solar Declination (δ)

$$d_r = 1 + 0.033 COS\left[\frac{2\pi}{365} J\right] \ldots\ldots (26)$$

$$\delta = 0.409 sin\left[\frac{2\pi}{365} J - 1.39\right] \ldots\ldots (27)$$

$$\omega_s = \arccos(-tan(\varphi)\, tan(\delta)) \quad \ldots\ldots (28)$$

9. Net Outgoing Long wave Solar Radiation (Rl)

The rate of long wave energy emission is proportional to the absolute temperature of the surface raised to the fourth power. This relation is expressed quantitatively by the Stefan-Boltzmann law

$$R_l \uparrow = \varepsilon \sigma T^4 \ldots\ldots (29)$$

Where ε is emissivity of water surface, taken as 0.97; σ is Stephan-Boltzman constant (5.67×10^{-8} $Wm^{-2}K^{-4}s^{-1}$); T is the water surface temperature (K), assumed to be the mean air temperature (Agizew, 2010).

3.12.3 Estimation of Water Losses Due to Evapotranspiration of Water Hyacinth

The volume of water lost due to evapotranspiration of water hyacinth was calculated using the following equation (equ. 30) (Rashed, 2014).

Reach water loss = (reach ETc x reach surface area) x 0.001 …… (30)

Where: reach water loss is in m^3, reach surface area is in m^2 and ETc is evapotranspiration of water hyacinth in mm/day.

3.13 Correlational Analysis

Pearson Correlation Coefficient used to test for a linear relationship between the monthly and seasonal area of water hyacinth with climatic elements (rainfall, temperature, and wind speed) and surface area of the Lake, and the correlation between rainfall and surface area of the Lake. The monthly and seasonal correlational analysis between variables was covering the time periods from 2016 September to 2018 December whereas the annual correlation covers from 2010 to 2019. The Pearson correlation coefficient is a measure of the linear relationship between two variables X and Y, giving a value between +1 and -1 inclusive, where 1 is a total positive correlation, 0 is no correlation, and -1 is a negative correlation (Guo et al., 2014). To analyzed the degree of the relationship between the dynamic of water hyacinth and climate elements the value of Pearson correlation coefficient was group based on the absolute value of the correlation coefficients into a weak correlation ($0 < |r| \leqslant 0.3$), a low correlation ($0.3 < |r| \leqslant 0.5$), a moderate correlation ($0.5 < |r| \leqslant 0.8$), and a strong correlation ($0.8 < |r| \leqslant 1$) (Changbin et al., 2014). The mathematical formulation of Pearson correlation coefficient is presented as follows.

$$r_{xy} = \frac{\sum_{i=1}^{n}(xi-xm)*(yi-ym)}{\sqrt{\sum_{i=1}^{n}(xi-xm)^2\sum_{i=1}^{n}(yi-ym)^2}} \qquad (31)$$

Where, rxy is the simple correlation coefficients of variables X and Y, xi is area of water hyacinth for the i^{th} year/month/season, Yi is climatic elements of the i^{th} year/month/season; Xm is the area cover for all years/month/season, Ym is the average climate element for all years/month/season (Li et al., 2004).

CHAPTER FOUR

4 RESULTS AND DISCUSSION

4.1 Image Classification Accuracy Assessment

A total of 51 Ground truth points (as shown in Figure 4.1) in three areas were collected using Handheld GPS instrument to discriminate water hyacinth from other land cover types and for image classification accuracy assessment. For the whole classification accuracy assessment and identification of the infested area in the Lake, 179 Google Earth points, and 23 Ground truth points which were collected in 2011 by Tewabe, (2015) during the preliminary survey of water hyacinth along the whole shore of Lake Tana have been employed in this study.

Figure 4.1 Ground GPS points overlaid over 2019 January Sentinel- 2 raw image (TCI).

The accuracy of LULC for the annual images classified along with the overall accuracy and the Kappa coefficient was summarized in Table 4.1. The results have shown that the spatial distribution and configuration of water hyacinth can be accurately detected and mapped with an overall classification accuracy ranged from 95.78% to 99.47% with a corresponding kappa statistics varied 0.92 to 0.99 of Landsat 8 and Sentinel 2 images respectively, which implies that the classification process is avoiding from 95.78% to 99.47% percent of the errors for each classified map that a completely random classification would generate. The producer‘s

accuracies and user‘s accuracies for water hyacinth consistently high, ranging from 90.24 to 98.86% and 94.20 to 100.00% respectively.

Table 4.1 Results of accuracy assessment of water hyacinth and water surface

Years	Class Name	Producer's Accuracy (%)	User's Accuracy (%)	Overall Accuracy (%)	Kappa Statistic	Omission Error	Commission Error
2014	Water	100	94.11	95.78	0.92	0.00	0.06
	WH	90.24	94.20			0.10	0.06
2015	Water	100.00	95.24	96.36	0.93	0.00	0.05
	WH	90.63	100.00			0.09	0.00
2016	Water	100.00	99.00	99.40	0.99	0.00	0.01
	WH	98.55	100.00			0.01	0.00
2017	Water	100.00	95.24	96.97	0.94	0.00	0.05
	WH	92.31	100.00			0.08	0.00
2018	Water	100.00	96.15	97.71	0.95	0.00	0.04
	WH	94.67	100.00			0.05	0.00
2019	Water	100.00	99.01	99.47	0.99	0.00	0.01
	WH	98.86	100.00			0.01	0.00

4.2 Water Hyacinth Spectral Response Profiles

Figure 4.2 illustrates the spectral response curves of water hyacinth and water body derived from Sentinel-2 and Landsat 8 remote sensing images. A sentinel-2 sensor provides more bands that have great potential than Landsat 8 in discriminating between the water hyacinth and other LULC. Band 5 (NIR), Band 7 (NIR), Band 8 (NIR) and Band 8a (NIR narrow) of Sentinel -2 image are the most critical and outstanding spectral regions for detecting and mapping water hyacinth from other land cover types. Water hyacinth generally had higher near-infrared (NIR) reflectance than the associated plant species and water (Kasaragod, 2003). On the contrary, the Band 2 (Blue), Band 3 (Green), Band 11 (SWIR1) and Band 12 (SWIR2) were the least influential in the discrimination of the weed. In Sentinel 2 image, water surface is more visible using Band 2 and 3. The spectral region from Band 4 to 7 of Landsat 8 is the most influential in detecting and mapping water hyacinth in freshwater ecosystems, whereas Band 2 to 4 are good for detecting the water body.

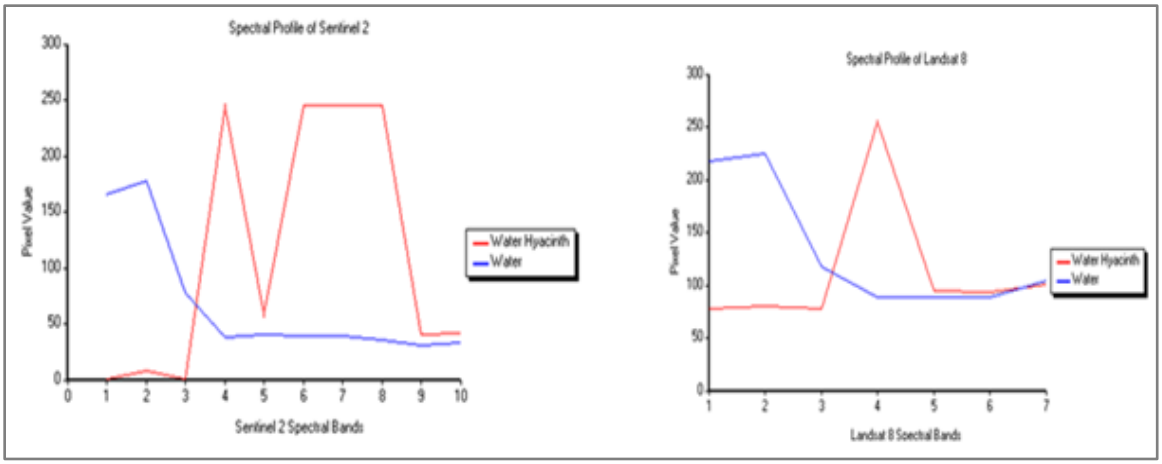

Figure 4.2 Spectral reflectance of water hyacinth derived from Sentinel-2 and Landsat 8 of Lake Tana *(for Sentinel-2 graph in the X-axis, 1=Band 2, 2=Band 3, 3=Band 4, 4= Band 5, 5= Band 6, 6 =Band 7, 7= Band 8, 8 = Band 8a, 9 =Band 11 and 10= Band 12; For Landsat 8, 1= Band 2, 2= Band 3, 3= Band 4, 4=Band 5, 5=Band 6, 6=Band 7 and 7= Band 9).*

4.3 Results of Spatio-Temporal Distribution of Water Hyacinth in Lake Tana

4.3.1 Annual Spatio-Temporal Distribution of Water Hyacinth in Lake Tana

The results of spatio-temporal water hyacinth mapping of satellite imagery available for the areas during the period from January 2011 to January 2019 are shown in Table 4.2. The results of the study indicated that there has been a rapid linearly increment of the invasive weed. The annual infestation area of water hyacinth was increased from 134ha in 2011 to 3019ha in 2019. The peak amount of annual water hyacinth coverage over the Lake in the study period determined directly from the imagery was 3019 ha in January 2019, which constitutes 0.99% of the entire Lake surface.

Table 4.2 Area of water hyacinth coverage from 2011 January to 2019 January

Year	2011	2012	2014	2015	2016	2017	2018	2019
Water (ha)	304786	306085	306195	306399	303188	303428	303406	302952
WH (ha)	134	512	854	1197	915	1504	2199	3019

As Tewabe, (2015), the first investigation of water hyacinth was conducted from October 27, 2011, to November 3, 2011 by interdisciplinary expedition groups and a total of 24 sites were delineated using the Global Positioning System (GPS) along the whole periphery of Lake Tana.

As the study noticed water hyacinth was started from Mitreha Abawarka Kebele of Gondar Zuria Woreda specifically around at Netseba Village with an estimated of 3ha area coverage and highest infestation of 80-100ha was estimated at Megech River Mouth (Between point 13 and 14) which supports the result of this study as shown in Figure 4.3.

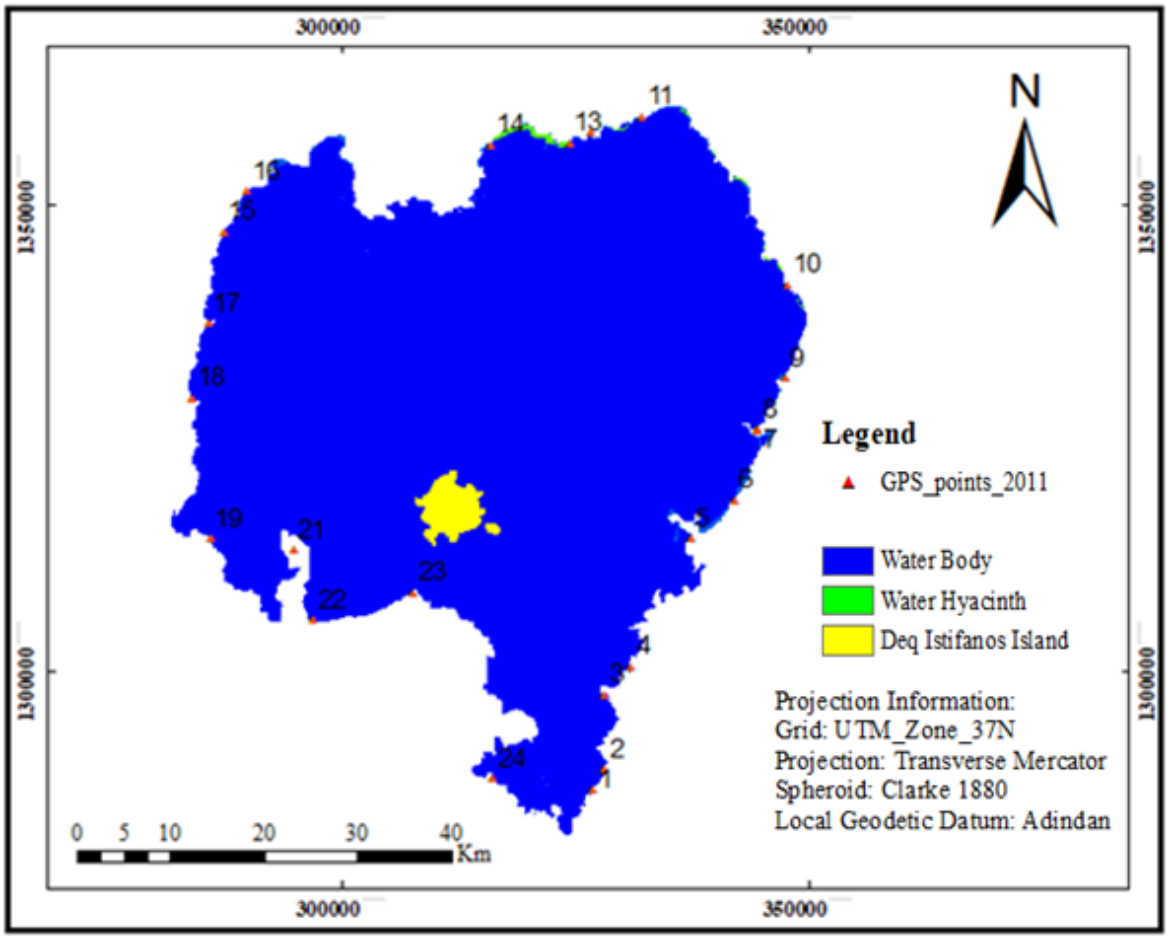

Figure 4.3 GPS points collected in 2011 by Tewabe, (2015) overlaid on a classified map of 2011 Jan in this study

Currently, five woredas such as Denbiya, Gondar Zuria, Libo Kemkem, Fogera and Dera Woredas are invaded by the weed. Gondar Zuria and Libo Kemkem Woredas are the most affected woredas whereas Denbiya and Dera Woredas are the least affected by the water hyacinth. However, Denbiya Woreda was the most adversely affected by water hyacinth invasive species than other woredas from 2011 to 2017 years and Gondar Zuria was the most infested woreda in 2018 year this shows that the severity infestation of water hyacinth is shifted from the

northern shore towards eastern parts the Lake. As Figure 4.4 depicts Fikra Dangurie, Lemba Arbaytu, Mitriha Kebeles from Gondar Zuria, and Agid Qiregna and Kab Abo Kebeles from Libo Kemkem Woreda were heavily infested with the dangerous weed.

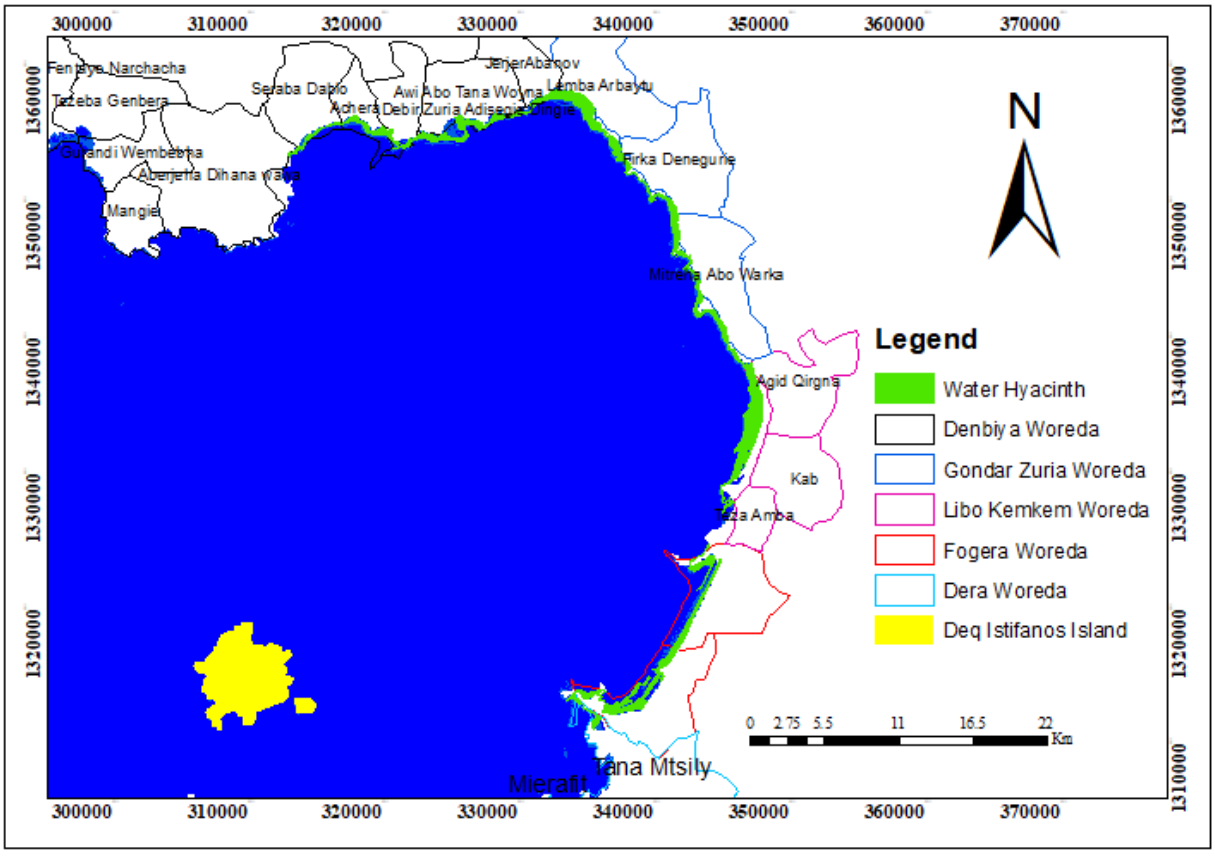

Figure 4.4 Water hyacinth infestation in 2019 hot-spot areas (Kebeles) within the Lakeshore

The infestation of water hyacinth in the whole study periods has been observed in the north and east shoreline of Lake Tana (Figure 4.5). This could be explained by the fact that the geographical setting of the Lake in northern and eastern seems to be favorable for water hyacinth expansion and distribution since the area is flat, the depth of the Lake is shallow below one meter, large portion of the Basin and four major rivers such as Megech, Rib, Gumara and Dirma are found in this direction of the Lake. These rivers are transport suspended sediments or nutrients from upstream during flood events that favor the proliferation of water hyacinth in this line. The study of Twongo, (1993); Hubble and Harper, (2002) and Albright et al., (2004) indicate that the presence of more suitable water hyacinth habitat/nutrient levels on the lake surface and at the shores helps for proliferation water hyacinth. In addition, Willoughby et al.,

(1993) stated that the shores of the lakes are the most severely infested with water hyacinth due to the large numbers of shallow, sheltered, and mostly papyrus-fringed bays and inlets. Shallow depth of Lake Tana is found on the northeast shore which is currently invaded by water hyacinth. The weed needs stagnant water, which is typical for the northeastern parts of the Lake due to their connection with the large flood plain (Derseh et al., 2019). The severity of water hyacinth infestation limited only to this portion of the Lake may be linked to the water currents and wind direction (Ouma et al., 2005) which may have pushed water hyacinth to the north and east.

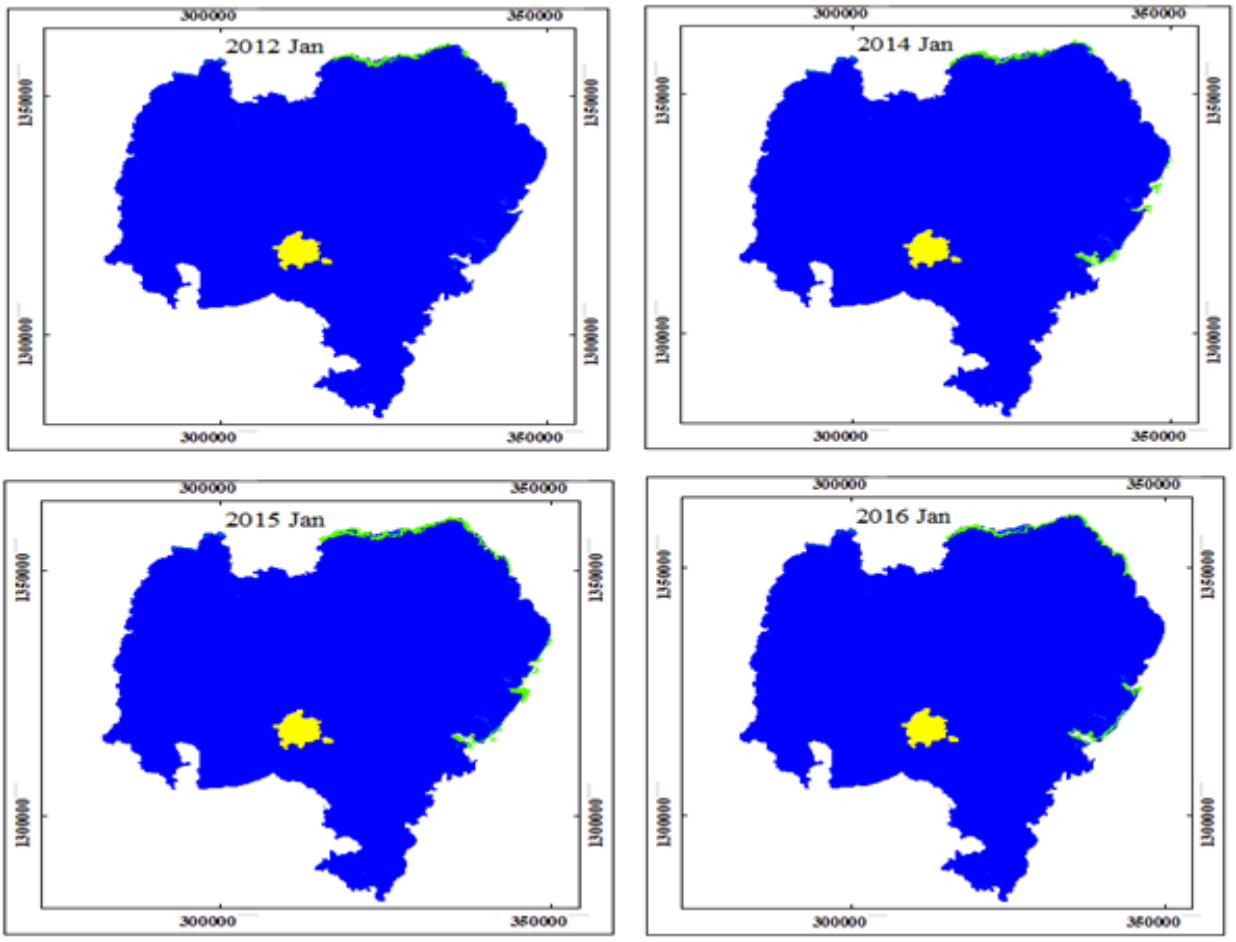

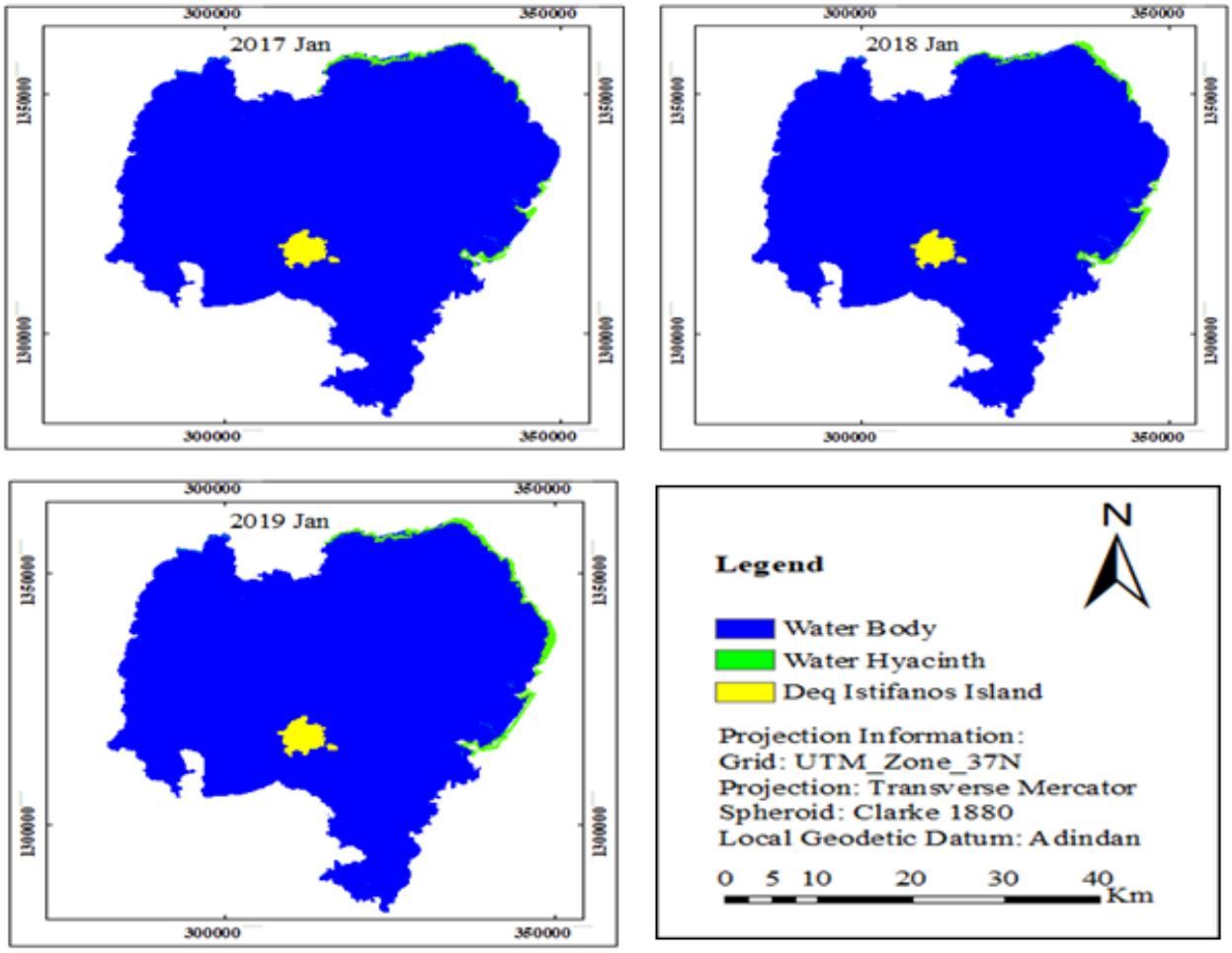

Figure 4.5 spatio-temporal distribution and extent of water hyacinth in Lake Tana (2011- 2019)

The previous studies carried out on the area estimation of water hyacinth in Lake Tana were overestimated and generally extremely higher than the estimates provided in this study. As Wassie et al., 2014 cited (in BoEPLAU, 2012) the areal coverage of water hyacinth in 2012 was 20,000ha found in three woredas such as Denbiya, Gondar Zuria, and Libo Kemkem. However, the estimated water hyacinth areal coverage from the Landsat 7 images in this study is 512ha which is near to 1500ha of area less than from the result of BoEPLAU, (2012). Wassie et al., (2014 and 2015), annual report 1 and 2 showed the water hyacinth infestation coverage was approximately 50,000ha and 34,500ha (3,000ha thick, 2,500ha intermediate and 29,000ha scattered) in 2014 and 2015 respectively. Besides this, the reports indicate that from the total of 385 km shoreline length of Lake Tana close to one-third or more than 30% of the shoreline (128 km distance) of the Lake's shore was invaded by water hyacinth. The area of water hyacinth

reported in 2014 and 2015 has a difference of 49,146ha and 32,794ha from 854ha and 1206ha which was mapped in this study for similar years.

It is difficult to explain why the areal coverage of water hyacinth reported in 2012, 2014 and 2015 have a large deviation with this study because of no clear procedure stated in their reports. A study conducted by Melaku, (nd) found out 5,394ha of water hyacinth areal coverage at five woredas along the coast of the Lake is closely related with the results of 3019ha in 2019 January than the above three reports. However, according to Derseh et al., (2019) the areal coverage of water hyacinth in Lake Tana estimated by the government offices was less than 5000ha in the peak growing season which exactly confirms the result made by this study.

4.3.2 Monthly Spatio-Temporal Distribution of Water Hyacinth in Lake Tana

The dynamics of water hyacinth distribution change patterns have been identified by analyzing the classified and manual digitized multi-temporal satellite images from 2016 September to 2019 January. Because the spatial coverage of water hyacinth had not been visible from 2016 February to 2016 August both in Sentinel-2 and Landsat 8 images, only four images (September to December) from 2016 years were used for mapping of the monthly area of water hyacinth.

Table 4.3 Monthly areal coverage of water hyacinth (ha) of the study area (2016 Sep -2018 Dec)

Month	Ja	Fe	Ma	Ap	Ma	Ju.	Jul	Au	Se	Oc	No	De
2016	915								598	1220	1546	1512
2017	1504	1159	970	677	524	439	396	772	1522	1590	2594	2308
2018	2199	1746	1729	1374	1273	908	821	957	1800	2857	3830	3237

As the result of the study reveals in the Table 4.3 above, the maximum area of water hyacinth in 2016 was observed in November (1546ha) followed by 1512ha (2016 Dec), 1220ha (2016 Oct) and 598ha (2016 Sep). Similarly, the maximum monthly infestation of water hyacinth in 2017 and 2018 was 2594ha (2017 Nov) and 3830ha (2018 Nov) while, the minimum spatial coverage was 396ha (2017 July) and 821ha (2018 July). The mean monthly area of the invasive water hyacinth in the study period was 1554ha with a standard deviation of 887ha. The analysis of monthly satellite images indicate that the peak areal extends of water hyacinth in the study area was 3830ha, observed in November 2018 followed by 3237ha (2018 Dec) and 3019ha (2019 Jan), while the minimum monthly infestations of water hyacinth was obtained as 396ha (2017 July). A cyclical pattern was seen in the areal distribution of water hyacinth in the monthly study

period, 2016 Sep – 2019 Jan (Figure 4.6). The area of the weed steadily increase from July month to November in both years while the amount started to decrease from December reaches low in July again. Therefore, November and July are the turning point, where a decrease and increase in the area of water hyacinth occurred. This result confirms with the study of Ongore et al., (2018), the spatial-temporal dynamics of water hyacinth in Lake Victoria from 2014 to 2017 exhibited periodic cyclical patterns of emergence, growth, disappearance, and reappearance within a year, reaching the highest peak between September and November and followed by a decline to almost complete disappearance in May.

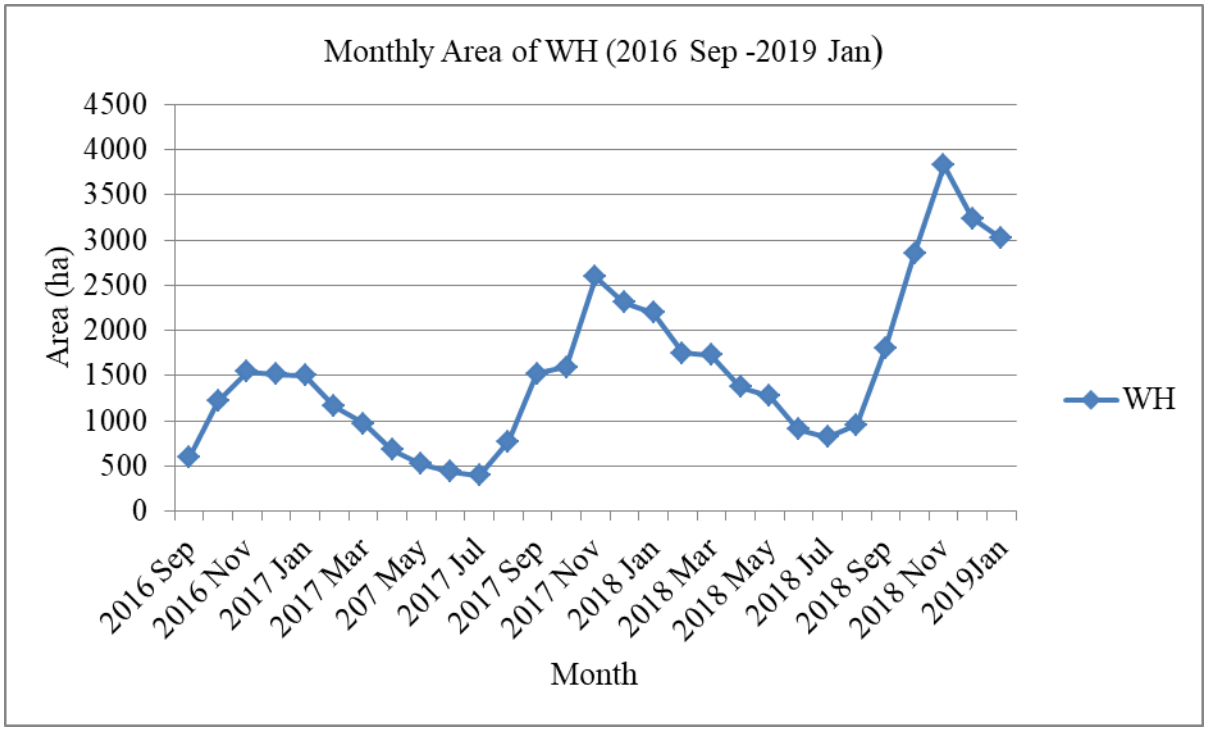

Figure 4.6 Monthly spatio-temporal variation of water hyacinth area in Lake Tana

The monthly spatial distribution and extent of water hyacinth in Lake Tana from 2018 February to 2018 December are shown in Figure 4.7, and the remaining maps from 2016 September to 2017 December months are appears in Appendix- 2.

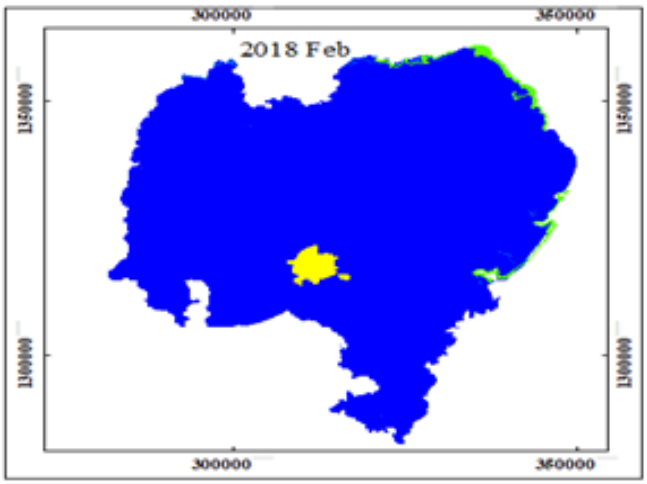
2018 Feb
300000
350000
1350000
1300000

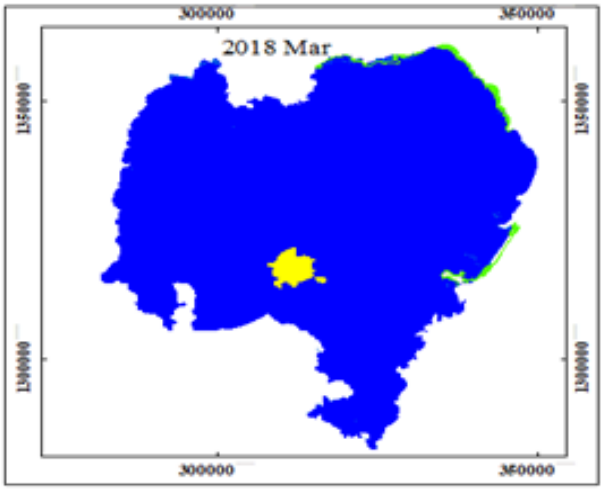
2018 Mar
300000
350000
1350000
1300000

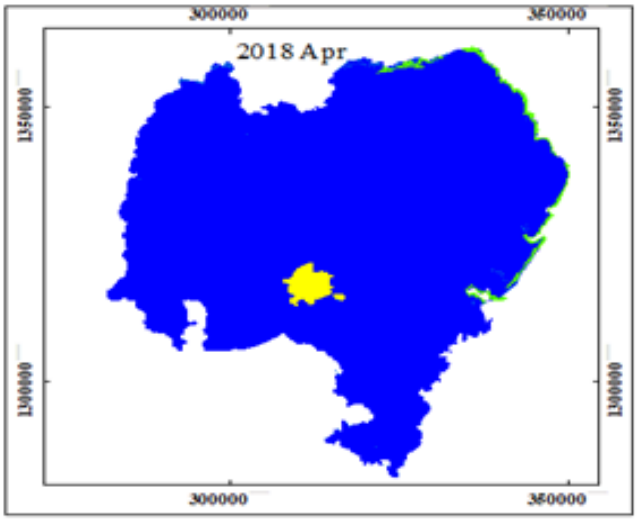
2018 Apr
300000
350000
1350000
1300000

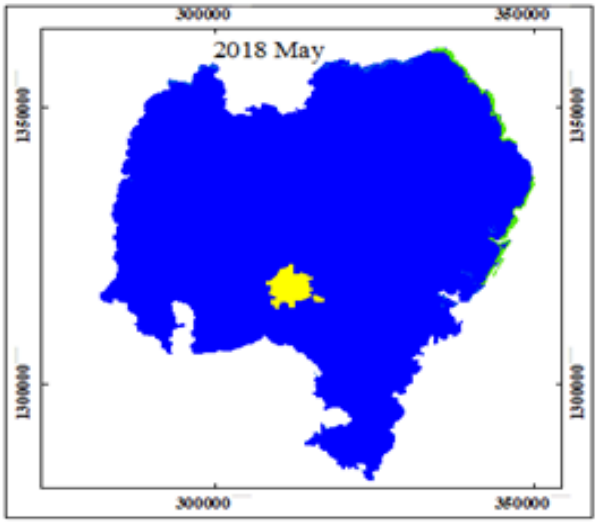
2018 May
300000
350000
1350000
1300000

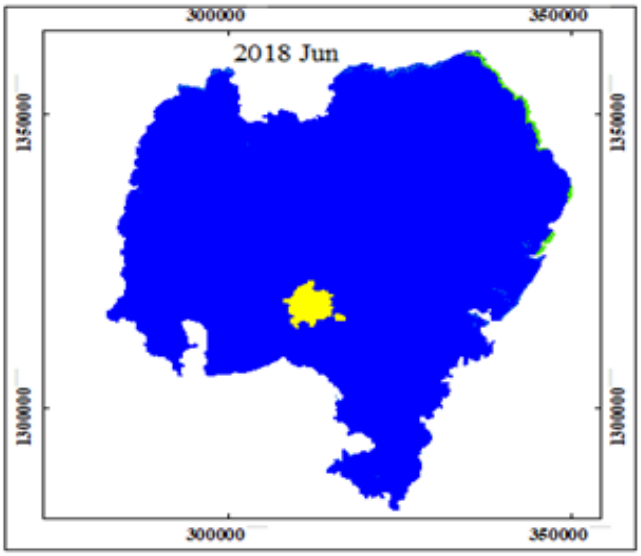
2018 Jun
300000
350000
1350000
1300000

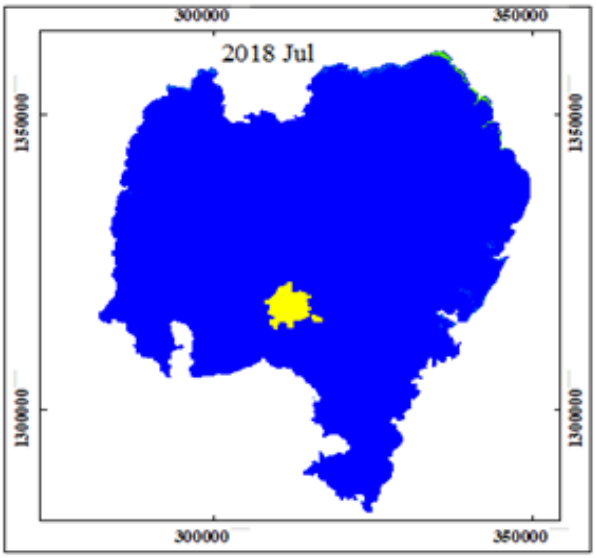
2018 Jul
300000
350000
1350000
1300000

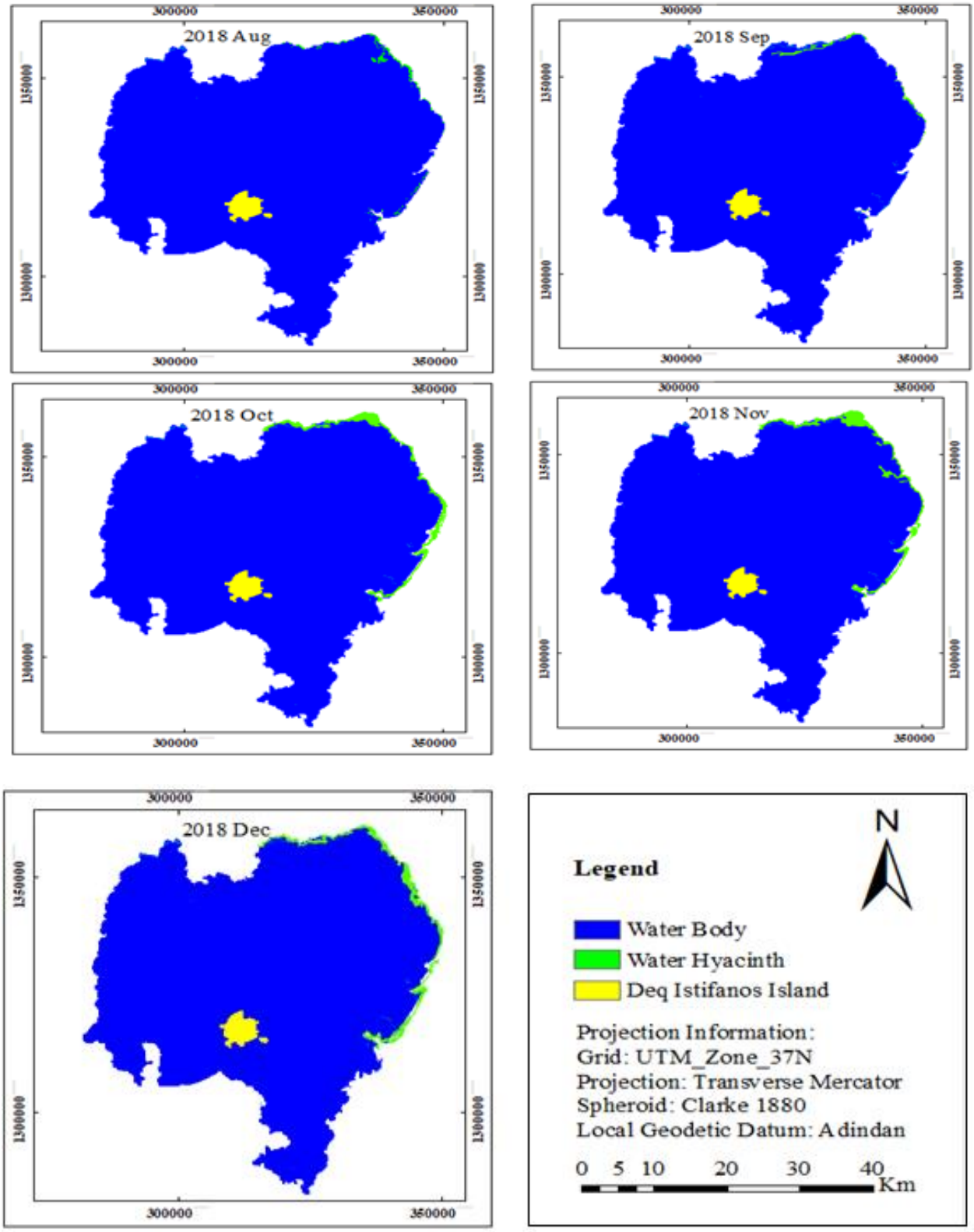

Figure 4.7 Monthly spatio-temporal distribution and extent of water hyacinth in Lake Tana

4.3.3 Seasonal Spatio-Temporal Distribution of Water Hyacinth in Lake Tana

Three seasons were identified according to NMSA, (1996) such as Kiremt (June-September), Bega (October-January), and Belg (February-May). Kiremt is the main rainy season, Belg is the small rainy season and Bega is the dry season. To assess the seasonal change of water hyacinth distribution, the average areas of water hyacinth for each season were calculated.

Table 4.4 Seasonal mean area of water hyacinth from 2016 Oct – 2019 Jan

Seasons		Mean area of WH (ha)	Season Type
2016 -2017 season	2016 Oc -2017 Ja	1446	Bega
	2017 Fe -2017 Ma	832	Belg
	2017 Ju -2017Se	782	Kiremt
2017 - 2018 season	2017 Oc -2018 Ja	2173	Bega
	2018 Fe -2018 Ma	1530	Belg
	2018 Ju -2018 Se	1121	Kiremt
2018 - 2019 season	2018 Oc -2019 Ja	3236	Bega

The maximum and minimum mean seasonal water hyacinth area from 2016 October to 2019 January season had been observed in Bega and Kiremt season. In Kiremt season, in addition, it's manifested the least quantity of water hyacinth during all the three seasons (Table 4.4), the weed were found scattered and moved from the coast to inside part of the Lake by the help of flood. A consistent concentration of water hyacinth along the north shore (around Lamba Arbaytu Kebele) of the Lake has been observed in Bega season. The reason of manifested the largest quantity of water hyacinth in Bega season during all the three seasons could be due to the surface area of the Lake and lake level decrease which enables the water hyacinth got new nutrient and inland surface. Because of the weed is mainly found in inshore and shallow areas to which it is swept by the current. It spreads fast in shallow (< 6m) bays and inlets with mud bed surfaces (Mitchell, 1976). The result of spatio-temporal distribution of six water quality parameters; phosphorus, nitrogen, temperature, pH, salinity, and lake depth study in Lake Tana shows the highest values of the total phosphorus (TP) concentration was observed in the dry season (December and March) and the lowest in the rainy season (August), (0.14 mg/ L in August, 0.18 mg/L in December, and 0.21 mg/L in March) (Derseh et al., 2019) because the availability of phosphorus is one of the most important factors for determining phytoplankton biomass and water quality in

lakes and temperate wetlands (Dilon and Rigler, 1974). Besides, a significant increase in the nutrient concentrations accelerates water hyacinth infestation (Adams et al., 2002; Mireri, 2005). The quantity of water hyacinth observed in Belg season show a decrease in magnitude as compared to Bega season and the geographic locations has also shifted evidently in the easterly direction i.e. from Gondar Zuria Woreda (Lemba Arbaytu Kebele) in the north towards Libo Kemkem Woreda (Agid Qiregna and Kab Kebeles) of the east shoreline of the Lake. The highest mean seasonal spatio-temporal infestation of water hyacinth was 3236ha seen between 2018 October to 2019 January, Bega season and the lowest be 782ha in 2017 Kiremt season. Ouma et al., (2005) studied the seasonal dynamism and abundance of water hyacinth in Winam Gulf of Lake Victoria with the seasonal climatic variability data, the study grouped three seasons as seasons 1, 2 and 3, each season were represented by March, July and November month. The results of the study revealed that the highest quantity of water hyacinth was observed in season 3 (November month), more than twice that in the first season which is consistent with this study. However the result of this study contradicted with the study of Mironga et al., (2014) and Thamaga and Dube, (2018) which shows high coverage of water hyacinth had observed in summer (wet season) than in dry season in Lake Naivasha, Kenya and Greater Letaba River System, South Africa respectively.

4.4 Spatio-Temporal Change Detection of Water Hyacinth in Lake Tana

4.4.1 Annual Spatio-Temporal Trend of Water Hyacinth in Lake Tana

The result of the Mann-Kendall trend test indicates that annual water hyacinth and surface area of Lake Tana exhibited an increased and a decreased trend respectively from 2011 -2019 over the study area. The results of the analysis revealed that there was a statistically significant increment of the annual area of water hyacinth as the computed p-value is lower than the significance level alpha value of 0.05 at 95% confidence level (Table 4.5). The area of water hyacinth has been increased by a Sen’s slope estimator of 343.80 per year. However, the Mann-Kendall trend analysis result shows that the annual surface area of Lake Tana has been deceased by 335.54ha per year with Kendall's tau of -0.43. The surface area of the Lake Tana in the study periods has shown a decreasing trend at a 95% confidence level for the last 9 years, although it is not statistically significant (p-value=0.95 > alpha 0.05).

Table 4.5 Result of the Mann-Kendall trend test for annual water hyacinth area and surface area of Lake Tana.

	Kendall's tau	S	P-value (one tailed)	Alpha value	Sen's slope
WH	0.93	26	0	0.05	343.8
water	-0.43	-12	0.95	0.05	-335.54

The evolution of water hyacinth infestation in Lake Tana has been shown fast growth between its existence since 2011 and the current coverage. The area of water hyacinth was increased from 134ha in 2011 to 3019ha in 2019 by 96%. As Figure 4.9 depicts the trend of the invasive weed increased steadily from 2011 to 2019 except the area was decreased from 1197.20ha in 2015 to 914.91ha by 30% in 2016. This declined may be attributed to the low rainfall received in the Basin in 2015 year than all the remaining study periods or removal of hyacinth mats by the surrounding community. Because the local communities are making weed removal campaigns every year since 2012. For the last six years, more than 1,018,227 people were participated in Lake Tana to remove the weed manually (Implementation Guideline on Use of Neochetina Weevils for Water Hyacinth Control around Lake Tana, 2018). On the other hand, the spatial coverage of the water hyacinth in 2014 was more than tripled of 2012 coverage though 90 – 95% of the water hyacinth was basically removed from the Lake through this manual/physical removal approach as Wassie et al., (2014).

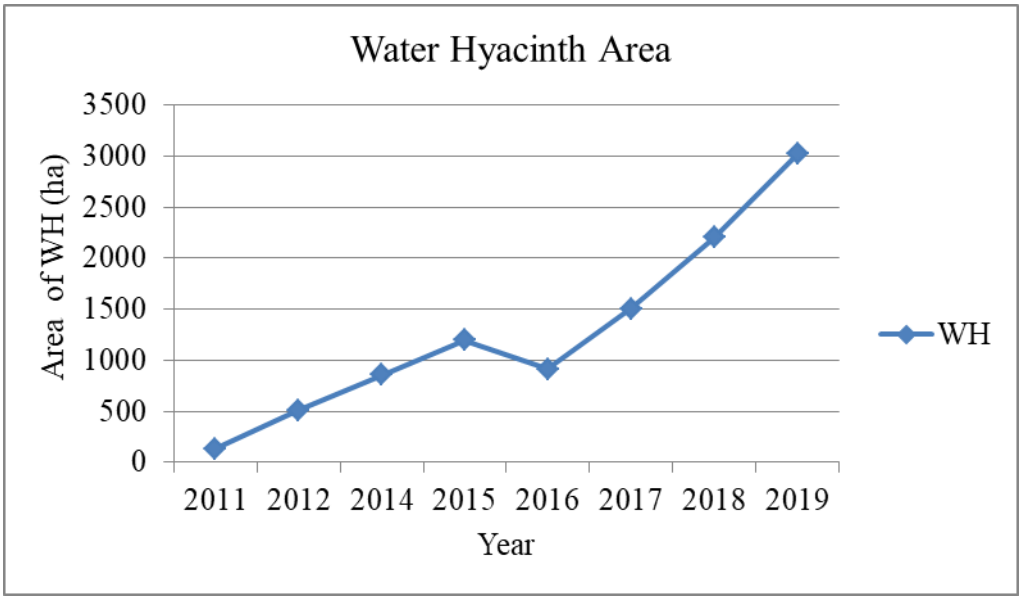

Figure 4.8 Area of Lake Tana occupied by water hyacinth as measured from satellite imagery

4.4.2 Monthly and Seasonal Spatio-Temporal Change Detection of Water Hyacinth

The analysis of consistent temporal satellite images showed that the areal extent and distribution of water hyacinth was fluctuating both monthly and seasonally from 2016 September to 2019 January time periods in the study area. Within consecutive months, the magnitude of change area of water hyacinth was varied from 34ha between November and December up to 622ha between October and September in 2016; 43ha between July and June up to 1004ha between October and November in 2017, and 17ha between February and March to 1057ha between September and October in 2018. This shows that the highest monthly variation has seen between September and December. However, within a year the highest change has been observed between November and July both in 2017 and 2018 years which was accounted for 85% and 79% change respectively. The proliferation pattern that manifests as high and low infestation periods observed in November and July possibly in correspondence with nutrient cycling, labor and mechanical removal of the weed and climatic regimes (Williams et al., 2005).

Table 4.6 Monthly spatio-temporal distribution change of water hyacinth (ha) in Lake Tana

2016	WH	Change	2017	WH	Change	2018	WH	Change
Ja	915		Ja	1504		Ja	2199	
Fe			Fe	1159	-345	Fe	1746	-453
Ma			Ma	970	-189	Ma	1729	-17
Ap			Ap	677	-293	Ap	1374	-355
Ma			Ma	524	-154	Ma	1273	-101
Ju			Ju	439	-85	Ju	908	-365
Jul			Jul	396	-43	Jul	821	-87
Au			Au	772	376	Au	957	136
Se	598		Se	1522	750	Se	1800	843
Oc	1220	622	Oc	1590	68	Oc	2857	1057
No	1546	326	No	2594	1004	No	3830	973
De	1512	-34	De	2308	-286	De	3237	-593
						2019 Ja	3019	-218

Note: the negative (-) sign is a decrease; the positive (+) sign is an increase of water hyacinth.

The spatial extent and distribution of water hyacinth considerably declined as the season cross from Bega to Kiremt in the same year. The area of weed in 2016 October to 2017 September time period has been decreased by 74% and 85% in Belg and Kiremt season respectively as compared to Bega season, then the proliferation of water hyacinth increase again by 64% from

2017 Kiremt (June - September) to Bega (2017 October - 2018 January) season. Similarly, the abundance of water hyacinth reduced from Bega to Belg by 42% and Kiremt by 93% from 2017 October to 2018 September time period and then rise up by 65 % in Bega (2018 October to 2019 January) season. Therefore, the seasonal change pattern of water hyacinth in Lake Tana from 2016 October to 2019 January time period revealed a periodic infestation reached a maximum in Bega and a minimum in Kiremt. The area of water hyacinth in the same season from 2017 Kiremt to 2018 Kiremt; 2017 Bega to 2018 Bega and 2017 Belg to 2018 Belg season was increase because as the season's changes (in months increasingly) every year the expansion of water hyacinth increase.

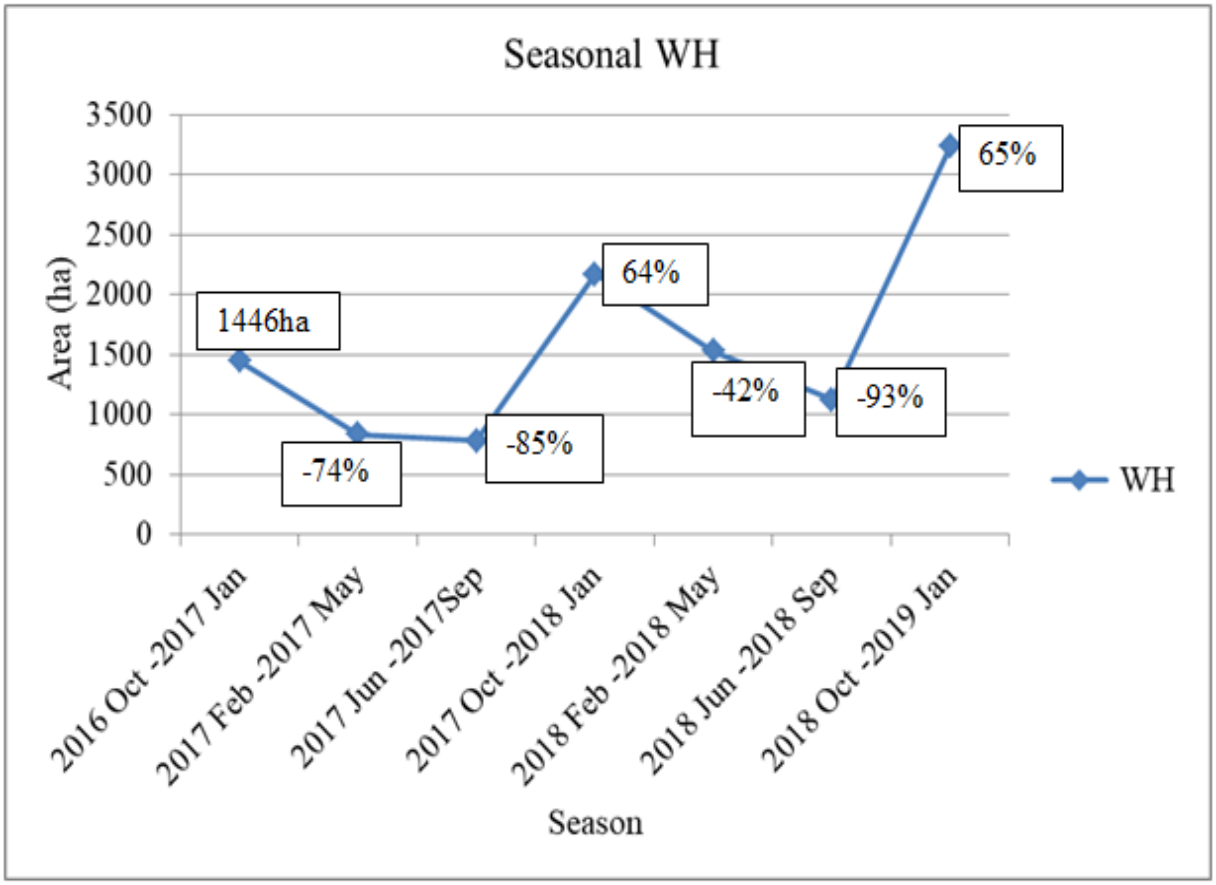

Figure 4.9 Seasonal change patterns of water hyacinth area from 2016 Oct to 2019 Jan

4.5 Spatio-Temporal Change Detection of Surface Area of Lake Tana

4.5.1 Spatio-Temporal Change of Annual Surface Area of Lake Tana

Timely and frequent observations of large water bodies can provide the information needed to reposition the resources at hand for interventions (e.g., mechanical removal) to mitigate the impact of aquatic vegetation such as water hyacinth (Cheruiyot et al, 2014). Surface water bodies are dynamic in nature as they shrink, expand, or change their appearance or course of flow with time, owing to different natural and human-induced factors (Karpatne et al., 2016). Variations in water bodies impact on other natural resources and human assets and further influence the environment. Therefore, it is crucial to efficiently detect the existence of a surface area of the Lake Tana, to extract its extent, to quantify and monitor its annual and seasonal dynamics. The result of satellite images analysis (summarized in Table 4.2) reveal that the annual maximum and minimum surface area of Lake Tana over the study period was 306,399ha (in 2015) and 302,952ha (in 2019) with an average surface area of 304,555ha and a standard deviation of 1,448 ha. The result further shows that the maximum annual surface area of the Lake change was about 3,448ha observed between 2015 and 2019, while a very small change occurred between 2017 and 2018 which was about 22ha (Figure 4.10). This is because of the rainfall influence in 2015, a high total annual mean rainfall of 1453mm was received in the Basin during 2014 year, while in 2019, 3,019ha of water surface was covered with water hyacinth. In addition, as Figure 4.10 clearly shows a minimum lake surface area next to 2019 was also observed during the year of 2016 due to the effect of 2015 year drought (total annual mean rainfall of 1214mm in the Basin which is less than all the remaining years in the study period) in Ethiopia. The total annual water surface area change of the Lake between 2011 and 2019 was about 1834ha implies an intense decreasing trend in Lake Tana surface area over the last 9 years. Therefore, the total change of the Lake over the study time period about 1834ha water surface which represents 0.6% of the average surface area of Lake Tana, (304,555ha). The maximal changes are observed around the northern and the eastern parts of the Lake due to the area are occupied by water hyacinth.

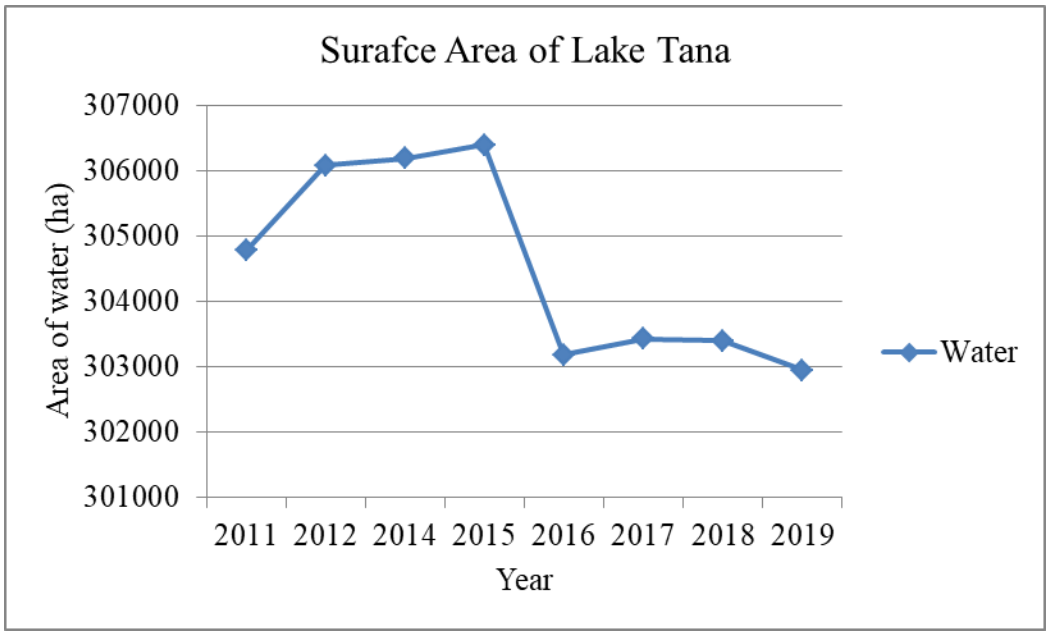

Figure 4.10 Annual water surface area change of Lake Tana from 2011 to 2019

4.5.2 Monthly and Seasonal Spatio-Temporal Change of Surface Area of Lake Tana

The analysis of the three years monthly satellite images indicate that the average monthly surface area of the Lake computed for 2016, 2017 and 2018 was 303,783ha, 304,382ha and 305,749ha. The highest surface area of the Lake was 311,586ha, 308,898ha and 317,257ha and the lowest area was 298,392ha, 300,199ha and 300,869ha respectively. The maximum surface area of Lake Tana during the whole monthly study period was 317,257ha observed in 2018 July, while the minimum was 298,392ha in 2016 June with a monthly average surface area of 304,638ha. All the minimum areas of the Lake of the three years were observed in June month while the maximum area of the Lake for 2016 and 2017 was seen in August and for 2018 year in July. The surface area change of the Lake Tana between the highest and the lowest area was varied from 8,699ha (2.82%) between 2017 August and June to 16, 388ha **(**5.20%) between 2018 July and June means that the amount of surface area of the Lake increased by rainfall per year was from 8,699ha up to 16, 388ha, and 13,194ha (4.23%) change was observed between 2016 August and June. The dynamic of the surface area of the Lake may be attributed to different natural and human-induced factors (Karpatne et al., 2016) in addition to the surface occupied by water hyacinth. The maximum surface area change of Lake Tana in consecutive months has been attained between July and June months to all the three years (Table 4.7).

Table 4.7 Monthly and seasonal surface area of Lake Tana (ha) from 2016 Jan to 2018 Dec

Month	2016	Change	2017	Change	2018	Change	Mean
Ja	303188		303428		303406		303341
Fe	302328	-860	302930	-498	303093	-313	302784
Ma	301428	-900	302091	-839	302780	-313	302100
Ap	300634	-794	301813	-278	302730	-50	301726
Ma	299233	-1401	300799	-1014	301747	-983	300593
Ju	298392	-841	300199	-600	300869	-878	299820
Jul	308989	10597	307106	6907	317257	16388	311117
Au	311586	2597	308898	1792	315229	-2028	311904
Se	306397	-5189	308453	-445	307271	-7958	307374
Oc	305532	-865	306944	-1509	305838	-1433	306105
No	304205	-1327	305501	-1443	304829	-1009	304845
De	303487	-718	304419	-1082	303943	-886	303950
Annual mean	303783		304382		305749		304638
Kiremt	306341		306164		310157		307554
Bega	304103	-2238	305073	-1091	304504	-5653	304560
Belg	300906	-3197	301908	-3165	302588	-1917	301801

Note: the negative (-) sign is a decrease; the positive (+) sign is an increase of area of the Lake.

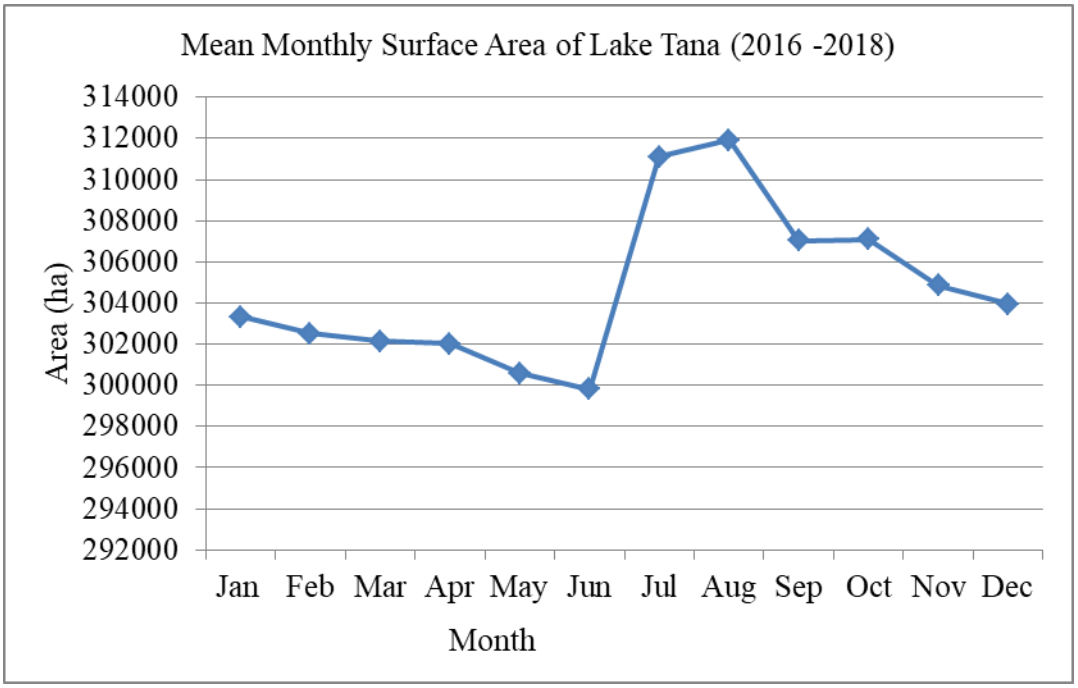

Figure 4.11 Monthly spatio-temporal variations in surface area of Lake Tana from 2016-2018

The mean seasonal amount of surface areas of the Lake have been analyzed and summarized in Table 4.7 as well. The seasonal surface area of Lake Tana in the seasonal study period varied from 300,906ha in 2016 Belg to 310,157ha in 2018 Kiremt. The mean seasonal surface area of Lake Tana ranged from 301,801ha (3018km^2) in Belg season to 307,471ha (3075km^2) in Kiremt season. This result has a small variation with surface area estimated by Amhara Design and Supervision Works Enterprise, 3035.3km^2 (dry season) – 3091.32km^2 (end of the rainy season), and seasonal lake level fluctuations, 2966km^2 to 3100km^2 (Derseh et al., 2019). This is could be the surface area of Lake Tana has been declined after the drought of the 2015 year and large areas of water surface have been occupied by water hyacinth. The maximum deviation in surface area of Lake Tana has been observed between Kiremt and Belg season which was about 5,435ha, 4,256ha and 7,569ha for 2016, 2017 and 2018 years respectively.

4.6 Analysis of Spatio-Temporal Distribution of Climate Variability in Lake Tana Basin

4.6.1 Analysis of Rainfall Data in Lake Tana Basin

The spatial and temporal variation of rainfall in Ethiopia is controlled by the movement of the position of the Inter-Tropical Convergence Zone, ITCZ (Agizew, 2010). The climate in the study area is largely influenced by western lies air from the Atlantic Ocean and minor rain is influenced by air movement from the Indian Ocean (Getachew, 2010). The mean total annual mean rainfall of the whole Basin was found to be 1331mm with a standard deviation of 76mm and a coefficient variation of 5.7% for a time period from 2011 to 2018 years (Table 4.8). Getachew, (2010) reported as the Lake Tana Sub Basin received an average total annual mean rainfall of 1329mm using 23 stations from 1992 – 2006 years. A similar result was found out by Agizew, (2010) the total annual mean rainfall of the whole Basin was 1330mm for a time series of 1992 – 2005 using a multiquadric method with a coefficient of variation of 2%. The lowest total annual mean rainfall (773mm) was observed in the northwestern part of the Basin, Delgi followed by Makisegnit (933mm) northern of the Basin and the highest rainfall 1751mm and 1723mm were recorded at Dangila and Wetet Abay of south west of the Basin respectively. This is supported by Birara et al., (2018), whose study confirms the highest and lowest total annual mean rainfall was observed in southwest and north of the Basin, respectively. Rainfall in the study area was found to be monomodal with the Kiremt season receiving more than 79% of the annual rainfall, while Bega and Belg contribute 8% and 13% to the annual rainfall. Total

seasonal mean rainfall in a rainy season mostly from June to September ranged from 896mm to 1232mm, Bega season (October -January) rainfall varied from 77mm to 135mm and Belg season (February -May) has deviated from 57mm to 305mm during last 8 years.

According to Hare, (2003) the coefficient of variation (CV) is used to classify the degree of variability of rainfall events as less (CV < 20), moderate (20 < CV < 30), and high (CV > 30). Based on this, the rainfall CV of Lake Tana Basin runs from 93 % to 148 % cross each season in a year which is extremely variable over the study period. From 2011 to 2018 time series Kiremt showed that low rainfall variability whereas Bega and Belg depicted moderate and high variability respectively which is consistent with the study of Birara et al., (2018).

Table 4.8 Total annual and seasonal mean rainfall (mm) from 2011 to 2018 years

Seasons	2011	2012	2013	2014	2015	2016	2017	2018	Mean	STD	CV1
Kiremt	885	1249	1136	1036	899	1019	964	1099	1036	123.3	11.9
Bega	74	77	137	124	136	85	81	147	108	31.1	28.8
Belg	169	57	97	366	181	233	239	118	182	97.7	53.7
CV2	118	148	129	93	106	113	110	123	117		
annual	1266	1368	1344	1453	1214	1386	1274	1343	1331	76.3	5.7

CV1 coefficient of variation for each season from 2011-2018, and CV2 is the coefficient of variation of the three seasons within a year from Kiremt to Belg both are in %.

Table 4.9 shows the monthly temporal variation of rainfall in the study area. The maximum mean monthly rainfall was observed in July month having a value of 354.3mm and the minimum mean rainfall was 1.1mm recorded in January. The mean monthly rainfall recorded from 2011 to 2018 was 110.9mm with a standard deviation and coefficient of variation 128mm and 115.42% respectively indicate that the monthly rainfall distribution is highly variable.

Table 4.9 Mean monthly rainfall (mm) of Lake Tana Basin from 2011-2018 years

Ja	Fe	Ma	Ap	Ma	Ju	Ju.	Au	Se	Oc	No	De
1.1	4	21	27	124.7	174	354.3	344.4	175.4	71.6	26.6	6.7

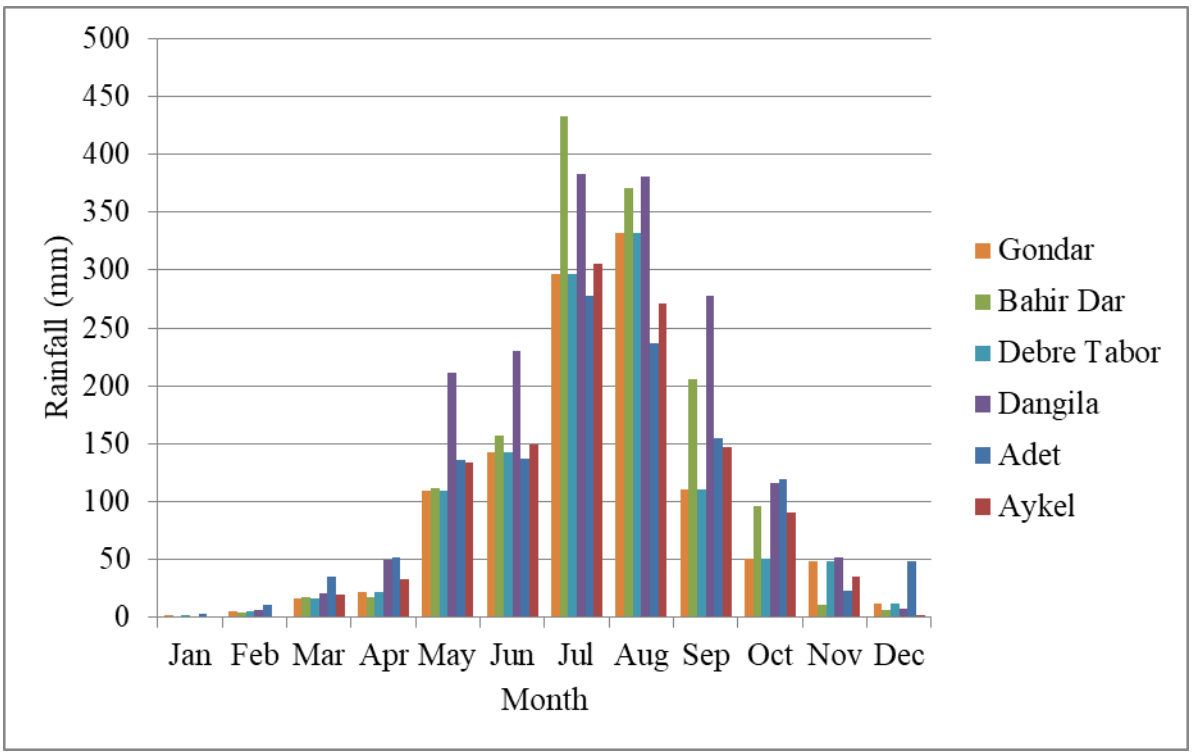

Figure 4.12 Mean monthly rainfall pattern of class 1 stations from 2011 to 2018 years

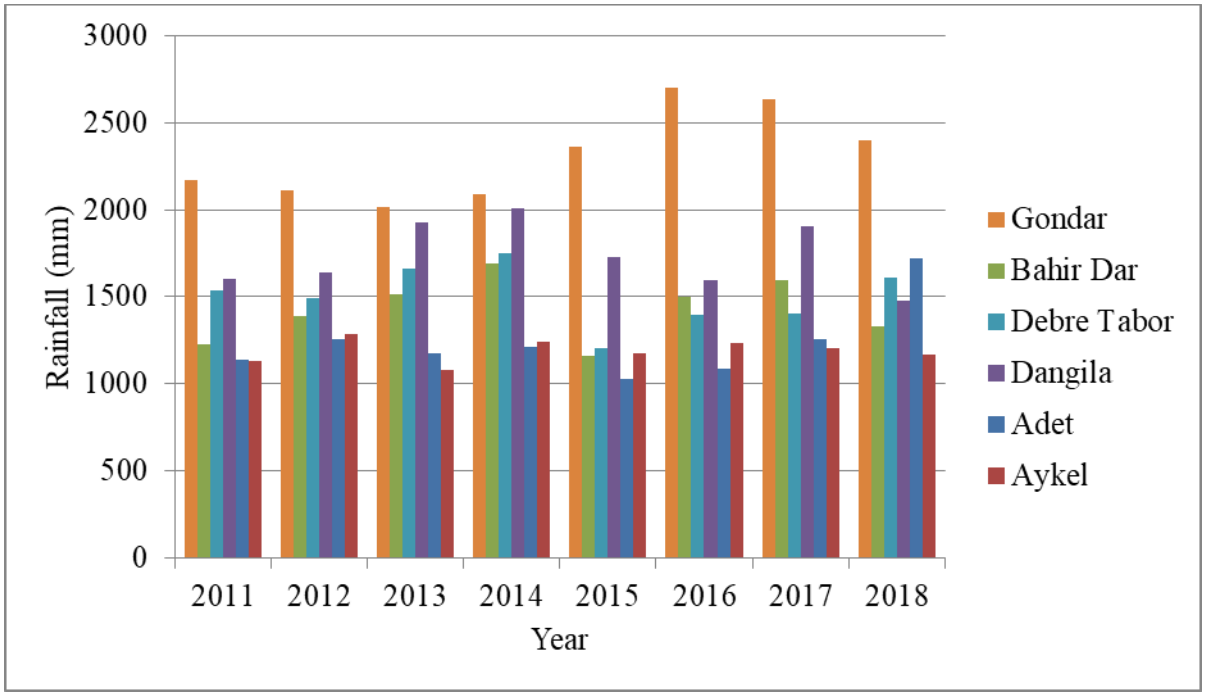

Figure 4.13 Variation of total annual rainfall in the Basin from 2011 to 2018 years

Spatial Distribution of Rainfall in the Lake Tana Sub-Basin

The mean total annual areal rainfall of Lake Tana Basin was taken to be 1355mm, 1362mm and 1372mm computed using inverse distance square, kriging, and Thiessen polygon spatial rainfall interpolation methods respectively. These values are differing from 1331mm value computed using simple arithmetic method. Within the study area, the distribution of rainfall varies locally, a higher amount of rainfall was observed in south and southeast mountainous side and relatively low rainfall was observed in the northern and western part, which indicates that precipitation increases with altitude (Agizew, 2010; Getachew, 2010; Birara et al., 2018).

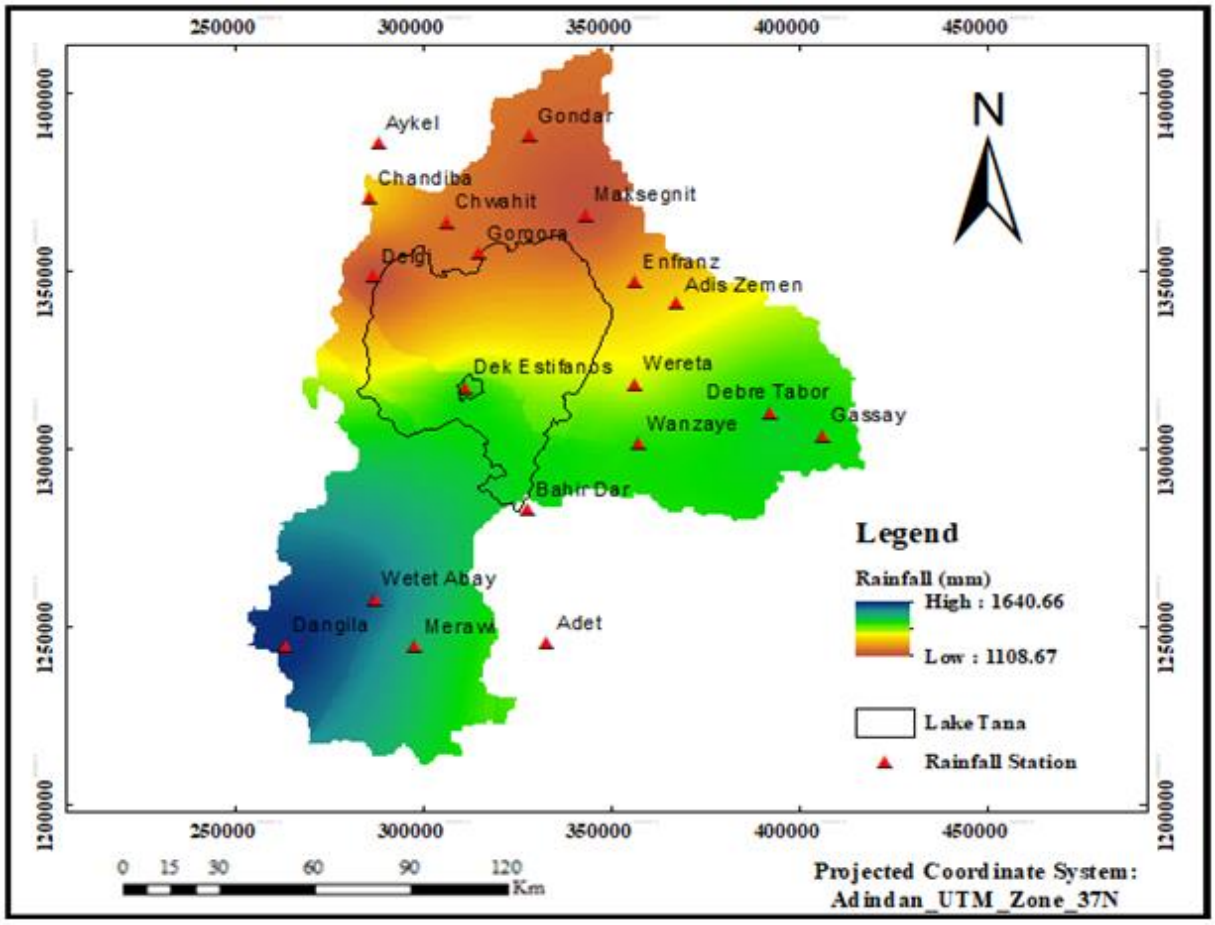

Figure 4.14 Spatial interpolation of total annual mean rainfall (mm) of Lake Tana Basin from 2011–2018 years using Ordinary Kriging method

4.6.2 Analysis of Temperature Data in Lake Tana Basin

The mean monthly temperature of Lake Tana Basin for the study period was varied from 12.3°C to 26.7°C with a mean of 19.5°C and a corresponding coefficient of variation of 0.1%. A close result of the mean annual temperature of the Basin was obtained as 19°C and 20°C by Agizew, (2010) and Getachew, (2010) respectively. The maximum and minimum annual mean temperatures were observed at Enfraz and Gasaye meteorological stations respectively.

Table 4.10 Mean annual and seasonal temperature variation in the study area (2011 -2018)

Season	2011	2012	2013	2014	2015	2016	2017	2018	Mean	STD	CV1
Kiremt	16.6	18.9	18.7	18.5	19.5	18.5	18.7	18.7	18.5	0.8	0.05
Bega	16.6	19.1	18.6	18.2	19.1	18.4	18.5	18.8	18.4	0.8	0.04
Belg	18.4	21.8	21.3	19.9	21.6	21.1	20.8	20.8	20.7	1.1	0.05
CV2	6.20	8.36	8.05	4.75	6.62	8.02	6.64	6.26	6.87		
Annual	17.2	20.0	19.6	18.9	20.1	19.3	19.3	19.4	19.2	0.9	0.05

CV1 coefficient of variation for each season from 2011-2018 and CV2 is coefficient of variation of the three seasons within a year from Kiremt to Belg both are in %.

The Basin experienced very little CV of annual and seasonal temperatures. Kiremt, Bega and Belg seasons had a CV of 0.05%, 0.04% and 0.05% respectively. A CV of the three seasons crosses within a year varied from 4.75 to 8.36% and the annual mean temperature of the Basin had a CV of 0.05%. Table 4.10 shows less seasonal variability of temperature in a year and the variability of each seasons was also less than 20%. The analysis of temperature recorded in 17 meteorological stations from 2011 to 2018 years indicated that the maximum mean monthly temperature was very high in Belg season (February-May) (NMA, 1996). The maximum mean monthly temperature was observed during April month was 29.4℃ followed by March (29.3℃) whereas the lowest maximum mean monthly temperature recorded during Kiremt season (June-September), mainly in July which was 23.7℃. Moreover, the highest minimum mean monthly temperature of the Basin was 13.7℃ which was occurred in the month of May, while the lowest was in December which was about 10℃. Therefore, April and December are warmest and the coldest months. Abel, (2018) found a similar results with only Bahir Dar station, and other study made by Addisu et al., (2015) based on 40 years meteorological data reveals the mean minimum and maximum temperature has recorded in the month of January and May in Lower Sub-Basin while, in the Upper Sub-Basin of Lake Tana has observed in February and March month. The

study of Birara et al., (2018) from 1980 - 2015 has shown April is the hottest month (28.8℃), followed by May (27.3℃) and July is the coolest month (13℃), followed by August (14.6℃).

Table 4.11 Maximum, mean and minimum monthly mean temperature (℃) variation of Lake Tana Basin from 2011 to 2018 years

	Ja	Fe	Ma	Ap	Ma	Ju	Jul	Au	Se	Oc	No	De	mean
Max	26.7	28.5	29.3	29.4	27.8	25.7	23.7	23.3	24.6	25.6	25.8	25.8	26.7
Mean	18.4	19.9	21.0	21.3	20.7	19.4	18.2	17.9	18.5	18.8	18.5	17.9	19.5
Min	10.1	11.3	12.7	13.2	13.7	13.1	12.6	12.6	12.4	12.0	11.1	10.0	12.3

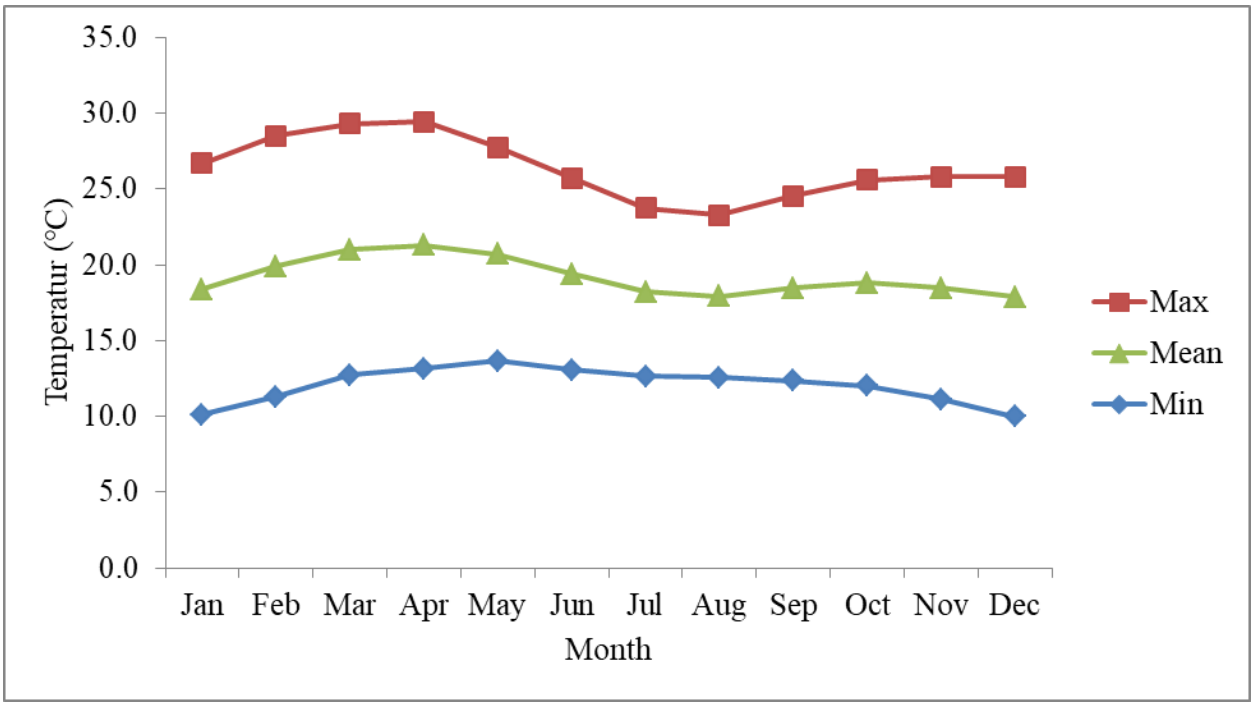

Figure 4.15 Maximum, mean and minimum monthly mean temperature distribution of Lake Tana Basin from 2011- 2018 years

High temperature value was recorded in the northern and eastern parts of the sub-basin, whereas low temperature is observed in the southern and southeastern of the Basin (Figure 4.16).

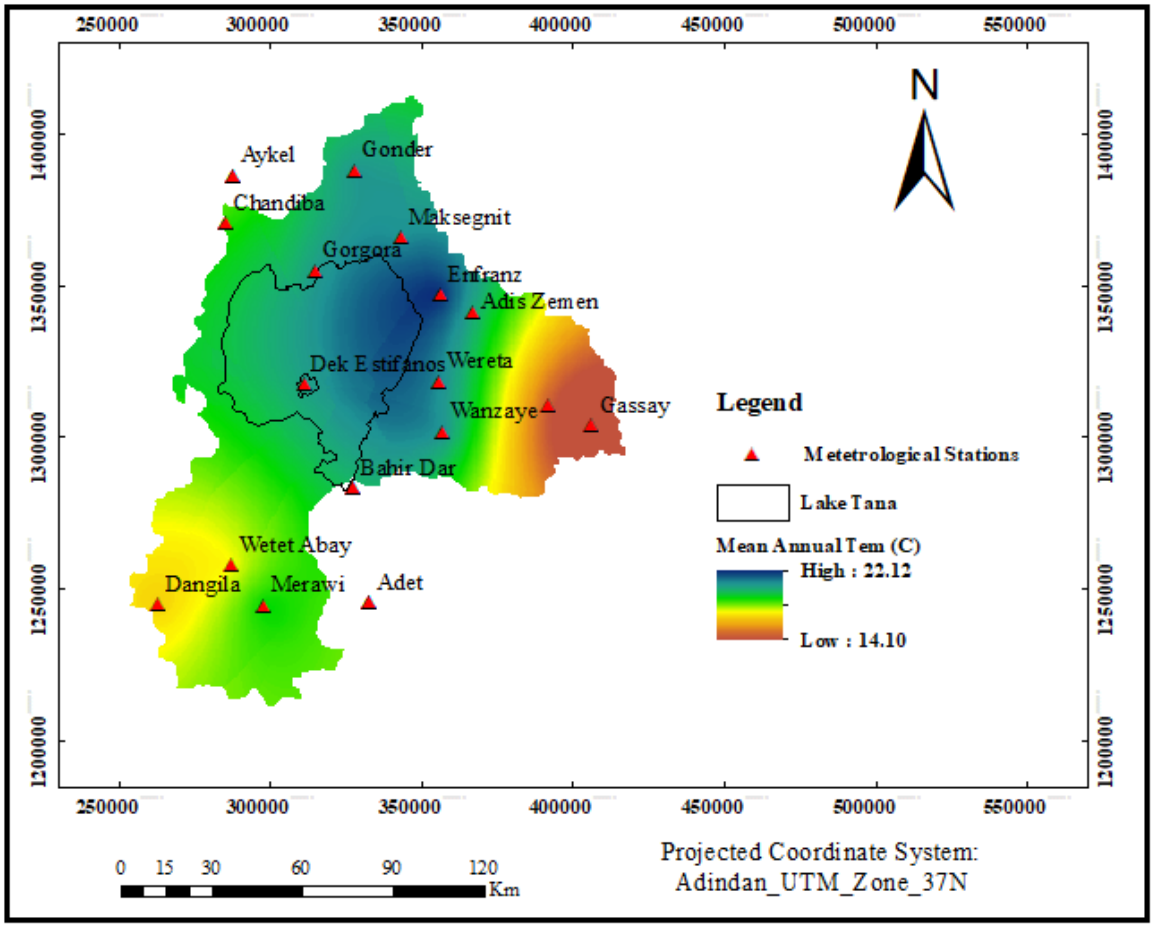

Figure 4.16 Spatial interpolation of annual mean temperature (°C) of the Basin from 2011 - 2018

4.6.3 Analysis of Wind Speed, Relative Humidity and Sunshine Hour Data

The mean monthly wind speed was ranged between 0.83m/s in September/October to 1.16m/s in April/May with a total mean monthly value of 0.96m/s and a standard deviation 0.12. The annual mean monthly wind speeds from 2011 to 2018 years were 1.02, 0.97, 1.10, 0.89, 0.91, 0.86, 0.90 and 0.43m/s respectively. Least mean seasonal wind speed variation was observed from 2011 to 2018 time period in the Basin which was about 0.98, 0.88 and 1.19 m/s for Kiremt, Bega and Belg season respectively. Wind speed also varies spatially in the study area; the maximum monthly wind speed was recorded at Gondar station and the minimum was at Bahir Dar station. A general south-north and west-east increase in wind energy distribution for Ethiopia characterized the wind speeds as stronger and weaker, respectively, during dry and wet seasons in the highland regions of Ethiopia (Mulugeta and Drake, 1996) confirms with the results in this study both in spatially and temporally.

Table 4.12 Monthly mean wind speed (m/s) at 2m above the ground surface from 2011 to 2018

Stations	Ja	Fe	Ma	Ap	Ma	Ju	Jul	Au	Se	Oc	No	De
Bahir Dar	0.69	0.78	0.93	1.00	0.93	0.84	0.76	0.66	0.68	0.62	0.68	0.59
Dangila	0.87	0.97	0.97	1.14	1.11	0.99	0.91	0.93	0.80	0.80	0.76	0.91
Debre Tabor	0.87	0.97	0.97	1.14	1.11	0.99	0.91	0.93	0.80	0.80	0.76	0.91
Gondar	1.18	1.32	1.38	1.37	1.50	1.37	1.07	1.05	1.05	1.08	0.95	1.09
Mean	0.90	1.01	1.06	1.16	1.16	1.05	0.92	0.89	0.83	0.83	0.79	0.88

The annual mean monthly values of relative humidity of the Basin from 2011 to 2018 years excluding 2013 were 59.7, 59.7, 60.1, 57.6, 60.9, 58.5 and 60.5 respectively while; the mean monthly relative humidity was ranged from 39.9% to 81.3% with an average value of 59.6%. The highest and lowest relative humidity values were recorded at Dangila and Bahir Dar station.

Table 4.13 Mean monthly relative humidity (%) of the study area from 2011 to 2018

Stations	Ja	Fe	Ma	Ap	Ma.	Ju	Jul	Au	Se	Oc	No	De
Bahir Dar	43.6	40.2	41.4	39.9	55.6	65.3	75.3	77.7	73.3	63.9	56.7	50.8
Dangila	54.5	47.0	44.9	42.2	58.6	76.0	83.0	83.2	79.1	74.1	69.4	62.1
Debre Tabor	44.9	44.8	40.3	42.3	60.8	68.3	77.6	82.2	75.4	69.4	61.2	51.9
Gondar	42.8	39.3	37.3	35.3	49.3	66.4	80.3	82.2	75.0	66.1	58.8	51.9
Mean	46.5	42.8	41.0	39.9	56.1	69.0	79.0	81.3	75.7	68.4	61.5	54.2

The annual mean sunshine hours in Lake Tana Basin from 2011 to 2018 time periods computed as 7.2, 7.3, 7.2, 6.9, 7.4, 7.2, 7.1 and 7.2 respectively. The maximum sunshine hour was recorded at Bahir Dar station and the minimum sunshine hour was observed at Gondar station. The sunshine hour decreases from May to August and rises from September to March. The whole mean monthly sunshine hour of the Basin derived from four class one stations found to be 7.2.

Table 4.14 Mean monthly sunshine hours (hr/day) of the study area from 2011 to 2018

Stations	Ja	Fe	Ma	Ap	Ma	Ju	Jul	Au	Se	Oc	No	De
Bahir Dar	9.7	9.8	9.2	9.3	8.0	6.8	5.1	4.4	6.4	8.6	9.3	9.7
Dangila	8.9	9.2	8.2	8.3	6.5	5.9	3.9	4.0	5.7	6.4	7.7	8.6
Debre Tabor	8.7	8.8	7.8	7.7	7.1	6.4	4.6	4.6	6.5	7.0	7.5	8.6
Gondar	8.8	9.0	7.4	7.4	6.5	4.5	4.0	4.4	5.5	7.4	8.3	8.5
Mean	8.4	8.8	9.1	9.2	7.0	5.9	4.4	4.4	6.0	7.3	8.1	8.2

4.7 Estimation Water Losses Due To Evapotranspiration of Water Hyacinth

The reference evapotranspiration (ETo) was computed by the FAO Penman-Monteith method, using decision support software – CROPWAT 8.0 developed by FAO (Sasaqi et al., 2019). The highest value of reference evapotranspiration was 4.7 mm/day recorded in the month of April 2017, while, the lowest value of reference evapotranspiration was 2.93 mm/day obtained in 2016 December. Table 4.15 presents the results calculation of reference evapotranspiration, evapotranspiration of water hyacinth and water losses from 2016 September to 2018 December.

Table 4.15 Reference evapotranspiration, evapotranspiration and water losses of water hyacinth from 2016 September to 2018 December

2016	Tmin	Tmax	RH	U_2	SHr	ETo	ET_C (0.65)	ET_C (1.90)	Water loss (Kc=0.65)	Water loss (Kc=1.90)
18-Se	12.9	26.0	74.7	0.7	5.3	3.17	2.06	6.02	12322	36018
20-Oc	13.2	27.6	65.0	0.6	6.8	3.26	2.12	6.19	25852	75567
21-No	11.9	27.5	53.0	0.7	8.7	3.13	2.03	5.95	31453	91941
23-De	11.7	27.8	46.5	0.9	9.4	2.93	1.90	5.57	28796	84173
Average	12.4	27.2	59.8	0.7	7.5	3.28	2.03	5.93	24606	71925
2017	Tmin	Tmax	RH	U_2	SHr	ETo	ETc (0.65)	ETc (1.90)	Water loss (Kc=0.65)	Water loss (Kc=1.90)
22-Ja	11.5	28.1	48.7	0.9	7.5	3.6	2.33	6.80	34998	102302
25-Fe	13.9	28.7	42.8	1.0	8.0	4.1	2.68	7.83	31038	90727
29-Ma	14.6	29.6	38.1	1.1	6.6	4.4	2.83	8.27	27427	80171
30-Ap	15.6	30.4	36.1	1.1	7.0	4.8	3.09	9.03	20916	61139
21-Ma	15.8	27.8	66.3	1.0	5.9	4.0	2.61	7.62	13646	39889
17-Ju	14.9	26.8	69.2	1.0	4.5	3.5	2.30	6.73	10096	29511
16-Jul	13.7	25.7	75.3	0.9	3.5	3.1	2.03	5.93	8032	23478
25-Au	13.4	25.3	78.1	0.8	3.3	3.0	1.94	5.68	15004	43857
24-Se	13.6	26.1	74.7	0.8	4.5	3.3	2.12	6.19	32250	94270
24-Oc	14.3	26.7	65.0	0.7	6.0	3.4	2.24	6.54	35558	103940
23-No	13.1	27.1	53.0	0.7	6.6	3.3	2.16	6.31	55983	163642
23-De	11.6	27.4	46.5	0.8	7.1	3.3	2.16	6.33	49952	146013
Average	13.8	27.5	57.8	0.9	5.9	3.7	2.37	6.94	27908	81578

2018	Tmin	Tmax	RH	U_2	SHr	ETo	ET_C (0.65)	ET_C (1.90)	Water loss (Kc=0.65)	Water loss (Kc=1.90)
27-Ja	12.3	27.3	45.0	0.9	9.0	3.8	2.44	7.14	53731	157061
22-Fe	13.6	28.5	39.4	0.9	8.9	4.2	2.71	7.92	47317	138311
16-Ma	14.4	29.3	33.6	1.0	9.7	4.9	3.19	9.33	55175	161282
27-Ap	14.6	29.4	36.4	1.0	8.8	4.9	3.19	9.33	43853	128185
19-Ma	15.3	29.6	49.8	1.1	7.6	4.7	3.04	8.87	38636	112936
4-Ju	15.1	27.0	72.1	1.0	5.9	3.8	2.48	7.24	22478	65706
31-Jul	14.8	25.3	77.0	0.9	3.8	3.2	2.05	5.99	16809	49133
15-Au	14.7	24.9	77.9	0.8	4.2	3.2	2.08	6.08	19906	58186
24-Se	14.9	26.4	68.8	0.8	6.4	3.8	2.44	7.14	43995	128602
26-Oc	15.0	27.0	65.8	0.7	6.4	3.5	2.29	6.71	65551	191611
11-No	14.6	27.0	61.3	0.6	7.3	3.4	2.20	6.42	84148	245971
18-De	12.9	28.0	54.1	0.7	8.5	3.5	2.29	6.69	74071	216515
Average	14.4	27.5	56.8	0.9	7.2	3.9	2.53	7.41	47139	137791

Note: Tmin & Tmax = minimum and maximum temperature (℃), RH = Relative humidity (%), U_2 = Wind speed at 2 meter height (m/s), SHr = Sunshine (Hr), ETo = Reference evapotranspiration (mm/day), ETc = Evapotranspiration (mm/day), water loss (m^3/day).

The highest daily evapotranspiration of water hyacinth in Lake Tana from 2016 September to 2018 December observed in April 2018 which was about 3.19 and 9.33 mm/day and the lowest value was about 1.90 and 5.57 mm/day revealed in 2016 December using crop coefficient value, Kc of 0.65 and 1.90 respectively, and the average daily evapotranspiration's of the weed using the these two Kc values in the above time frame were 2.39 mm/day and 6.99 mm/day. For Kc value of 0.65, the evapotranspiration water hyacinth is less than the reference evapotranspiration in the study period (Table 4.15) disagrees with the results of Timmer and Weldon, (1967); Gopal, (1987); Ali and El-Din Khedr, (2018) and Sasaqi et al., (2019) which study revealed that the evapotranspiration of water hyacinth is higher than the evaporation from free water surface, while it agrees with results of Agutu et al., (2018); Gavin and Agnew, (2000), areas covered by water hyacinth has lower evapotranspiration than open water surface areas of the lake.

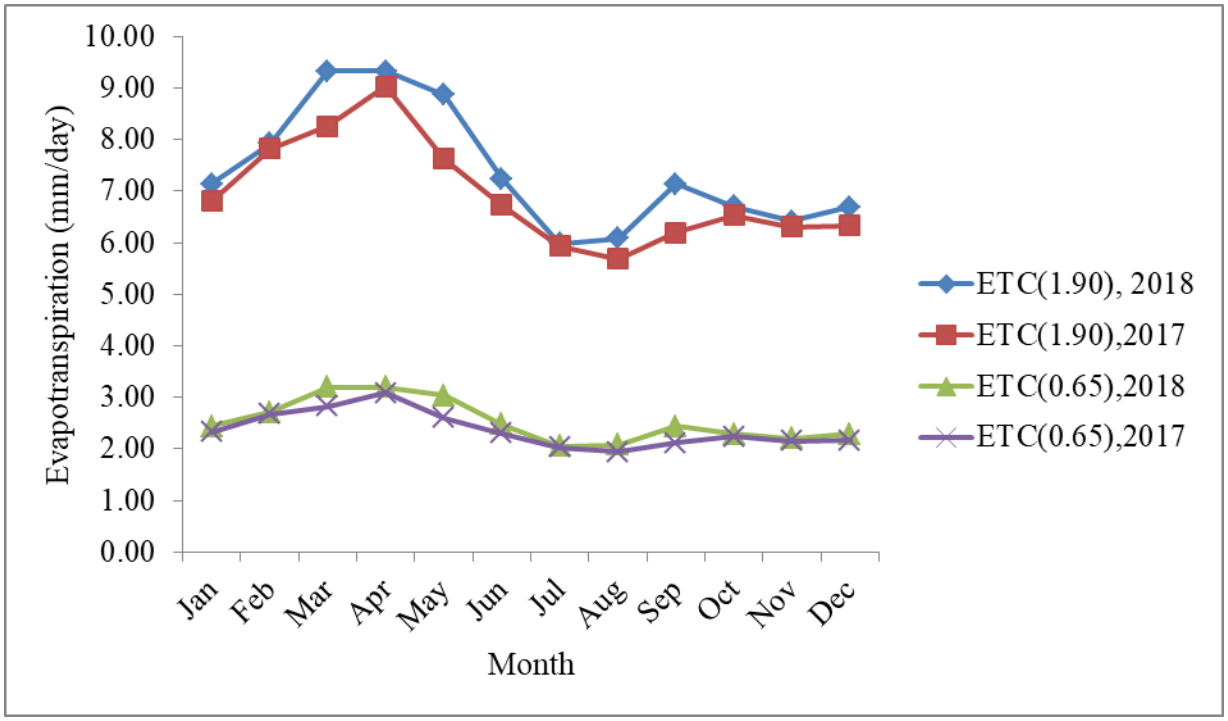

Figure 4.17 water hyacinth evapotranspiration in Lake Tana from 2017 Jan – 2018 Dec

The water losses due water hyacinth evapotranspiration using Kc value of 0.65 was between 8,032 m^3/day on July 21, 2017 and 84,148 m^3/day on November 11, 2018 having an average value of 35,678 m^3/day, while the water losses using Kc value = 1.90 varied from 23,478 m^3/day on 21, July 2017 to 245,971 m^3/day on November 11, 2018 having an average value of 104,290 m^3/day. Although the highest evapotranspiration of water hyacinth observed in 2017 April month, the greater water losses was observed in November 2018 due to high infestation of water hyacinth in this month. The surface area of water hyacinth influences the amount of water loss; extensive coverage of water hyacinth causes greater water loss and low coverage causes low water loss (Ali and El-Din Khedr, 2018 and Sasaqi et al., 2019). The total amount of water losses from Lake Tana from 2016 September to 2018 December time period (with only 2.4 years) through evapotranspiration of water hyacinth was 30,397,918 m^3 and 88,855,452 m^3 using Kc value of 0.65 and 1.90 respectively. This means that a minimum of 30,397,918 m^3 and maximum of 88,855,452 m^3 volume of water was lost from Lake Tana due to the invasive water hyacinth. The average of the two volumes is approximately 60,000,000 m^3 represents 0.21 % of the volume (28.4 km^3) of Lake Tana.

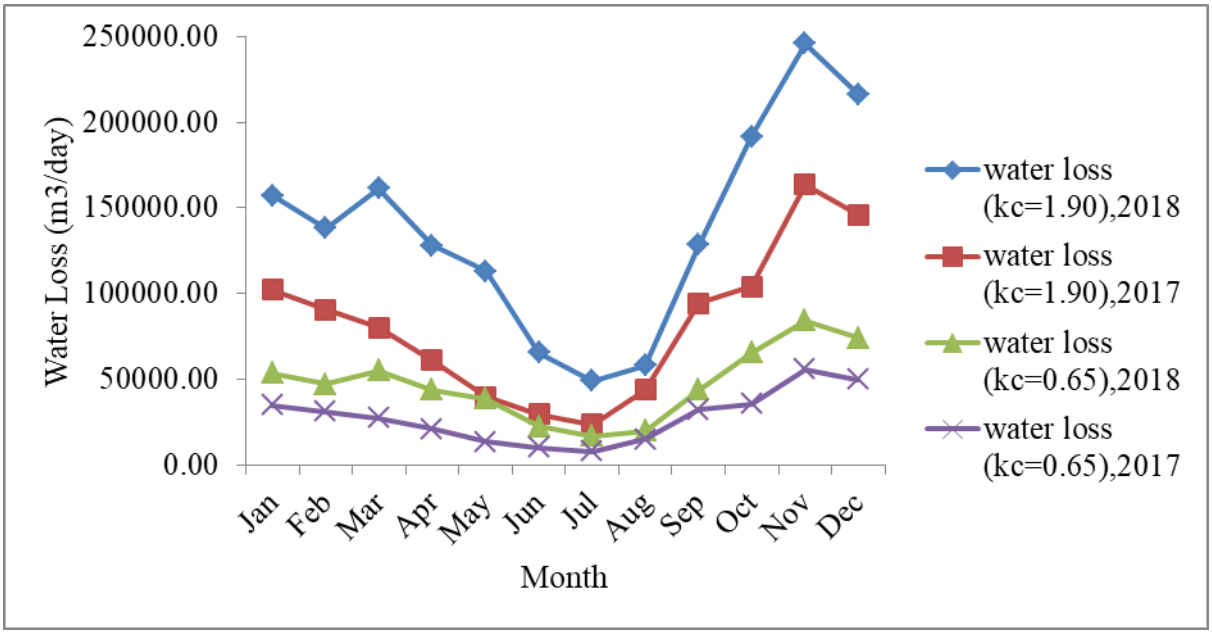

Figure 4.18 water losses due to water hyacinth evapotranspiration in Lake Tana (2017 -2018)

4.8 The Association of Water Hyacinth Area with Climate Elements and Surfaces Area of Lake Tana

The impacts of climate changes on the water hyacinth dynamics are of paramount importance even if nothing can be done to control the climatic conditions and whatever their contributions to the proliferation of hyacinth. It is necessary to understand the effects or contributions of climate in the scientific sense and as an early warning system for economic reasons (Ouma et al., 2005). To analyze the effects of variability in climatic elements on water hyacinth dynamics, the Pearson correlation coefficient was used to see the relationship between the area of water hyacinth with rainfall, temperature, wind speed and surface area of Lake Tana (Table 4.16).

Table 4.16 Result of correlation of water hyacinth with climatic elements and surface area of Lake Tana

	WH vs RF		WH vs Water		Water vs RF		WH vs T		WH vs Wind Speed	
	R	P	R	P	R	P	R	P	R	P
Annual	0.34	0.41	-0.60	0.11	0.29	0.49				
Seasonal	-0.72	0.49	-0.15	0.90	0.79	0.42	-0.36	0.76	-0.62	0.57
Monthly	-0.63	0.03	-0.03	0.92	0.69	0.01	-0.34	0.28	-0.59	0.04

WH=area of water hyacinth, RF= rainfall, T = temperature, water = surface area of the Lake.

The statistical Pearson correlation analysis have shown that low positive correlation was exist between annual area of water hyacinth and rainfall (r =0.34, p=0.41), moderate negative correlation between annual area of water hyacinth and surface area of the Lake (r= -0.60, p=0.11), weak positive correlation between surface area of the Lake and rainfall (r=0.29, p=0.49) with a significance level alpha at 0.05 in Lake Tana Basin from 2010 to 2019, all of these correlations are insignificant (as the p-value >alpha value).

The monthly Pearson correlation analysis result revealed that monthly water hyacinth and monthly rainfall in the Basin had a moderately negative correlation with a coefficient of determination (r = -0.63, p = 0.03, less than the alpha value which is significant). The correlation of mean monthly temperature and mean monthly wind speed with water hyacinth was low negative (r = -0.34, p = 0.28) and moderately negative (r = -0.59, p = 0.04) respectively. This indicates that the effect of monthly temperature on the distribution of water hyacinth is insignificant while wind speed has a significant negative effect on the spread of the weed. On the other hand, the relationship between monthly water hyacinth area and monthly surface area of the Lake was insignificant weakly negative (r = - 0.03, p = 0.92 > a = 0.05). However, the surface area of the Lake showed significant moderately positive correlation with monthly rainfall in the Basin, (r = 0.69, p = 0.01) with alpha value of 0.05 over the monthly study period.

The Pearson correlation coefficient of the seasonal area of water hyacinth with the seasonal mean rainfall and wind speed was moderately negative (r= -0.72, p=0.49) and (r= -0.62, p=0.57) with a significance level alpha of 0.05 respectively. Low negative correlation (r = -0.36, p = 0.76) with mean temperature was also attained in seasonal period. The negative linear relationship that exists between the variables was insignificant since the p-value 0.49, 0.76 and 0.57 for rainfall, temperature and wind speed are greater than the alpha value (0.05). Close to this result, Krishnaveni, (2010) found a low correlation between the aquatic weed area with average rainfall and temperature which was 0.38 and -0.50 respectively. The correlation of seasonal lake surface area with seasonal water hyacinth area and rainfall was insignificant weakly negative (r = -0.15, p = 0.90) and moderately positive (r = 0.79, p = 0.42) respectively. This implies that the seasonal surface area of Lake Tana is more importantly affected by the total amount of rainfall in the Basin than the area of water hyacinth due to the total areal coverage of water hyacinth in Lake Tana is almost equal to 1 % of the surface area of the Lake.

The negative correlation between rainfall and area of water hyacinth in seasonal and monthly time periods could be due to signal saturation above certain biomass values, to a deficit of solar radiation used for the photosynthesis because of cloud (Camberlin et al., 2007; Song and Ma, 2008). Heavy rains that manifest the higher rates of run-off (Humberto et al., 2012), and rainfall in the form of runoff is a major cause for population size reduction in aquatic plants (Kitamura et al., 2016). Water hyacinth needs stagnant water and shallow depth of lake (Derseh et al., 2019). Similarly, the study of Ouma et al., (2005) reveals that moderate rainfall amounts are optimal for water hyacinth propagation, very high and very low rainfall slows the proliferation of the weed.

Based on the above relationship, it is possible to say that rainfall has indirectly contribution for proliferation of water hyacinth by transporting nutrients during rainy season from the Basin despite the correlational analysis between the area of water hyacinth and rainfall shows a negative relationship in both seasonal and monthly time periods. It is important to considered that the highest infestation of water hyacinth observed in Bega season after Kiremt, for instance, 1091 to 5653 hectares of the Lake surface has been changed to land surface from 2016 Sep to 2019 Jan as the season cross from Kiremt to Bega which creates comfortable situation for growth of water hyacinth because the weed spreads fast in inshore and shallow areas with mud bed surfaces (Mitchell, 1976; Willoughby et al., 1993), and in high nutrient level shores (Twongo, 1993; Albright et al., 2004). However, the spatial correlation of rainfall in Lake Tana Basin with the existence location of water hyacinth is opposite, higher rainfall value has been observed in southern (with no water hyacinth) and southeastern (low water hyacinth) of the sub-basin and relatively low rainfall in the northern (with high water hyacinth) and western part of the Basin (see Figure 4.14). Large area of the weed has been observed in northern and eastern shoreline of the Lake in which the area has manifest higher temperature values (Figure 4.16). The correlation between water hyacinth and wind speed was moderately negative in monthly and seasonal periods implies that as the wind speed increase, the area of water hyacinth decrease this is only happens when the wind blows from lake surface towards to the land surface otherwise the reverse is true since the influence of current and wind speed on the distribution of water hyacinth is depend on the direction of wind blows.

CHAPTER FIVE

5 CONCLUSIONS AND RECOMMENDATIONS

5.1 Conclusions

Reliable estimates of water hyacinth distribution and extent are required to gauge the severity of the problem through time, relate water hyacinth abundance to environmental factors, identify areas requiring management action, and assess the efficacy of management actions. The study used 41 different date periods of satellite images from Landsat 7 ETM+, Landsat 8 OLI and Sentinel 2 images, and meteorological data from NMA. The combined use of satellite images such as Landsat 8 and Sentinel 2 is highly important to overcome the problem of heavy cloud noise of the images in summer season by using them alternatively. A hybrid image classification approach of supervised, unsupervised and manual digitizing image classification was employed to detect the annual and seasonal distribution and extent of water hyacinth and surface area of Lake Tana. Mann-Kendall trend test was employed to see the trend of water hyacinth and surface area of the Lake. The impact of climate variability on water hyacinth spreads was studied using Pearson correlation coefficient, and the evapotranspiration and water losses were estimate from reference evapotranspiration which was computed using FAO-56 Penman-Monteith method, and a crop coefficient value of 0.65 and 1.90.

Unlike the previous studies made in Lake Tana, the results of this study indicate that there has been a statistically significant increment of annual spatial coverage of water hyacinth in the Lake from 2011 to 2019. The annual area of water hyacinth increased from 134ha in 2011 to 3019ha in 2019 by 96%. The infestation of water hyacinth has been observed in the north and east shoreline of Lake Tana in the whole study periods. However, the surface area of the Lake showed a decreasing trend while the rainfall availability does not show any trend in the Basin. A total of 1834ha of surface area of the Lake (0.6 % of the average surface area of the Lake) has lost over the last nine years. The annual maximum and minimum lake surface area observed was 306,399ha (in 2015) and 302,952ha (in 2019) with an average surface area of 304,555ha.

The monthly and seasonal spatial-temporal dynamics of water hyacinth in Lake Tana from 2016 September to 2019 January exhibit a periodic cyclical patterns, reaching the highest peak in Bega (October to January) and followed by a decline to least coverage level in Kiremt season (June to

September). The peak areal extent of monthly water hyacinth was 3830ha observed in November 2018 while the minimum was 396ha in 2017 July. The surface area of the Lake was varied from 298,392ha in Belg (2016 June) to 317,257ha in Kiremt season (2018 July) with a monthly average surface area of 304,699ha. The lowest and the highest seasonal average surface area of the Lake were 301,817ha in Belg and 307,471ha in Kiremt season from 2016 Jan -2018 Jan.

The evapotranspiration of water hyacinth in Lake Tana varied from 1.9 mm/day in December 2016 to 9.33 mm/day in April 2018. The water losses due water hyacinth evapotranspiration was ranged from 8,032 m^3/day on July 21, 2017 to 245,971 m^3/day on November 11, 2018, and the total amount of water losses from 2016 September to 2018 December in Lake Tana due to water hyacinth was between 30,397,918 m^3 and 88,855,452 m^3 using a Kc value of 0.65 and 1.90.

The statistical Pearson correlation analysis has shown insignificant low positive correlation between annual area of water hyacinth and rainfall (r = 0.34, p =0.41), insignificant moderately negative correlation between annual area of water hyacinth and surface area of the Lake (r = -0.60, p=0.11), insignificant weakly positive correlation between surface area of the Lake and rainfall (r=0.29, p=0.49) with a significance level alpha 0.05. The correlation of monthly water hyacinth and rainfall in the Basin had a moderately negative correlation (r = -0.63 and p = 0.03, less than the alpha value) which is significant. The correlation of mean monthly temperature and mean monthly wind speed with water hyacinth was negative (r = -0.34, p = 0.28) and (r = -0.59, p = 0.04) respectively. The correlation between the monthly water hyacinth area and surface area of the Lake was statistically insignificant weakly negative (r = - 0.03 and p = 0.92 > alpha value). However, the surface area of the Lake showed a moderately significant positive correlation with monthly rainfall in the Basin (r = 0.69 and p = 0.01) with alpha value of 0.05. The seasonal Pearson correlation of area of water hyacinth with rainfall and wind speed was insignificant moderately negative (r= -0.72, p=0.49) and (r= -0.62, p=0.57) respectively. Insignificant low negative correlation (r = -0.36, p = 76) with mean temperature was also attained. The correlation of seasonal lake surface area with water hyacinth and rainfall was insignificant weakly negative (r = -0.15, p = 0.90) and positive (r = 0.79, p = 0.42) respectively. The negative correlation between rainfall and area of water hyacinth in seasonal and monthly periods may be due to heavy rains that manifest the higher rates of run-off which causes the reduction of water hyacinth biomass and because of the weed needs stagnant water and shallow depth of lake. The climate

variability in Lake Tana Basin in general showed a less and insignificant contribution for distribution and spread of water hyacinth over the Lake this may be linked to spatio-temporal variability of nutrient level inshore in the Lake influence more than the seasonal climate variability.

The spatial coverage of water hyacinth increases steadily from year to year while a manual and mechanical removal of the weed management made since 2012. The control and management methods of the weed employed so far should be critically and thoroughly evaluated, and an important mitigation approach against the rapid spread of the weed in Lake Tana Basin should be adopted may focus on a better land management practices and strategies aimed at limiting pollution and soil erosion within the Lake's Basin.

5.2 Recommendations

Based on the finding of the study, the following recommendations are suggested for future research.

- No single factor may possibly be responsible for the proliferation of water hyacinth in the aquatic system. In addition to climate factors, the spatio-temporal concentrations of nutrients and alterations to the composition of the shore; human activities and agricultural practices and managements in Lake Tana Basin need to be assessed.
- The current study tried to address only the infestation of water hyacinth in Lake Tana, the future research needs to study the land-based water hyacinth and other water bodies (rivers) system which requires more involvement of ground survey-based approach.
- It is advisable for future research to study the long term spatio-temporal dynamics of Lake Tana before and after the existence of water hyacinth to understand other factors contributes to the reduction of the Lake size.
- In this study only the impact of evapotranspiration of water hyacinth has been studied, it is important to study the effect of the weed on the water balance and lake level of Tana.
- The influence of monthly and seasonal Lake wind and current speeds and their directions should be investigated critically in the future works and,
- The monthly crop coefficient (Kc) of water hyacinth in Lake Tana should be studied with some sort of experiment to estimate the evapotranspiration of the weed accurately.

REFERENCE

Abel Belete. (2018). Impacts of land-use and land-cover changes on land surface temperature distribution in Bahir Dar town and its surrounding using remote sensing. MSc. Thesis Addis Ababa University, Ethiopia.

Acharya, T. D., Lee, D. H., Yang, I. T., & Lee, J. K. (2016). Identification of water bodies in a Landsat 8 OLI image using a J48 Decision Tree. *Sensors*, 16(7), 1075.

Adams, C.S. Boar, R.R., Hubble D.S., Gikungu, M. Harper, D.M. Hickley H. and Tarras Wahlberg, N. (2002). The dynamics and ecology of exotic tropical species in floating plant mats: Lake Naivasha, Kenya, *Hydrobiologia,*Vol. 488 No. 168, pp. 115-122.

Addisu, S., Selassie, Y. G., Fissha, G., and Gedif, B. (2015). Time series trend analysis of temperature and rainfall in lake Tana Sub-basin, Ethiopia. *Environmental Systems Research*, 4(1). Doi: 10.1186/s40068-015-0051-0.

Agizew Nigussie. (2010). Hydrological and suspended sediment modeling in the Lake Tana Basin, Ethiopia. Hydrology. Université Joseph-Fourier - Grenoble I, 2010.

Agutu, P., O., Gachari, M., K., and Mundia, C.,N. (2018). An assessment of the role of water hyacinth in the water level changes of Lake Naivasha using GIS and remote sensing. *American Journal of Remote Sensing*. Vol. 6, No. 2, 2018, pp. 74-88. doi: 10.11648/j.ajrs.20180602.13.

Albright, T., Moorhouse, T., McNabb, T., (2004). The rise and fall of water hyacinth in Lake Victoria and the Kagera River Basin, 1989–2001. *J. Aquat. Plant Manag*. 42, 73–84.

Alexandridis, T. K., Takavakoglou, V., Crisman, T. L., & Zalidis, G. C. (2006). Remote sensing and GIS techniques for selecting a sustainable scenario for Lake Koronia, Greece. *Environmental Management*, 39(2), 278–290. Doi: 10.1007/s00267-005-0364-2.

Ali, Y. M., & El-Din Khedr, I. S. (2018). Estimation of water losses through evapotranspiration of aquatic weeds in the Nile River (Case study: Rosetta Branch). *Water Science*, 32(2), 259 275. https://doi.org/10.1016/j.wsj.2018.08.002.

Allen, R. G., L. S. Pereira, D. Raes, and M. Smith. (1998). Crop evapotranspiration: guidelines for computing crop water requirements. International proceedings of the irrigation and drainage paper No. 56. Food and Agricultural Organization, United Nations, Rome, Italy.

Amare, S. (2015). Land use/cover change at Infraz Watershed, Northwestern Ethiopia. *Journal of Landscape Ecology, 8(1):69-83.*

Aplin, P. (2005). Remote sensing: ecology. *Progress on Physical Geography*, 29:104-113.

Bicudo, D., Fonseca, B., Bini, L., Crossetti, L., Bicudo, C. and Araujo-Jesus, T. (2007). Undesirable side-effects of water hyacinth control in a shallow tropical reservoir. *Freshwater Biology*, 52, 1120–1133.

Birara, H., Pandey, R. P., & Mishra, S. K. (2018). Trend and variability analysis of rainfall and temperature in the Tana basin region, Ethiopia. *Journal of Water and Climate Change*, jwc2018080. doi:10.2166/wcc.2018.080. .

Callisto, M., Molozzi, J., & Barbosa, J. L. E. (2013). Eutrophication of lakes. Eutrophication: causes, consequences and control, 55–71. Doi: 10.1007/978-94-007-7814-6_5.

Camberlin, P., Martiny, N., Philippon, N., Richard, Y. (2007). Determinants of the inter annual relationships between remote sensed photosynthetic activity and rainfall in tropical Africa. *Remote Sensing of Environment*, 106, 199-216.

Cavalli, R.M., Laneve, G., Fusilli, L., Pignatti, S., Santini, F. (2009). Remote sensing water observation for supporting Lake Victoria weed management. *Journal of Environment Managment.* 90, 2199–2211.

Center, T. D., Hill, M. P., Cordo, H., & Julien, M. H. (2002). Water hyacinth. biological control of invasive plants in the Eastern United States. *USDA Forest Service Publication FHTET*.

Changbin, L., Jiaguo Q., Linshan, Y.,Shuaibing W, Wenjin, Y., Gaofeng, Z., Songbing, Z.,and Feng, Z. (2014). Regional vegetation dynamics and its response to climate change: a case study in the Tao River Basin in Northwestern China. *Environmental Research Letters*, vol. *300*, pp. 1560–1563.

Chen, X., (2000). Using remote sensing and GIS to analyze land cover change and its impacts on the regional sustainable development. *Intern. Jou.of Remote Sensing,* 23(1), 107-114.

Cheruiyot, E., Mito, C., Menenti, M., Gorte, B., Koenders, R., & Akdim, N. (2014). Evaluating MERIS-based aquatic vegetation mapping in Lake Victoria. *Remote Sensing*, 6(8), 7762–7782. doi:10.3390/rs6087762.

Cobbing, B. (2006). The use of Landsat ETM imagery as a suitable data capture source for alien Acacia species for the WFW Programme. M.Sc. Thesis Rhodes University, Grahamstown, South Africa.

Congalton, R.G., (1991). A Review of assessing the accuracy of classifications of remotely sensed data. *Remote sensing of environment,* 37, 35-46.

Conway, D. (2000). The climate and hydrology of the Upper Blue Nile River. *The Geographical Journal* 166(1): 49-62.

Dagno, K., Lahlali, R., Diourte, M., & Haissam, J. (2012). Fungi occurring on water hyacinth, Eichhornia crassipes (Martius) Solms-Laubach in Niger River in Mali and their evaluation as Mycoherbicides. *Journal of Aquatic Plant Management*, 50, 25–32.

Dagno, K., Lahlali, R., Friel, D., Bajji, M., and Jijakli, H. (2007). Review: problems of the water hyacinth, Eichhornia crassipes in the tropical and subtropical areas of the world, in particular its eradication using biological control method by means of plant pathogens. *Biotechnol. Agron. Soc. Environment*, 11(4), 299–311.

DeFries, R.S., Asner, G.P. and Houghton, R., (2004). Trade-offs in land-use decisions: towards a framework for assessing multiple ecosystem responses to land-use change. *Ecosystem Land Use Change*, 2:1-9.

Derseh, Kibret, Tilahun, Worqlul, Moges, Dagnew, and Melesse. (2019). Potential of water hyacinth infestation on Lake Tana, Ethiopia: a prediction using a GIS-based multi criteria technique. *Water*, 11(9), 1921. Doi: 10.3390/w11091921.

Dhir, D. (2015). Status of aquatic macrophytes in changing climate: A perspective. *Journal of Environmental Science and Technology* 8 (4): 139-148, DOI: 10.3923/jest.2015.139.148.

Dillon, P., J., and Rigler, F., H. (1974). A test of a simple nutrient budget model predicting the phosphorus concentration in lake water. *Journal of Fish Res Board Can* 31:1771–1778.

Donald, W., Meals, Spooner, J., Steven, A., Dressing, and Harcum, J., B. (2011). Statistical analysis for monotonic trends, Tech Notes 6, November 2011. Developed for U.S. Environmental Protection Agency by Tetra Tech, Inc., Fairfax, VA, 23 p.

Dooenboss, J., & Pruitt, W., O. (1992). Crop water requirements (FAO irrigation and drainage paper 24) (Revised 19). Rome: Food and Agriculture Organization of the United Nations.

Dube, T., Mutanga, O., Sibanda, M., Bangamwabo, V. and Shoko, C. (2017a). Testing the detection and discrimination potential of the new Landsat 8 satellite data on the invasion of the water hyacinth, eichhornia crassipes (Mart.)

Dube, T., Mutanga, O., Sibanda, M., Bangamwabo, V. and Shoko, C. (2017b). Evaluating the performance of the newly-launched Landsat8 sensor in detecting and mapping the spatial configuration of water hyacinth (Eichhornia crassipes) in inland lakes, Zimbabwe. *Physics and Chemistry of the Earth*, http:// dx.doi.org/10.1016/j.pce.2017.02.015.

Dube, T., W. Gumindoga, and M. Chawira. (2014). Detection of land cover changes around Lake Mutirikwi, Zimbambwe, Based on traditional remote sensing classification techniques. *African Journal of Aquatic Science*, 39 (1): 89–95. doi:10.2989/16085914.2013.870068.

Edwards, D., and Musil, CJ. (1975). Eichhornia crassipes in South Africa – a general review. Journal of *Limnological Soc. Southern Africa*.; 1: 23-27.

EEA, (2012). The impacts of invasive alien species in Europe. EEA technical reports No 16/2012. Luxembourg: Publications Office of the European Union, 2012. http://www.eea.europa.eu/publications/impacts-of-invasive-alien-species Ethiopia II: wind energy. *Solar Energy* 57(4): 323-334.

Erkie Asmare. (2017). Current trend of water hyacinth expansion and its consequence on the Fisheries around North Eastern part of Lake Tana, Ethiopia. *Journal of Biodiversity & Endangered Species*, 05(02). doi:10.4172/2332-2543.1000189.

Erwin, K. L. (2008). Wetlands and global climate change: the role of wetland restoration in a changing world. *Wetlands Ecology and Management*, 17(1), 71–84. Doi: 10.1007/s11273-008-9119-1

Everitt, J.H., Yang, C., Escobar, D.E., Webster, C.F., Lonard, R.I., and Davis, M.R. (1999). Using remote sensing and spatial information technologies to detect and map two aquatic macrophytes. *Journal of Aquatic Plant Management* 37: 71-79

Firehun, Y. (2017). Management of water hyacinth (Eichhornia crassipes [Mart.] Solms) using bioagents in the Rift Valley of Ethiopia, PhD thesis, Wageningen University, Wageningen, the Netherlands, 174 pp.

Firehun, Y., Struik, P.C., Lantinga, E.A., and Taye, T. (2014). Water hyacinth in the Rift Valley Water Bodies of Ethiopia: its distribution, socioeconomic importance, and management, Ethiopia.

Fordham, C., J. (2012). A spatial and temporal analysis of the changes in alien macrophyte communities and a baseline assessment of the macro invertebrates associated with Eurasian watermilfoil, Myriophyllum spicatum L. (Haloragaceae) in the Vaal River. M.Sc. Thesis Rhodes University, Grahamstown, South Africa.

Frazier, P. S., and Page, K. J. (2000). Water body detection and delineation with Landsat TM data. *Photogrammetric Engineering and Remote Sensing*, 66(12), 1461–1467.

Fundament of remote sensing: a Canada Centre for remote sensing tutorial, nd

Fusilli, L., Collins, M. O., Laneve, G., Palombo, A., Pignatti, S., and Santini, F. (2013). Assessment of the abnormal growth of floating macrophytes in Winam Gulf (Kenya) by using MODIS imagery time series. *International Journal of Applied Earth Observation and Geoinformation*, 20, 33–41. doi:10.1016/j.jag.2011.09.002.

Gao, J. (2009). Digital analysis of remotely sensed imagery. McGraw-Hill.

Gavin, H., and Agnew, C.T., (2000). Estimating evaporation and surface resistance from a wet grassland. *Phys. Chem. Earth*, 25 (7–8), 599–603.

Getachew Bayable. (2017). Evaluating the nexus between climate variability and vegetation dynamics: the case of Upper Awash Basin, Ethiopia. MSc. Thesis Addis Ababa University, Ethiopia

Getachew Zewude. (2010). Base flow analysis of rivers in Lake Tana Sub Basin.

Gichuki, J, Omondi, R., Boera, P., Okorut, T., Matano. A., S. (2012). Water hyacinth eichhornia crassipes; laubach dynamics and succession in the nyanza. *Sci World J pp*: 106-429.

Gopal, B. (1987). Water Hyacinth. *Elsevier Science Publishers*, Amsterdam, the Netherlands.

Goraw Goshu and Shimelis Aynalem, (2017). Chapter 2: Problem overview of the Lake Tana Basin.

Guo, W., Ni. X., Jing, D., and Shuheng, L. (2014). Spatial-temporal patterns of vegetation dynamics and their relationships to climate variations in Qinghai Lake Basin using MODIS time series data. *Journal of Geographical Sciences*, 2014, 24(6):1009-1021.

Haider, S. Z. (1989). Recent work in Bangladesh on the utilisation of water hyacinth. *Recent work in Bangladesh on the utilization of water hyacinth*., (278).

Hailu, S., T., Demel, N. Sileshi, and A. Fassil. (2004). Some biological characteristics that foster the invasion of Prosopis juliflora (Sw.) DC. At Middle Awash Rift Valley, North-Eastern *Ethiopian Journal of Arid Environment*, 58:135 -154.

Hare, W. (2003). Assessment of knowledge on impacts of climate change, contribution to the specification of Art, 2 of the UNFCCC, WBGU.

Hill, M., P., and Coetzee, J.,A. (2008). Integrated control of water hyacinth in Africa. *EPPO Bull*. 38: 452-457.

Holm, L.G., Plucknett, D.L., Pancho, J.V., and Herberoer, J., P. (1977). The world's worst aquatic weeds: distribution and biology. Honolulu, the University Press Hawaii.

http://projects.infonile.org/a_weed_grown_out_of_control/index.html.

https://web.uri.edu/ltrs/files/415AccuracyAssessment2018.pdf.

https://www.youtube.com/watch?v=520VZV9LoNk.

Huang, C., Chen, Y., Zhang, S., and Wu, J. (2018). Detecting, extracting, and monitoring surface water from space using optical sensors: a review. *Reviews of Geo physics*, 56. https://doi.org/10.1029/2018RG000598.

Hubble, S., and Harper, D., M. (2002). Phytoplankton community structure and succession in the water column of a shallow tropical lake (Lake Naivasha, Kenya). Hydrobiologia 488 (Developments in Hydrobiology 168).

Humberto A. Barbosa and T. V. Lakshmi Kumar. (2012). Strengthening regional capacities for providing remote sensing decision support in dry lands in the context of climate variability and change, international perspectives on global environmental change, Dr. Stephen Young (Ed.), ISBN: 978-953-307-815-1, InTech,

Implementation guideline on use of Neochetina Weevils for water hyacinth control around Lake Tana, (2018). Prepared by ANRS Environment, Forest and Wildlife Protection and Development Authority, Bahir Dar University and Global Coalition for Lake Tana Restoration.

Jensen, J.R. (2005). Introductory digital image processing: a remote sensing perspective. 3rd edition, Prentice Hall, Upper Saddle River, 505-512.

Ji, L., Zhang, L., and Wylie, B. (2009). Analysis of dynamic thresholds for the normalized difference water index. *Photogrammetric Engineering and RS*, 75(11), 1307–1317.

Jiménez-Rodríguez, C., Esquivel-Vargas, C., Coenders-Gerrits, M., and Sasa-Marín, M. (2019). Quantification of the evaporation rates from six types of wetland cover in Palo Verde National Park, Costa Rica. *Water*, 11(4), 674. doi:10.3390/w11040674.

Joshi, C., de Leeuw J., van Duren, I., and C. (2004). Remote sensing and GIS applications for mapping and spatial modelling of invasive species.

Karpatne, A., Khandelwal, A., Chen, X., Mithal, V., Faghmous, J., and Kumar, V. (2016). Global monitoring of inland water dynamics: State-of-theart, challenges, and opportunities. *International Journal of Lässig, K. Kersting, & K. Morik (Eds.), Computational Sustainability* (pp. 121–147).

Kasaragod, G., R. (2003). Assessment of changes in water-hyacinth coverage of water bodies in northern part of Bangalore city using temporal remote sensing data. *Research Gate*, vol. 84, no. 6, 25.

Kebede, S., Travi, Y., Alemayehu T., and Marc, V. (2006). Water balance of Lake Tana and its sensitivity to fluctuations in rainfall, Blue Nile Basin, Ethiopia. *Journal of Hydrology* 316(1–4): 233–247.

Khanna, S., Santos, M., Ustin, S., Haverkamp, P. (2011). An integrated approach to a biophysiologically based classification of floating aquatic macrophytes. *International Journal Remote Sensing* 32:067–1094.

Kitaka, N. (2000). Phosphorus supply to a shallow tropical lake and its consequences Lake Naivasha, Kenya. PhD, University of Leicester.

Kitamura, K., Kakishima, S., Uehara, T., Morita, S., Tainaka, K., & Yoshimura, J. (2016). The Effects of Rainfall on the Population Dynamics of an Endangered Aquatic Plant, Schoenoplectus gemmifer (Cyperaceae). *PLOS ONE*, 11(6), e0157773. doi:10.1371/journal.pone.0157773.

Krishnaveni, R., Y. (2015). Spatiotemporal distribution of aquatic invasive plants in Kuttanad Wetland Ecosystem. Academy of climate change education and research Vellanikkara, Thrissur – 680 656 Kerala, India.

Landgrebe, D.A. (2003). Signal theory methods in multispectral remote sensing. Hoboken,NJ: John Wiley and Sons.

Leica Geosystems. (2005). ERDAS imagine tour guides. Leica Geosystems Geospatial, Norcross, Georgia, US.

Li, J., Lewis, J., Rowland, J., Tappan, G., and Tieszen, L.L. (2004). Evaluation of land performance in Senegal using multi-temporal NDVI and rainfall series. *Journal of Arid Environments*, 59:463–480.

Lillisand, M.T. and Kiefer, W.R. (2008). Remote sensing and image interpretation. Sixth ed. New York, USA: John Wiley & Sons, Inc.

Lu, D., P. Mausel, E., Brondi, Z., and Moran, E. (2004). Change detection techniques. *International Journal of Remote Sensing, 24, 23652407.*

Lunetta, R. S., and Elvidge, C. D. E. (1999). Applications, project formulation and analytical approach, remote sensing change detection, environmental monitoring methods and applications. London: Taylor & Francis, pp: 1-20.

Mailu, A., M. (2001). Preliminary assessment of the social, economic and environmental impacts of water hyacinth in the Lake Victoria Basin and the status of control. In: Biological and Integrated control of water hyacinth, Erchhorniacrassipes. Julien, M.H., M. P. Hill, T. D.

Marangoz, A.M., Sekertekin, A.A., and Akçin, h. (2017). Analysis of land use land cover classification results derived from Sentinel-2 image, Bulent Ecevit University, Engineering.

McFeeters, S.K. (1996). The use of the normalized difference water index (NDWI) in the delineation of open water features. *Int. Journal. Remote Sensing*. 1996, *17*, 1425–1432.

Melaku Getachew Ayalew. (nd). Spatial coverage of water hyacinth infestation around Lake Tana, Ethiopia. *Earth Sciences: an International Journal (ESIJ),* Vol 1 No 1.

Meleha, M.E. (2005). Calculation of water consumptive use of hayacinth Elchhornia Crasslpes. *Water Sci*. 38, 69–76.

Minakawa, N., Sonye, G., Dida, G., Futami, K. and Kaneko, S. (2008). Recent reduction in the water level of Lake Victoria has created more habitats for Anopheles funestus. *Malaria Journal* 7:119.

Ministry of Natural Resources (MNR). (1994). State of the environment report for Uganda. Uganda: National Environmental Information Centre.

Mireri, E. (2005). DAAD Summer School. Topics of integrated watershed management. Siegen University, 89-98.

Mironga, J., Mathooko, J. and Onywere, S. (2011). The effect of water hyacinth (eichhornia crassipes) infestation on phytoplankton productivity in Lake Naivasha and the status of control. *Journal of Environmental Science and Engineering* 5(10) 1252-1261.

Mironga, J.M., Mathooko, J.M. and Onywere, S.M. (2014). Effects of spreading patterns of water hyacinth (Eichhornia crassipes) on zooplankton population in Lake Naivasha, Kenya. *Int. Journal of Development and Sustainability*, vol. 3 No. 10, pp. 1971-1987.

Mitchell D., S. (1976). The growth and management of Eichhornia crassipes and salvinia spp. In their native and alien situations. In Varshney C.K and Rzoska J. eds. Aquatic weeds in South East Asia. The Hague: Junk.

Mohamed, Y.A., Bastiaanssen, W.G.M., Savenije, H.H.G., van den Hurk, B.J.J.M., and Finlayson, C.M. (2011). Wetland versus open water evaporation: An analysis and literature review. *Physics and Chemistry of the Earth*, 47–48 (2012), 114–12. doi:10.1016/j.pce.2011.08.005

Mohammed, M., R., A. (2016). Mapping and assessing impacts of land use and land cover change by means of an advanced remote sensing approach: A case study of Gash Agricultural Scheme, Eastern Sudan. Dissertation for awarding the academic degree Doctor of Natural Science (Dr.rer.Nat.).

Mohr, P. A. (1962). The Geology of Ethiopia. *Addis Ababa University-College Press*, Addis Ababa.

Molinos, J. G., Viana, M., Brennan, M. and Donohue, I. (2015). Importance of long-term cycles for predicting water level dynamics in natural lakes. *Plus one*, 10(3): e0119253.

Mondal, A., Kundu, S., and Mukhopadhyay, A. (2012). Rainfall trend analysis by Mann Kendall test: a case study of North-Eastern Part of Cuttack District, Orissa. *International Journal of Geology, Earth and Environmental Sciences, 2(1)*:70-78.

Mountrakis, G.I. J. and Ogole, C. (2011). Support vector machines in remote sensing: A review. *ISPRS Journal of Photogrammetry and Remote Sensing*, 66:247-259.

Mujere, N. (2015). Water hyacinth: characteristics, problems, control options, and beneficial uses. *Research Gate*, DOI: 10.4018/978-1-4666-9559-7.ch015.

Mulugeta, Yacob and F. Drake. (1996). Assessment of solar and wind energy resources in Ethiopia II: wind energy. *Solar Energy* 57(4): 323-334.

Nath, S.S, Mishra,G., Kar J., Chakraborty,S., and Dey,N. (2014). A survey of image classification methods and techniques. *International Conference on Control, Instrumentation, Communication and Computational Technologies* (ICCICCT), Kanyakumari, 2014, pp. 554-557, doi: 10.1109/ICCICCT.2014.6993023

Navarro, L., and Phiri, G. (2000). Water hyacinth in Africa and the Middle East. A survey of problems and solutions. *International Development Research Centre*, Ottawa.

Ndimele, P. E., Kumolu-Johnson, C. A., and Anetekhai, M. A. (2011). The invasive aquatic macrophyte, water hyacinth {Eichhornia crassipes (Mart.) Solm-Laubach: Pontedericeae}: problems and prospects. Research Journal of Environmental Sciences, 5(6), 509.

Ndimele, P., & Jimoh, A. (2011). Water hyacinth, Eichhornia crassipes (Mart. Solms.) in phytoremediation of heavy metal polluted water of Ologe lagoon, Lagos, Nigeria. *Research Journal of Environmental Sciences*, 5(5), 424-433.

NMSA. (1996). Climatic and agro-climatic resources of Ethiopia. Meteorological research report series, vol. 1, no. 1, Addis Ababa.

Nohara, S. (1991). A study on annual changes in surface cover of floating-leaved plants in a lake using aerial photography. *Vegetation*, 97:125-136.

Olthof, I. (2017). Mapping seasonal inundation frequency (1985–2016) along the St-John River, New Brunswick, Canada using the Landsat archive. *Remote Sensing*, 9(2), 143.

Omo-Irabor, O.O. (2016). A comparative study of image classification algorithms for landscape assessment of the Niger Delta Region. J. of Geographic Information System, 8, 163-170.

Ongore C., O., Aura C., M., James, Z., O., Njiru, M., and Nyamweya, C., S. (2018). Spatial temporal dynamics of water hyacinth, Eichhornia crassipes (Mart.), other macrophytes and their impact on fisheries in Lake Victoria, Kenya. *Journal of Great Lakes Research*.

Ouma, Y.O., Shalaby, A., and Tateishi, R. (2005). Dynamism and abundance of water hyacinth in the Winam Gulf of Lake Victoria: evidence from remote sensing and seasonal climate data. *International. Journal of Environment. Stud.* 62(4).

Ozesmi, S. L. and Bauer, M. E. (2002). Satellite remote sensing of wetlands. *Wetlands Ecology and Management*, 10:381-402.

Palmer, S.C.J., Kutser, T. and Hunter, P. D., (2015). Remote sensing of inland waters challenges, progress and future directions. *Remote Sensing of Environment*, 157:1-8.

Panetta, F.D. and Lawes. R., 2005. Evaluation of the performance of weed eradication programs: the delimitation of extent. *Diversity and Distributions*, 11: 435-442.

Patel, S. (2012). Threats, management and envisaged utilizations of aquatic weed Eichhornia crassipes: an overview. *Rev. Environment Science of Biotechnology*, 11:249-259.

Penatti, N.C., Almeida, T.I.R.d., Ferreira, L.G., Arantes, A.E. and Coe, M.T. (2015). Satellite based hydrological dynamics of the world's largest continuous wetland. *Remote Sensing of Environment*, 170:1-13.

Penfound, W.T., and Earle, T.T. (1948). The biology of the water hyacinth. *Ecological Monographs*, 18:447-472.

Rahman, A., and Begum, M. (2013). Application of non-parametric test for trend detection of rainfall in the largest island of Bangladesh. *ARPN Journal of Earth Sciences, 2(2)*: 40-44.

Rajapakse, S. S., Khanna, S., Andrew, M. E., Ustin, S. L., and Lay, M. (2006). Identifying and classifying water hyacinth (Eichhornia crassipes) using the HyMap sensor. *Remote Sensing and Modeling of Ecosystems for Sustainability III*. doi:10.1117/12.676265.

Rashed, A., A. (2014). Assessment of aquatic plants evapotranspiration for secondary agriculture drains (case study: Edfina drain, Egypt). *Egyptian Journal of Aquatic Research*, 40(2), 117 124. https://doi.org/10.1016/j.ejar.2014.07.001.

Rezene, F. (2005). Water hyacinth (Eichhornia crassipes): A review of its weed status in Ethiopia. Arem, 6:105-111.

Richards, J.A., and Jia, X. (2006). Remote sensing digital image analysis: An introduction, 4th edition. Springer-Verlag Berlin Heidelberg 2006, Germany.S27-S31.

Şahin, H., Topan, H., Karakış, S., & Marangoz, A. (2004). Comparison of object oriented image analysis and manual digitizing for feature extraction.

Samuel, T., and Netsanet, A. (2014). Prevalence and intensity of water hyacinth infestation in the water bodies of rift valley, Ethiopia.

Sasaqi, D., Pranoto, & Setyono, P. (2019). Estimation of water losses through evapotranspiration of water hyacinth (Eichhornia crassipes). Caraka Tani: *Journal of Sustainable Agriculture*, 34(1), 86-100. doi:http://dx.doi.org/10.20961/carakatani.v34i1.28214.

Scavia, D., J.C. Field, D.F. Boesch, R.W. Buddemeier and V. Burkett. (2002). Climate change impacts on U.S. coastal and marine ecosystems. *Estuaries*, 25: 149-164.

Sewnet, A., and Kameswara, K., R. (2011). Hydrological dynamics and human impact on ecosystems of Lake Tana, Northwestern, Ethiopia, doi:10.4314/ejesm.v4i1.7.

Shanab, S., Shalaby, E., Lightfoot, D. and El-Shemy, H. (2010). Allelopathic effects of water hyacinth (Eichhornia crassipes). *PLoS One*, 5(10):1320.

Shekede, M.D., Kusangaya, S., and Schmidt, K. (2008). Spatio-temporal variations of aquatic weeds abundance and coverage in Lake Chivero, Zimbabwe. *Phys. Chem. Earth. 33*: 714 721

Shoko, C. and Mutanga, O. (2017). Examining the strength of the newly-launched Sentinel-2 MSI sensor in detecting and discriminating subtle differences between C3 and C4 grass species. *ISPRS Journal of Photogrammetry and Remote Sensing*, 129:32-40.

Sibanda, M., Mutanga, O. and Rouget, M. (2015). Examining the potential of Sentinel-2 MSI spectral resolution in quantifying above ground biomass across different fertilizer treatments. *ISPRS Journal Photogrammetry of Remote Sensing*, 110:55-65.

Sisay, H., Teshome, S., and Demel, T. (2016). Land use and land cover change in the Bale Mountain Eco-Region of Ethiopia during 1985 to 2015. *Land, 5(4)*:41.

Sithranjan, S. (2012). Statistical analysis to detect climate change and its implications on water resources, Msc. Thesis, Victoria University, Australia.

Song, Y., and Ma, M. G. (2008). Variation of AVHRR NDVI and its relationship with climate in Chinese Arid And Cold Regions. *Journal of Remote Sensing*, vol. 12(3), pp. 499–505.

Soni, S. (2017). Evaluation of land-use land-cover change with changing climatic parameters of a watershed of Madhya Pradesh, India. *An International Journal of Society for Tropical Plant Research, 4(1)*: 115–125.

Sophia, R., and Ndambuki, J. M., (2017). Accuracy assessment of land use/land cover classification using remote sensing and GIS. *International Journal of Geosciences, 8*: 611 622.

Stephenson, M. G., Turner, G., Pope, P., Colt, J., Knight, A., & Tchobanoglous, G. (1980). The use and potential of aquatic species for wastewater treatment. Publication No. 65. California State Water Resources Control Board.

Stroud, A. (1994). Water hyacinth (Eichhornia crassipes [Mart.] Solms) in Ethiopia. proceedings of the 9th annual conference of Ethiopian Weed Science Committee, Addis Ababa, Ethiopia, pp. 7-16.

Tellez, T.R., de Rodrigo Lopez, E.M., Granado, G.L., Perez, E.A., Lopez, R.M., and Guzman, J.M.S. (2008). The water hyacinth, Eichhornia crassipes: an invasive plant in the Guadiana River Basin (Spain). *Aquatic Invasions: 3(1): 42-53.*

Tewabe, Dereje. (2015). Preliminary survey of water hyacinth in Lake Tana, Ethiopia. *Global Journal Allergy 1(1)*: 013-018. DOI: 10.17352/2455-8141.000003.

Teygeler, R. (2000). Water hyacinth paper, contribution to a sustainable future [bi-lingual]. In (Torley and Gentenaar (eds.): Publishers, pp.168-188.

Thamaga, K. H., & Dube, T. (2018). Remote sensing of invasive water hyacinth (Eichhornia crassipes): A review on applications and challenges. *Remote Sensing Applications: Society and Environment*, 10(17), 36–46. https://doi.org/10.1016/j.rsase.2018.02.005.

Thamaga, K., H., & Dube, T. (2018). Testing two methods for mapping water hyacinth (Eichhorniacrassipes) in the Greater Letaba River System, South Africa: discrimination and mapping potential of the polar-orbiting Sentinel-2 MSI and Landsat 8 OLI sensors, *International Journal of Remote Sensing.*

Thenmozhi, M., and Kottiswaran, S.V. (2016). Analysis of rainfall trend using Mann– Kendall test and the sen's slope estimator in Udumalpet of Tirupur district in Tamil Nadu. *International Journal of Agricultural Science and Research, 6(2)*:131-138.

Timmer, C.E., Weldon, L.W. (1966). Evapotranspiration and pollution of water by water hyacinth. Annual report. In: Soil and Water Conservation. Research Division. Southern Branch, Florida.

Tiwari, S., Dixit, S. and Verma, N. (2007). An effective means of bio filtration of heavy metal contaminated water bodies using aquatic weed Eichhornia crassipes. *Environmental Monitoring and Assessment*, 129:253-256.

Topaloğlu, R.H., Sertel, E., and Musaoğlu, N. (2016). Assessment of classification accuracies of Sentinel-2 and Landsat-8 data for land cover / use mapping. ITU, Civil Engineering Faculty, Geomatics Engineering Department, 34469, Istanbul, Turkey.

Twongo, T. (1993), Status of the water hyacinth in Uganda. In: Great head A and P de Groot (ed) control of Africa's water weeds. Series Number CSC (93) AGR-18 Proceedings 295.

United Nations Environment Programme (UNEP). (2012). Fifth global environment outlook (GEO5): environment for the future we want. Nairobi: United Nations Environment Programme.

United Nations Environment Programme (UNEP). (2013). Global Environment Alert Service. Taking the pulse of the planet connecting science with policy, United Nation Environment Programme.

United States Geological Survey (USGS). (2013). Using the USGS Landsat 8 product. http://landsat.usgs.gov/Landsat8_Using_Product.php (29 Jun. 2015).

Vapnik, V. (1998). Statistical Learning Theory, John Wiley and Sons, New York.

Venter, N., Hill, M., Hutchinson, S., & Ripley, B. (2012). Weevil borne microbes contribute as much to the reduction of photosynthesis in water hyacinth as does herbivory. *Biological Control*, 64(2), 138–142. doi:10.1016/j.biocontrol.2012.10.011.

Vila, M., Espinar, J., Hejda, M., Hulme, P., Jarošík, V., Maron, J., & Pyšek, P. (2011). Ecological impacts of invasive alien plants: A meta-analysis of their effects on species, communities and ecosystems. *Ecology Letters*, 14(7), 702–708. doi:10.1111/j.1461 0248.2011.01628.x PMID: 21592274.

Villamagna, A. and Murphy, B. (2010). Ecological and socio-economic impacts of invasive water hyacinth (Eichhornia crassipes): A review. *Freshwater Biology* (2010) 55, 282–298 doi:10.1111/j.1365-2427.2009.02294.x.

Wassie A, Dereje T, Addisalem A, Abebaw Z, %eia T, et al. (2015). Water hyacinth coverage survey report on Lake Tana biosphere reserve. Technical survey report series 2.

Wassie, A., Minwuyelet, M., Ayalew, W., Dereje, T., Woldegebrael G., Addisalem, A., and Wondie, E. (2014). Water hyacinth coverage survey report on Lake Tana. Technical report series 1, 28 pp.

Welch, R., Remilliard, R.R., and Slack, R.B. (1988). Remote sensing and geographic information system techniques for aquatic resource evaluation. *Photogrammetric Engineering and Remote Sensing 54*:177-185.

Williams, A. E., Duthie, H.C., Hecky, R. E., 2005.Water hyacinth in Lake Victoria: Why did it vanish so quickly and will it return? *Aquat. Bot.*. 81 (4), 300-314.

Willoughby, N. G., Watson, I., Lauer, S. and Grant, I. F. (1993). The effects of water hyacinth in the biodiversity and abundance of fish and invertebrates in Lake Victoria, Uganda. Final Technical Report. NRI Project No. 10066 and A038, Natural Resources Institute, Overseas Development Administration. United Kingdom.

Worku, Melese and Sahile, Samuel. (2018). Impact of water hyacinth, Eichhornia crassipes (Martius) (Pontederiaceae) in Lake Tana, Ethiopia: a review. *Journal Aquatic Res Development* 9: 520. DOI: 10.4172/2155-9546.1000520.

Worku Nega. (2018). The impacts of vegetation cover change on rainfall and land surface temperature using remote sensing: a case study of North Gondar zone. M.Sc. Thesis Addis Ababa University, Ethiopia .

Wrona, F.J., T.D. Prowse, J.D. Reist, J.E. Hobbie, L.M.J. Levesque and W.F. Vincent, (2006). Climate change effects on aquatic biota, ecosystem structure and function. AMBIO. *Journal Hum. Environment*, 35: 359-369.

Xie, Y., Sha, Z. and Yu, M., (2008). Remote sensing imagery in vegetation mapping: a review. *Journal of Plant Ecology*, 1(1):9-23.

Xu, H. Q. (2006). Modification of normalized difference water index (NDWI) to enhance open water features in remotely sensed imagery. *In. Jour. of Remote Sensing, 27*, 3025- 3033.

Xu, M., Watanachaturaporn, P., Varshney, P. K. and Arora, M. K., (2005). Decision tree regression for soft classification of remote sensing data. *Remote Sensing of Environment*, 97(3):322-336.

Zhang, T., Su, J., Liu, C. and Chen, W.H. (2017). Potential bands of sentinel-2a satellite for classification problems in precision agriculture, proceedings of the 23rd international conference on automation & computing, University of Huddersfield, UK. 7-8 Sep 2017.

Appendices

Appendix 1:The status of water hyacinth in 2019 May during the field survey.






Appendix 2: Spatio-temporal distribution and extent of water hyacinth from 2016 September to 2017 December.

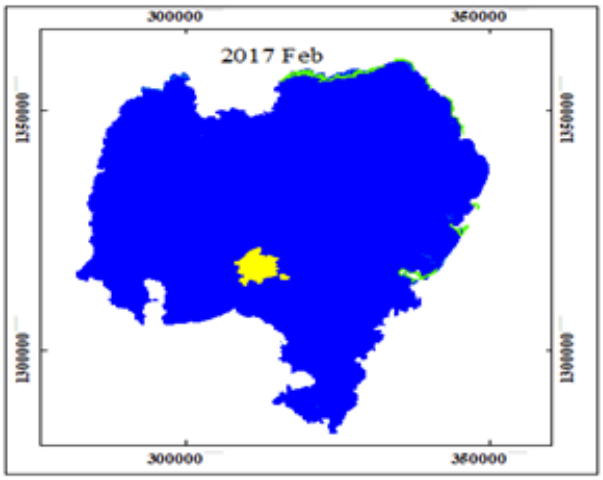
2017 Feb
300000
350000
1350000
1300000

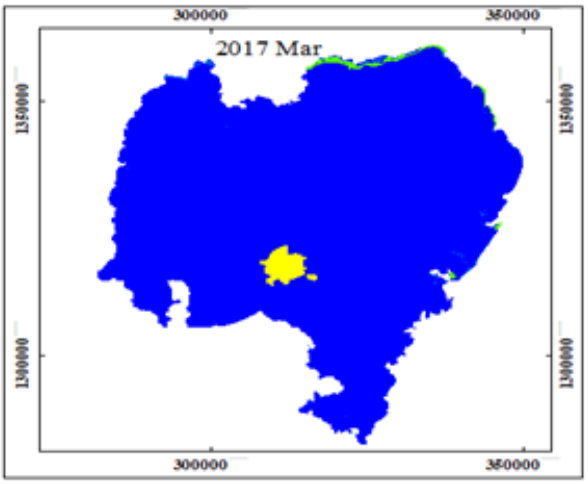
2017 Mar
300000
350000
1350000
1300000

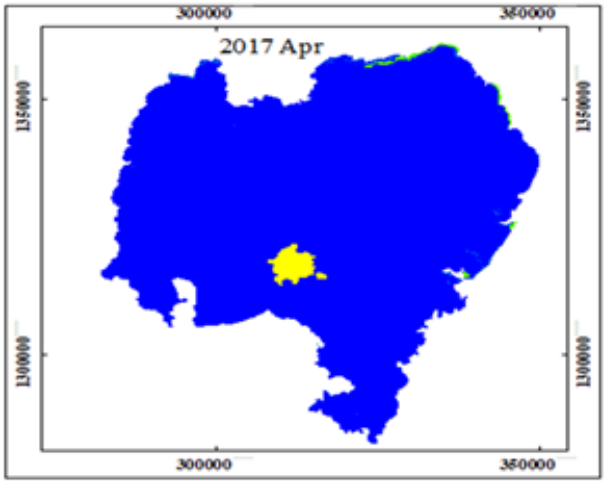
2017 Apr
300000
350000
1350000
1300000

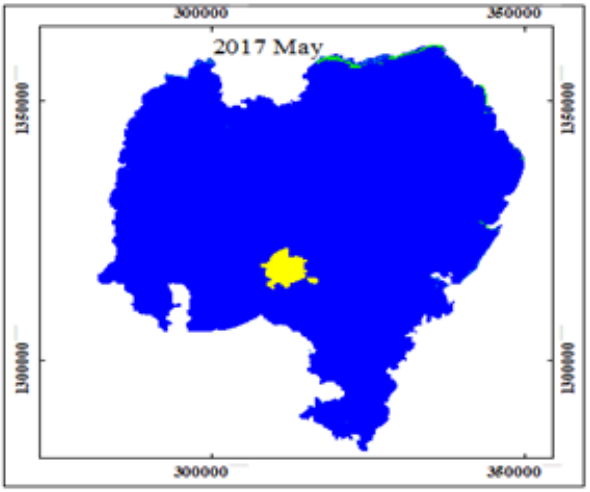
2017 May
300000
350000
1350000
1300000

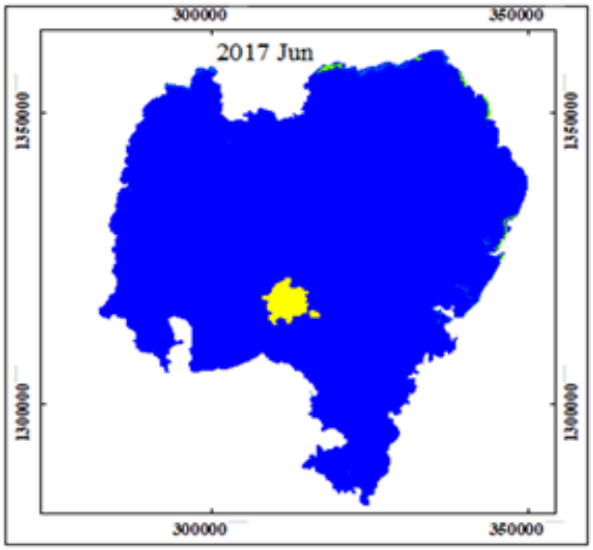
2017 Jun
300000
350000
1350000
1300000

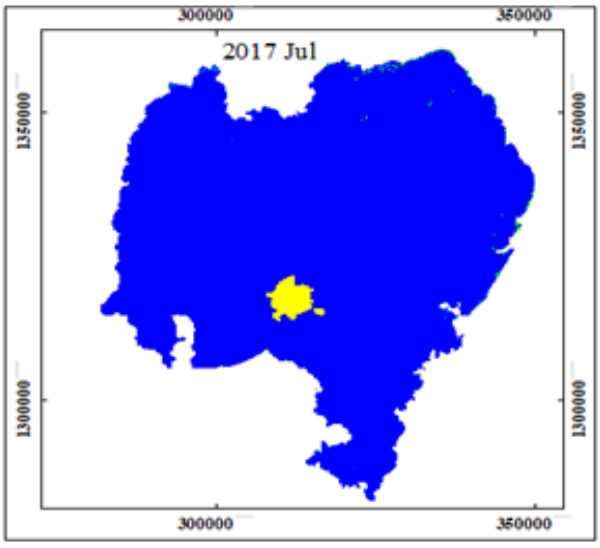
2017 Jul
300000
350000
1350000
1300000

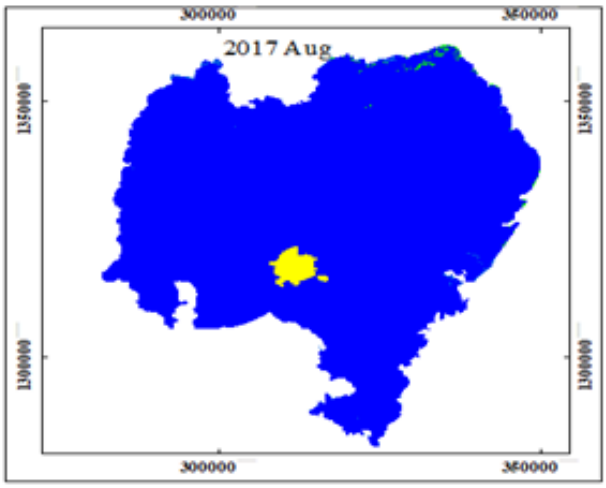
2017 Aug
300000
350000
1350000
1300000

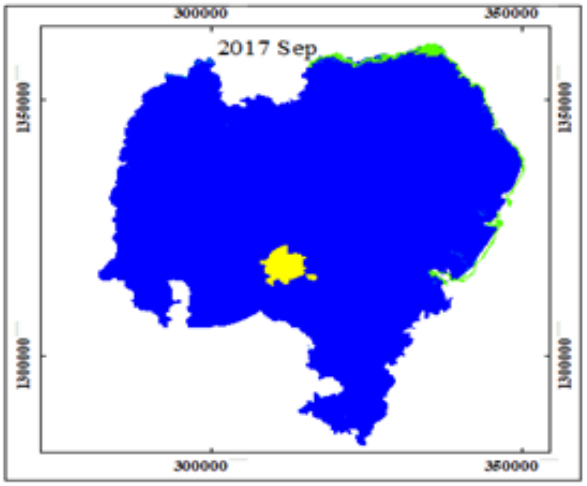
2017 Sep
300000
350000
1350000
1300000

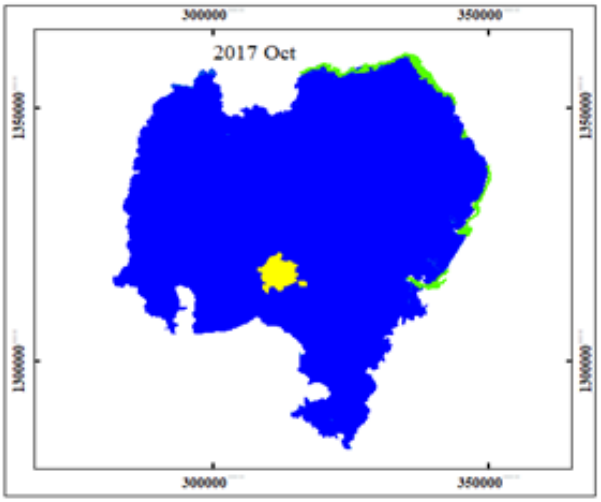
2017 Oct
300000
350000
1350000
1300000

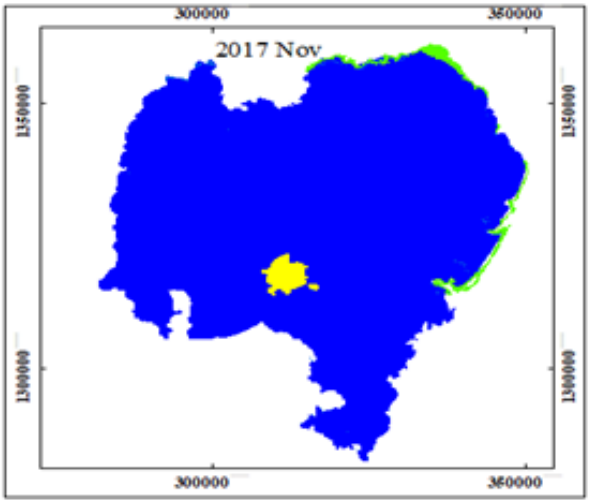
2017 Nov
300000
350000
1350000
1300000

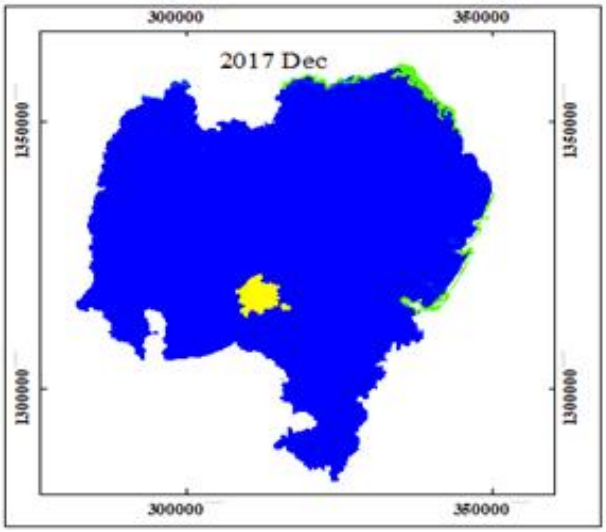
2017 Dec
300000
350000
1350000
1300000

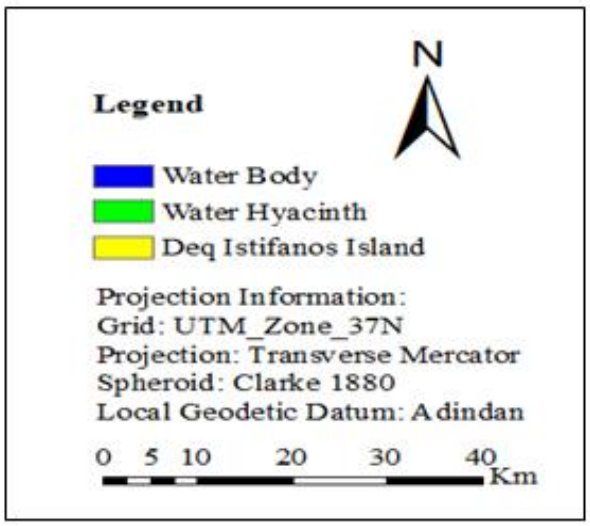
Legend
N
Water Body
Water Hyacinth
Deq Istifanos Island
Projection Information:
Grid: UTM_Zone_37N
Projection: Transverse Mercator
Spheroid: Clarke 1880
Local Geodetic Datum: Adindan
0 5 10 20 30 40
Km

Appendix 3: Meteorological stations used within and near Lake Tana Basin.

No.	Stations	Class	UTM Coordinate		Elevation above MSL
			East (m)	North (m)	
1	Adis Zemen	3	367246.68	1341225.9	1970
2	Adet	1	332986.66	1245163.53	2195
3	Aykel	1	288111.2	1385943.64	2172
4	Bahir Dar	1	327733.01	1282800.77	1824
5	Chandiba	3	285822.25	1370469.98	2071
6	Chwahit	4	306441.23	1363687.05	1890
7	Dangila	1	263090.2	1244497.86	2127
8	Debre Tabor	1	392165.34	1310158.37	2700
9	Dek Estifanos	4	311585.17	1317188.85	1808
10	Delgi	4	286748.65	1348334.05	1814
11	Enfranz	3	356390.4	1346806.91	1882
12	Gassay	3	406306.09	1303476.13	2850
13	Gondar	1	328339.37	1387887.2	2094
14	Gorgora	3	315086.98	1354780.61	1786
15	Maksegnit	3	343432.98	1365677.35	1897
16	Merawi	3	298038.47	1244258.57	2020
17	Wanzaye	3	357263.36	1301453.82	1934
18	Wereta	3	356252.06	1318049.5	1801
19	Wetet Abay	3	287206.46	1257605.12	1922